# Economic, Environmental, and Health Impact Analysis of Developing Hydrogen Economy in Canada

by

Hamidreza Shamsi

A thesis

presented to the University of Waterloo

in fulfillment of the

thesis requirement for the degree of

Doctor of Philosophy

in

Mechanical and Mechatronics Engineering

Waterloo, Ontario, Canada, 2022

# Examining Committee

The following served on the Examining Committee for this thesis. The decision of the Examining Committee is by majority vote.

External Examiner      Dr. Hossam Gaber

            Professor

Supervisor         Dr. Michael Fowler

            Professor

Internal Member       Dr. Roydon Fraser

            Professor

Internal Member       Dr. John Wen

            Professor

Internal-external Member    Dr. Rebecca Saari

            Assistant Professor

# Author's Declaration

This thesis consists of material all of which I authored or co-authored: see Statement of Contribution included in the thesis. This is a true copy of the thesis, including any required final revisions, as accepted by my examiners.

I understand that my thesis may be made electronically available to the public.

# Statement of Contributions

The body of this thesis is based on a combination of published work. Various sections are adapted from the following list of publications:

**Chapter 3**

Shamsi, H., Haghi, E., Raahemifar, K., & Fowler, M. (2019). Five-year technology selection optimization to achieve specific $CO_2$ emission reduction targets. *International Journal of Hydrogen Energy*, *44*(7), 3966-3984.

> Dr. Haghi and I developed the energy system optimization model. Dr. Haghi and I analyzed the results and worked on different scenarios. I wrote the final manuscript. Dr. Raahemifar and Dr. Fowler reviewed the manuscript.

**Chapter 4**

Shamsi, H., Tran, M. K., Akbarpour, S., Maroufmashat, A., & Fowler, M. (2021). Macro-Level optimization of hydrogen infrastructure and supply chain for zero-emission vehicles on a Canadian corridor. *Journal of Cleaner Production*, *289*, 125163.

> I developed the modeling framework, Dr. Maroufmashat assisted with the computer simulation, and Dr. Fowler was the advisor for model development and results generation. I prepared all the results and Mr. Tran and I wrote the final manuscript. Ms. Akbarpour prepared the maps. Dr. Fowler and Dr. Maroufmashat reviewed the manuscript.

**Chapter 5**

Shamsi, H., Munshed, M., Tran, M. K., Lee, Y., Walker, S., The, J., Raahemifar, K., & Fowler, M. (2021). Health Cost Estimation of Traffic-Related Air Pollution and Assessing the Pollution Reduction Potential of Zero-Emission Vehicles in Toronto, Canada. *Energies*, *14*(16), 4956.

> Mr. Munshed and I developed the air pollution simulation model and Dr. The assisted with computer simulation. Dr. Walker and I developed the emission calculation model. I developed the risk analysis model and health cost calculation. Mr. Tran, Mr. Lee, and I wrote the final manuscript. Dr. Fowler and Dr. Raahemifar reviewed the manuscript.

# Abstract

The greatest challenge to the development of a cleaner energy system is economic issues. However, if the environmental and health externalities of the current energy system is considered, other energy alternatives become economically competitive. Therefore, hydrogen can become an option in different energy sectors. As an energy vector, hydrogen can be represented as the missing link between clean energy sources and energy consumers. The real cost of an energy system includes environmental and health-related hidden costs. The current energy system imposes lots of critical damages to the environment and human lives. All these damages are avoidable if governments follow the prevention policy instead of the cure policy. In other words, governments can support developing clean energy solutions by incentivizing them. In this regard, the government should be aware of the hidden costs of energy for both fossil-fuel-based and hydrogen-based energy systems. Therefore, in this work, a comprehensive cost calculation is conducted for using hydrogen in different energy sectors in this work. The result from this work shows that the idea of Hydrogen Economy is economically competitive with the current energy system, if the hidden costs of environmental and health effects are taken into account.

The first study is focused on developing a five-year mathematical model for finding the optimal sizing of renewable energy technologies for achieving specific $CO_2$ emission reduction targets. An industrial manufacturing facility that uses CHP for electricity generation and natural gas for heating is considered the base case in this work. The CHP capacity is 4500 kW and the furnace is operated 8 AM to 4 PM with a natural gas

consumption of 4000 $m^3$/h. Different renewable energy technologies are assumed to be developed each year to achieve a 4.53% annual $CO_2$ emission reduction target. The results of this study show that wind power is the most cost-effective technology for reducing emissions in the first and second years, with a cost of 44 and 69 CAD per tonne of $CO_2$, respectively. On the other hand, hydrogen is more cost-effective than wind power in reducing $CO_2$ emissions from the third year onward. The cost of $CO_2$ emission reduction with hydrogen doesn't change drastically from the first year to the fifth year (107 and 130 CAD per tonne of $CO_2$). Solar power is a more expensive technology than wind power for reducing $CO_2$ emissions in all years due to lower capacity factor (in Ontario), more intermittency (requiring mores storage capacity), and higher investment cost. A hybrid wind/battery/hydrogen energy system has the lowest emission reduction cost over five years. The emission reduction cost of such a hybrid system increases from 44 CAD per tonne of $CO_2$ in the first year to 156 CAD per tonne of $CO_2$ in the fifth year. The developed model can be used for long-term planning of energy systems to achieve GHG emission targets in regions/countries with fossil fuel-based electricity and heat generation infrastructure.

The second study develops a multi-objective model to determine the optimal sizes and locations of the hydrogen infrastructure needed to generate and distribute hydrogen for the critical Highway Corridor (HWY 401) in Ontario. The model is used to aid the early-stage transition plan for converting conventional vehicles to FCEVs in Ontario by proposing a feasible solution to the infrastructure dilemma posed by the initial adoption of hydrogen as fuel in the general market. The health benefit from the pollution reduction is also determined to show the potential social and economic incentives of using FCEVs. The results show that

hydrogen production and delivery cost can reduce from \$22.7/kg H2 in a 0.1% market share scenario to \$14.7/kg H2 in a 1% market share scenario. The environmental and health benefit of developing hydrogen refueling infrastructure for heavy-duty vehicles is 1.63 million dollar per year and 1.45 million dollars per year, respectively. Also, every kilogram of H2 can avoid 11.09 kg $CO_2$ from entering the atmosphere. In a 1% market share scenario, the proposed hydrogen network avoids more than 37,000 tonnes of $CO_2$ per year.

The third study aims to determine the economic burden of environmental and health impacts caused by Highway 401 traffic. Due to the high volume of vehicles driving on the Toronto Highway 401 corridor, there is an annual release of 3771 tonnes of carbon dioxide equivalent ($CO_2e$). These emissions are mainly emitted onsite through the combustion of gasoline and diesel fuel. The integration of electric and hydrogen vehicles shows maximum reductions of 405–476 g $CO_2e$ per vehicle kilometer. Besides these carbon dioxide emissions, there is also a large number of hazardous air pollutants. The mass and concentrations of criteria pollutants of $PM_{2.5}$ and $NO_x$ emitted by passenger vehicles and commercial trucks on Highway 401 were determined using the MOVES2014b software to examine the impact of air pollution on human health. Then, an air dispersion model (AERMOD) was used to find the concentration of different pollutants at the receptor's location. The increased risk of health issues was calculated using hazard ratios from literature. Finally, the health cost of air pollution from Highway 401 traffic was estimated to be CAD 416 million per year using the value of statistical life, which is significantly higher than the climate change costs of CAD 55 million per year due to air pollution.

The fourth study discovers the health benefit of reducing fossil-fuel vehicle market share and utilizing more Zero-Emission Vehicles (ZEVs). A historical dataset from 2015-2017 is used to learn a Long Short-Term Memory (LSTM) model that can predict future $NO_x$ concentration based on traffic volume, weather condition, time, and past $NO_x$ concentration. The developed model is used in a modified manner to predict $NO_x$ concentration in the long term. Then, the developed model is utilized to predict annual average $NO_x$ reduction in four different scenarios. Interpolation methods are used to predict pollution reduction in all Dissemination Areas (DA) of Toronto. Finally, a health cost assessment is conducted to estimate the health benefit from different scenarios. The results show that the western areas of Toronto experience more $NO_x$ concentration reduction in all scenarios, which is the result of a stronger correlation between traffic volume and pollution in those areas. Also, by 10% reduction in fossil-fuel traffic volume, 70 deaths can be prevented annually, equivalent to CAD 560 million health benefit per year.

There are plenty of opportunities for future work in this area to make more robust energy models which can take all aspects of implementing the idea of Hydrogen Economy. First, the impact of using different types of hydrogen storage can be investigated in terms of cost. Also, a comprehensive hydrogen-based energy model can be optimized if the cost-benefit analysis is conducted in all energy sectors. Finally, different objective functions such as energy, environmental, health, and social costs can be optimized to reach an optimal sustainable energy system for Ontario.

# Acknowledgments

First of all, I am deeply grateful to my supervisor: Professor Michael Fowler, for his invaluable supervision, support, and tutelage during my Ph.D. degree. Also, I would like to offer my special thanks to colleagues I've worked with at the University of Waterloo, especially Dr. Ehsan Haghi, Dr. Azadeh Maroufmashat, and Mr. Manh-Kien Tran.

I would like to express gratitude to my Ph.D. examining committee, Professor Roydon Fraser, Professor John Wen, Professor Rebecca Saari from the University of Waterloo, and Professor Hossam Gaber as my external examiner from Ontario Tech University for their time and contributions.

Finally, I'd like to acknowledge the help and support I received from my family and friends, especially my wife, Hosna. Without their love and care, I would not have been able to make it this far.

# Dedication

In dedication to my mother, Mahshid, my father, Dariush, and my wife, Hosna, whose wholehearted love, wisdom, and support constantly encouraged me throughout life.

**Table of Contents**

# List of Figures

# List of Tables

# List of Symbols

CapCost          Capital Cost

D          Demand

Ecap          Energy Capacity

Ein          Input Energy

Em          Total emission

EmLim          Limit of total emission

Enewcap          New Energy Capacity

Eout          Output Energy

HENGlimit          Hydrogen perecentage limit in HENG

Hout          Output Heat

NGCost          Natural Gas Cost

Scap          Storage Capacity

Sstored          Stored electricity or hydrogen

v          Binary value for hydrogen production plants

w          Binary value for hydrogen refueling stations

X          Hydrogen delivered to stations

| | |
|---|---|
| Z | Objective function |

*Subscripts*

| | |
|---|---|
| h | hour |
| m | Energy Conversion Technology |
| s | Storage technology |
| t | Year |

# List of Acronyms

| | |
|---|---|
| AADT | Annual Average Daily Traffic |
| BEV | Battery Electric Vehicle |
| CHP | Combined Heat and Power |
| EPA | Environmental Protection Agency |
| FCEV | Fuel Cell Electric Vehicle |
| GA | Global Adjustment |
| GAMS | General Algebraic Modeling Software |
| GHG | Greenhouse Gas |
| HDSAM | Hydrogen Delivery Scenario Analysis Model |
| HENG | Hydrogen-Enriched Natural Gas |
| HFS | Hydrogen Fueling Station |
| HOEP | Hourly Ontario Electricity Price |
| HWY | Highway |
| IESO | Independent Electricity System Operator |
| LCA | Life Cycle Assessment |
| LCOE | Levelized Cost of Electricity |
| LSTM | Long Short-Term Memory |

| | |
|---|---|
| MILP | Mixed-Integer Linear Programming |
| MOVES | Motor Vehicle Emission Simulator |
| NASCO | North American Superhighway Corridor |
| NG | Natural Gas |
| O&M | Operation and Maintenance |
| TRAQS | Transportation Air Quality System |
| VSL | Value of Statistical Life |
| WHO | World Health Organization |
| WTW | Well to Wheel |
| ZEV | Zero-Emission Vehicle |

# 1. Introduction

## 1.1    Overview and Objectives

In 1987, The United Nations (the UN) defined "sustainability" as "meeting the needs of the present without compromising the ability of future generations to meet their own needs" [1]. Today's energy system, however, does not have the signs of a sustainable system. The current energy system compromises future generations' needs and has many adverse effects on living human beings. Two significant problems with the global energy system are environmental issues and health issues.

According to the International Energy Agency, the world energy demand in 2040 will be 50% more than 2015 [2]. Fossil fuels will be the dominant source to meet this additional amount of global energy demand. On the other hand, atmospheric $CO_2$ concentration is 30% more than pre-industrial levels[3]. Previous research estimates the Social Cost of Carbon (SCC) to be \$31 per ton of $CO_2$ in 2010 US\$ [4]. However, recent studies show that global SCC is US\$417 per tonne of $CO_2$, which results in a \$250 billion financial loss just for the U.S. [5].

According to the International Energy Agency's (IEA) Executive Director, 70 percent of worldwide energy investments are from governmental sources[6]. "The message is clear – the world's energy destiny lies with government decisions," said Dr. Fatih Birol [6]. Lots of efforts have been made to guarantee that the GHG-related global temperature increase will stop by 2050. The Kyoto Protocol and Paris agreement are the most known global agreement on GHG emission reduction, which have not been successful. According to

World Energy Outlook 2018, in a sustainable development scenario, the current 32 Gtonne/year of energy-related $CO_2$ emissions could reduce to less than 20 Gtonne/year in 2040 [7]. However, pursuing current policies could result in 36 Gton of energy-related $CO_2$ emission in 2040 [7]. This shows that governments have a crucial role in developing a sustainable global energy system.

The other major problem with the current energy system is health effects. According to [8], the fifth-ranking mortality risk factor in 2015 is related to $PM_{2.5}$. $PM_{2.5}$ caused more than 4 million deaths (more than 7% of total global deaths) and 100 million disability-adjusted life-years (DALYs) in 2015 [8]. The $PM_{2.5}$-related deaths in 2015 are 20% more than in 1990 [8]. These statistics become worse when ozone-related health impacts are considered. More than 250000 annual deaths and 4 million DALYs are related to ozone pollution [8]. In total, air pollution is responsible for around 8 million deaths each year [9]. Air pollution-related health cost in 2015 was USD 21 billion and is anticipated to increase to USD 176 billion by 2060 [9]. The market cost of air pollution will reach 1% of global GDP by 2060 [9].

One of the biggest challenges with energy systems of different sizes around the world is providing enough storage capacity required to cover the intermittent behavior of renewable energy sources. Renewable energy sources are the most recent alternatives to fossil fuel sources. Daily, monthly, and yearly intermittency of renewable sources has increased the need for higher storage capacity. Electricity as the most common energy vector is not capable of being stored easily in its form. Lots of researchers around the world

are working on the development of batteries. However, storing electricity in large scales and for long times seems to be unachievable using batteries.

GHG emissions and air pollution are the most significant negative consequences of the current energy system. The scarcity of energy resources, non-homogenous distribution of energy resources, and intermittency of existing alternative energy sources are other drawbacks of the current energy system. "Hydrogen Economy", which was first defined in the 1970s, could be a natural solution for worldwide energy system problems. The hydrogen economy can amend all energy sectors through different pathways - household, industry, and transportation. However, the biggest obstacle against the idea of a hydrogen-based energy system is economic barriers. Based on economic assessments, the idea of rebuilding the global energy system is not logical. However, it might change everything if the adverse side effects of the current energy system are taken into consideration.

The optimal energy system parameters would change if total cost - not only direct costs- is considered. For instance, in the transportation sector, governments worldwide can incentivize Zero-Emission Vehicles (ZEVs) to make more money out of fewer healthcare costs. Based on estimations, people around the world are willing to pay USD 3 trillion to reduce the risk of air pollution-related premature deaths [9]. In all energy sectors, renewable alternatives can reduce GHG emissions and mitigate air pollutions. Reduction in GHG emissions and air pollution can lower the social cost of carbon and premature deaths.

As an energy vector and in integration with other clean energy sources, Hydrogen can present a new energy system with fewer consequences for people around the world. This work will study the possibility of different hydrogen pathways using economic,

environmental, and health impact analysis. Also, optimal sizing and planning of hydrogen-based energy systems will be presented in different energy sectors.

As the most significant fossil fuel-dependent energy sector, the transportation sector is the greatest challenge for government in terms of emission and pollution. Spending money in the transportation sector to reduce the side effects of using fossil fuels is unavoidable. The unanswered questions are the amount of incentives by the government and incentive policies. A slight reduction in GHG emissions and air pollution in the transportation sector needs less investment. As reduction targets become more ambitious, the marginal cost of air pollution reduction becomes higher. That is why the optimum amount of investment has to be found.

The industrial sector in Ontario can benefit from the surplus amount of electricity generation. Now, Ontario is selling its surplus electricity at low prices. The government of Ontario can sell the surplus electricity to the manufacturing companies at lower prices to encourage them to reduce their GHG emissions. Additionally, manufacturing companies need to reduce their GHG emissions to meet their emission reduction targets. Moving toward a cleaner future, those companies require a step-by-step plan. The optimum plan must be designed for every individual facility.

Seasonal changes in energy supply and demand are relatively high in Ontario. Hydrogen is a great storage solution for significant amounts of energy for long periods. Storage sizing and planning at the province level needs a comprehensive optimization process that can lead to the most logical decisions.

All in all, a comprehensive model is required to propose an optimal energy system benefitting from clean energy sources, sustainable energy vectors, and storage media. To

find the optimum sizing and planning of a sustainable energy system, environmental and health-related costs must be taken into account. As a result, an energy model based on different energy options in different sectors needed to be developed to find the best energy decisions for a sustainable future.

## 1.2    Thesis Layout

This thesis includes 7 chapters wherein chapter 1 depicts the motivation and objectives of the overall studies along with the thesis layout. Chapter 2 reviews the background information used in the next chapters. Chapters 3 to 5 consists of papers all of which I co-authored as principal lead author (Please refer to the statement of contributions included in the thesis).

Chapter 3 presents five-year technology selection optimization to achieve specific $CO_2$ emission reduction targets published by Shamsi et al. [10]. In this study, the optimal sizing and scheduling of an industrial facility is analyzed in different scenarios including a hydrogen-based system scenario.

Chapter 4 introduces  macro-level optimization of hydrogen infrastructure and supply chain for zero-emission vehicles on a Canadian Corridor published by Shamsi et al. [11]. In this study, the optimal location and sizing of hydrogen refueling stations along Highway 401 is investigated. It is assumed that the demand of the different shares of heavy-duty trucks are met using a network of hydrogen refueling stations.

Chapter 5 studies health cost estimation of traffic-related air pollution and assessing the pollution reduction potential of zero-emission vehicles in Toronto, Canada published by

Shamsi et al. [12]. In this study, an integrated model is developed to assess the environmental and health cost of traffic-related emission from Highway 401. The study utilizes MOVES, AERMOD, and GREET as well as Concentration Response Function (CRF) for calculation the increased risk of mortality.

Chapter 6 discusses Traffic air pollution prediction and health cost estimation using machine learning: A case study of Toronto, Canada. In this study, Machine Learning (ML) techniques are used to estimate the impact of traffic volume on the air pollution in Toronto. Then, different scenarios are defined to assess the impact of lower share of fossil-fuel vehicles on human's health in term of mortality and monetary units.

Chapter 7 summarizes the conclusions and provides recommendations for future work.

# 2. Background

## 2.1 Hydrogen as an energy carrier

Since the 1920s, ammonia replaced saltpeter for explosive and fertilizer purposes. So, hydrogen has been used to produce ammonia for almost a century [2]. Then, until the 1960s, many countries used hydrogen to produce town gas, which was a mixture of H2, CO, and CH4. This mixture was used for residential purposes as well as street lighting [2]. Today, total hydrogen production is around 700 billion $Nm^3$- enough to fuel more than 600 million FCEVs- and around 50% of total hydrogen consumption is for ammonia production [2]. More than 90% of total hydrogen production comes from fossil fuels – around half from natural gas and one-third from oil- and just 4% comes from electricity [13].

## 2.2 Hydrogen: from production to consumption

In this section, a brief description of the $H_2$ journey from production to consumption is presented.

### 2.2.1 Hydrogen production

Hydrogen can be produced from different sources. Common hydrogen production methods are listed below

- Steam Methane Reforming (SMR)

- Gasification

- Electrolysis

- Hydrogen from biomass

- Hydrogen from nuclear energy

Below, each production method is described briefly.

### 2.2.1.1   Steam Methane Reforming (SMR)

In SMR natural gas reacts with water in the presence of a catalyst to produce H2 and $CO_2$. The amount of hydrogen produced in the SMR process is around 70-75% [14]. As mentioned in the previous section, natural gas reforming produces around half the total hydrogen production. However, this process is not a key process in a sustainable energy system because it needs natural gas as feed, which is scarce and heterogeneously distributed around the world. Additionally, without a carbon capture system, SMR produces as much $CO_2$ as burning natural gas.

### 2.2.1.2   Gasification

Gasification can produce H2 and CO from coal, heavy residual oils, and low-value refinery production in a less than stoichiometric ratio reaction. The reaction temperature in this process is around 1200 0C to 1400 0C [14].

### 2.2.1.3   Electrolysis

In the electrolysis process, water molecules are directly split into hydrogen and oxygen molecules using electricity. Two common electrolyzers are PEM and alkaline. PEM electrolyzers utilize solid polymer membrane electrolytes [14]. Alkaline electrolyzers employ potassium hydroxide electrolytes.

Electrolysis would play a key role in future energy systems, as it can be a bridge between intermittent renewable sources and the energy storage sector. One of the biggest problems with this technology is its high cost. Therefore, the application of this technology is limited to low scales and it produces less than 5% of total hydrogen production [14].

### 2.2.1.4 Hydrogen from biomass

In this method, hydrogen can be produced by thermochemical processes at high temperatures. In this process, syngas -which is a mixture of H2 and CO- can be achieved by gasification or pyrolysis. As this process is less dependent on insecure fossil fuels, it is identified as a more sustainable way of hydrogen production than SMR and coal gasification [ref]. Additionally, this process can lead to other useful products such as polymers, fertilizers, ethanol, methanol, etc. [14].

### 2.2.1.5 Hydrogen from nuclear energy

As stated before, the cleanest hydrogen production method is water electrolysis using renewable sources, however, the cost of such a system is high. One of the solutions to this problem is to use nuclear energy instead of renewable energies. Although nuclear energy is a non-renewable energy source, it has a low life-cycle $CO_2$ emission. However, there are many environmental concerns about the mining and processing of uranium.

Figure 2-1 shows different methods of producing hydrogen.
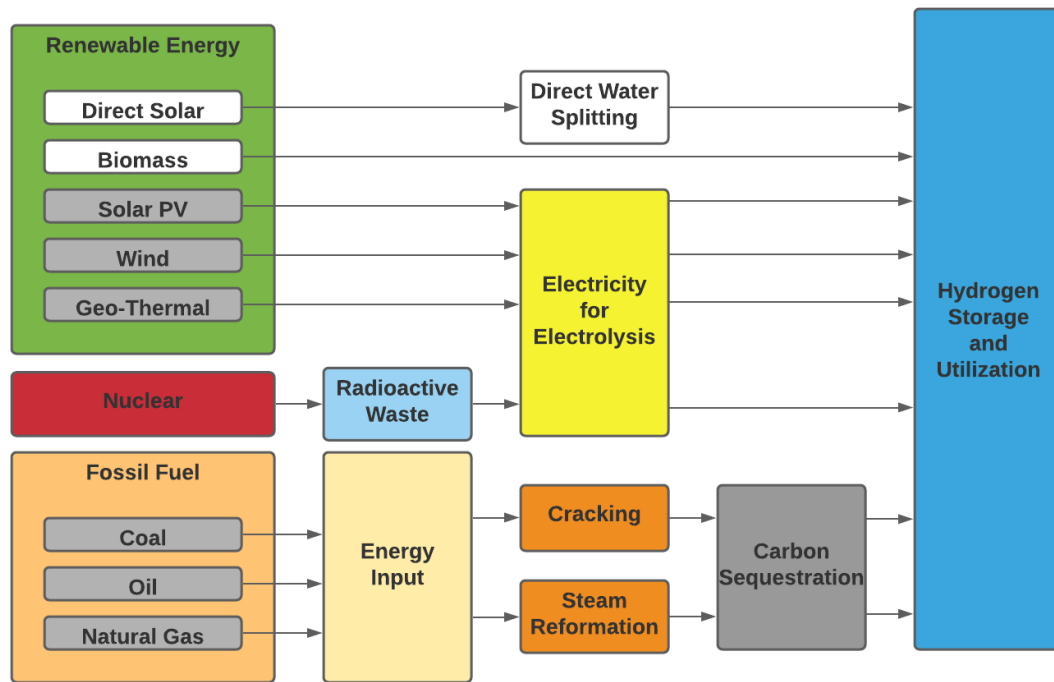
**Figure 2-1 - Hydrogen production from different energy sources [15]**

### 2.2.2 Hydrogen Storage

One of the greatest challenges facing a hydrogen-based energy system is hydrogen storage. Because of low volumetric energy density, hydrogen storage tanks require large volumes. This would be the greatest problem with storing energy in hydrogen molecules, especially in the transportation sector. To overcome this problem, different methods are employed. Figure 2-2 shows some of these methods.
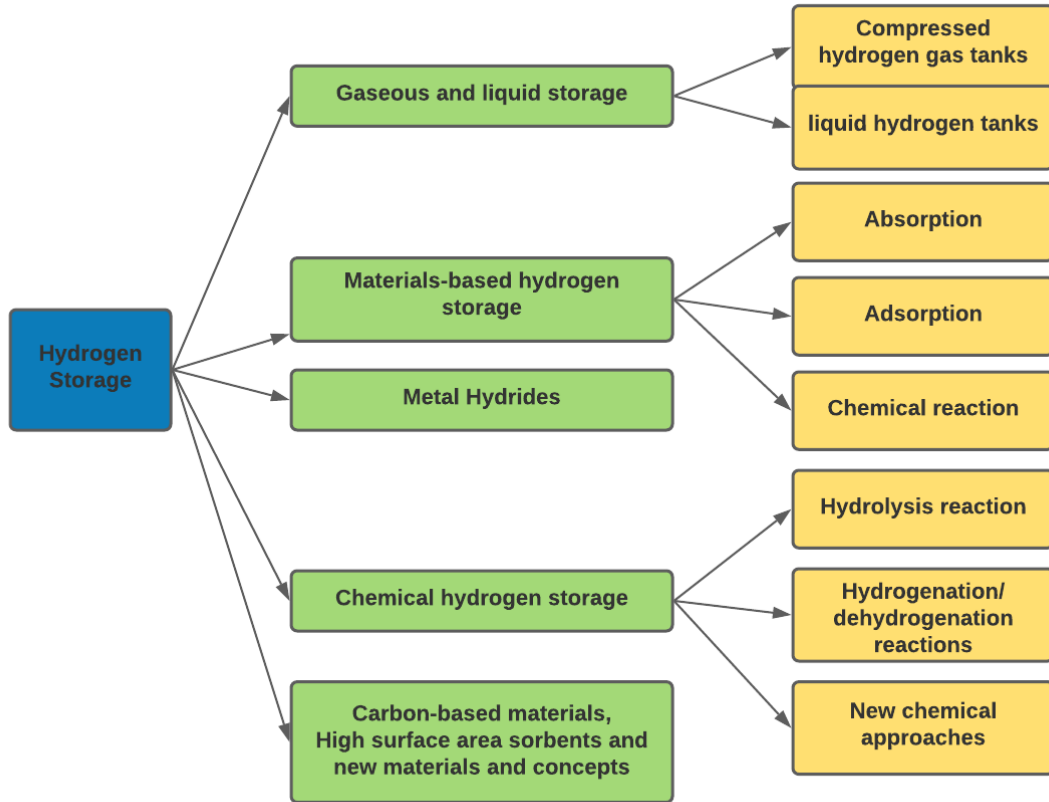
**Figure 2-2 - Different hydrogen storage methods [14]**

### 2.2.3 Hydrogen consumption

There are three major energy demands which can be met using hydrogen

• Transportation

• Residential

• Industry

In this section, hydrogen application in these three sectors is explained.

### 2.2.3.1 Hydrogen in Transportation

The transportation sector accounts for around 20% of total energy consumption around the world. Moreover, transport is responsible for almost a quarter of global energy-related $CO_2$ emissions [16]. Furthermore, fossil-fuel vehicles are estimated to be the cause of 6.5 million premature deaths in 2012 [16]. Hydrogen can be the substitute for diesel and petrol in the future energy system, as it emits less $CO_2$, even if it is produced by the SMR process. In the case of using clean electricity for hydrogen production by electrolysis, FCEVs (Fuel Cell Electric Vehicles) can be categorized as ZEVs (Zero Emission Vehicles). Toyota's Mirai, Hyundai's Tuscan FCEV, and Honda's Clarity Fuel Cell are some of the commercial FCEVs which are released in the last 5 years [16]. A McKinsey analysis anticipates that total ownership cost for the different types of vehicles will decrease after 2025, due to learning and economies of scale [16].

### 2.2.3.2 Hydrogen in the residential sector

The residential sector accounts for about 40% of global energy consumption in building and industry. There are lots of alternatives to replace current hydrocarbon fuels used for heat generation with low-carbon energy carriers to meet climate change mitigation targets by 2050. Air and ground-source heat pumps, solar heating and biomass are of the residential energy solution. However, these options are costly, due to high capital expenditure and no alternative function in periods of low heat demand, especially for countries closer to the poles [16]. So, hydrogen, as a new solution was identified in recent publications. Existing

natural gas networks could be utilized to transport hydrogen instead of natural gas. Then, heat could be produced using hydrogen boilers or micro-CHP fuel cells.

**2.2.3.3    Hydrogen in industry**

Today, most of the hydrogen demand is related to the industry sector. 53% of hydrogen is used by ammonia production, 40% by the oil industry and methanol synthesis, and 7% by polymer and resin production. Hydrogen can be utilized for refining crude oil via hydrocracking and hydrotreating to eliminate sulphur from transportation fuels. The hydrogen demand in the oil industry is increasing, as the decline in light crude oils.

## 2.3   Hydrogen Economy: History and Definition

After the oil crisis in the 1970s, the term "Hydrogen Economy" was first brought up by General Motors in connection with the future fuel supply in the transport sector. The idea of the hydrogen economy is constructed on a hydrogen-based energy system, in which, hydrogen, as an energy vector, plays the key role to connect different energy networks together. Figure 2-3 shows the idea of the hydrogen economy. As it can be seen in Figure 2-3, hydrogen is a communication tool between the heat network, electricity grid, and fuel network.
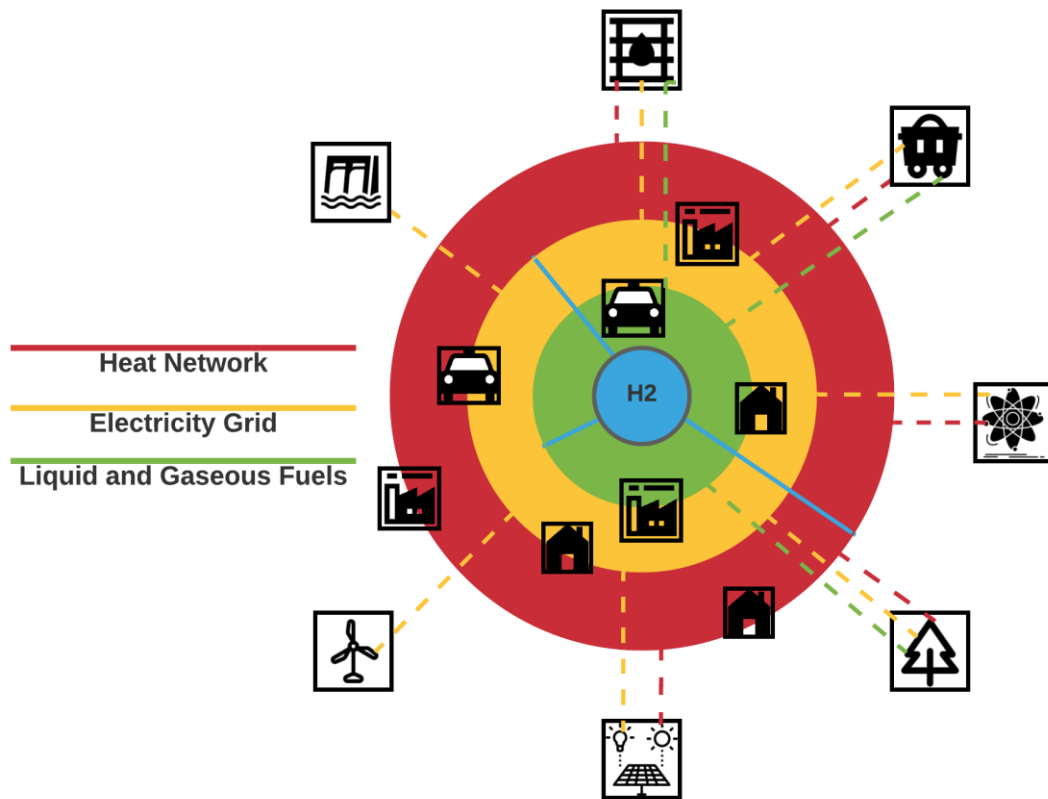
**Figure 2-3 - Hydrogen connects different energy networks in the future energy system**

## 2.4   Hydrogen Pathways

There are three major pathways for hydrogen in a large energy system, which are shown in

Figure 2-4. These pathways are described in this section.
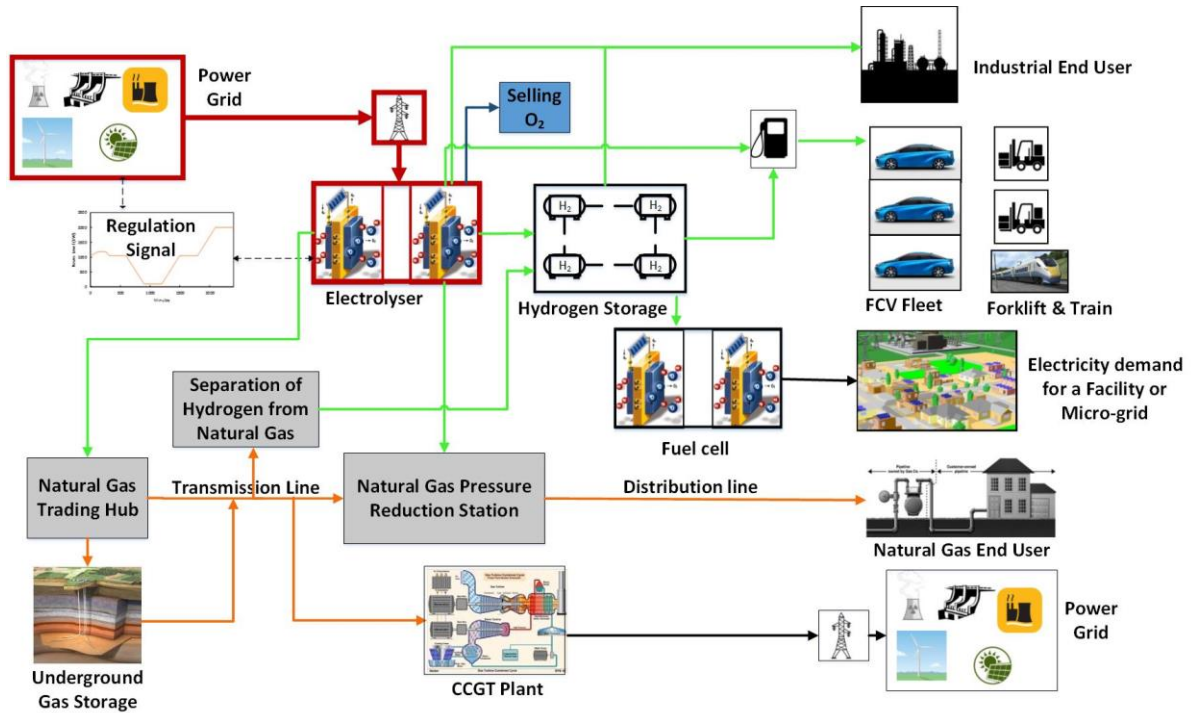
**Figure 2-4 - Hydrogen pathways** [17]

## 2.4.1 Power-to-Gas (P2G)

In this pathway, electricity is the source for producing hydrogen through the electrolysis process. The produced hydrogen in the P2G pathway can be blended with natural gas or go through the methanation process. HENG (Hydrogen Enriched Natural Gas) has less energy density rather than natural gas, however, it could be a method to decrease $CO_2$ emission. Different countries around the world have different limitations for adding hydrogen to the natural gas pipeline. Figure 2-5 shows the limitation on hydrogen injection into the natural gas network for some European countries.
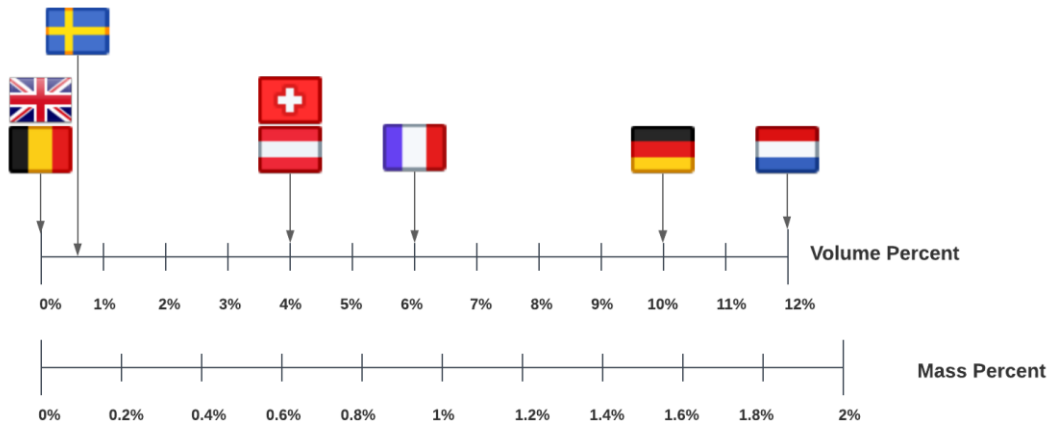
**Figure 2-5 - Hydrogen limit in different national gas networks** [18]

One of the greatest advantages of the hydrogen economy is that hydrogen can utilize the current natural gas network system with some modifications. HENG would be a step toward moving from natural gas to hydrogen.

Methanation is the process of combining $CO_2$ and H2 in a high-temperature reactor in the presence of a catalyst. If the $CO_2$ in the methanation process comes from a CCS (Carbon Capturing System), it could result in $CO_2$ reduction emission.

### 2.4.2 Power-to-Power (P2P)

P2P is the key pathway of the hydrogen economy, as in this process surplus power could convert to hydrogen by electrolysis. Then, the produced hydrogen could be stored in large amount for long periods of time. Using fuel cells, stored hydrogen could produce power again. This pathway is important because, in the future energy system, there would be lots of intermittent energy resources. In other words, the different pattern of power production and consumption could match using P2P. Moreover, the produces hydrogen can be utilized in

FCEVs to meet the transportation demand. So, Power-to-Fuel (P2F) is categorized under P2P pathway.

### 2.4.3   Gas-to-Gas (G2G)

To decarbonize natural gas, SMR process can be combined with CCS. In this case, methane could be converted to hydrogen without any by-product.

Figure 2-6 shows the overall efficiency for different hydrogen economy pathways. Low overall efficiency can be expressed as one of the major barriers against hydrogen economy. For instance, P2F efficiency is less than 30%, which is too low in comparison with that of BEVs.
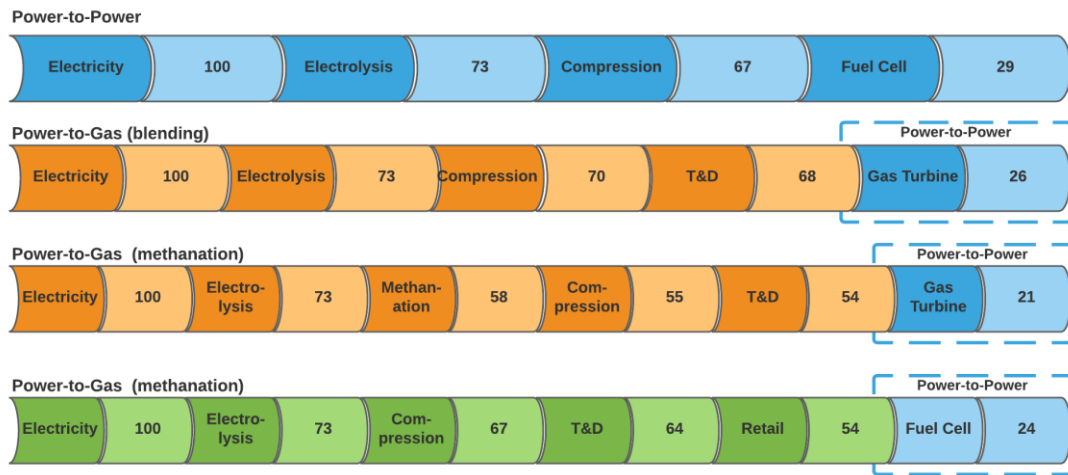


**Figure 2-6 - Hydrogen pathways overall efficiency** [19]

# 3. Five-year technology selection optimization to achieve specific CO$_2$ emission reduction targets

## 3.1 Introduction

Greenhouse Gas (GHG) emissions and the climate change challenge they may cause are the concern of many governments around the world. Despite this concern, worldwide emissions have increased more than 93% from 1970 to 2012 [20]. In 2013, Canada was among the top 10 CO$_2$ emitting countries in the world, with emissions of about 517 megatonnes of CO$_2$ [21]. In that year Canada contributed to 1.6% of global GHG emissions [22]. The province of Ontario had the highest GHG emissions among all provinces in Canada in 2016, only after Alberta [23].

Figure 3-1 shows the GHG emission by sector in Ontario in 2013. As shown in Figure 3-1, the transportation, industry, and building sectors are the top three emitting sectors and accounted for 36%, 28%, and 19% of GHG emissions in Ontario in 2013, respectively.
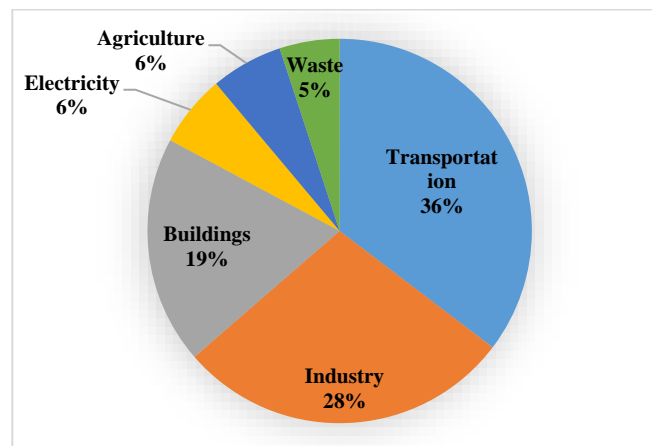


**Figure 3-1. GHG emission by sector in Ontario in 2013** [24]

Replacement of conventional energy sources with renewables is a challenging task. Lower prices of fossil fuels compared to renewable sources of energy, ease of transport and storage, and the already developed infrastructure are the main factors for the widespread use of fossil fuels.

Despite these challenges, there has been a tendency toward investment in renewable energy technologies as reducing the share of fossil fuel generation in the electricity sector is essential for addressing the climate change challenge [25]. There seems to be a consensus on the role of renewable electricity generation capacity in reducing GHG emissions in the literature. Robalino-López et al. [26] stated that an increased share of renewable energies would lead to $CO_2$ emission control while maintaining economic development. Bassi and Baer [27] noted that the development of renewable energies to replace fossil fuels in the energy sector is essential for long-term GHG emission reduction.

High investment cost and intermittency are the drawbacks of the high penetration of renewable energies in energy systems. The intermittency of these systems may impose technical and economic challenges to the grid [28]. Stamford and Azapagic [29] stated that a mix of wind, solar, and nuclear electricity generation is not feasible due to the intermittency of wind and solar and the low flexibility of nuclear. To address these challenges, mathematical models for finding the optimum configuration of hybrid renewable systems have been developed. Different combination of technologies has been investigated in this stream of literature. Haghi et al. [30], for instance, investigated the feasibility of a small hydropower/PV hybrid system for meeting the electricity demand of a grid-connected area in northern Iran. The authors developed an optimization model to determine the

19

system's configuration that leads to the lowest cost for the consumer. Agarwal et al. [31] developed a multi-objective optimization model to find the optimal size of a solar-diesel-battery hybrid system. The hybrid system was supposed to be used in a remote village, and the objectives were lifecycle cost and $CO_2$ emissions. Bala and Siddique [32] developed an optimization model to design and control a solar-diesel-battery hybrid system for an isolated island in Bangladesh. The outputs of the models determined the system's optimized configuration and operation schedule.

Similarly, Hrayshat [33] performed a similar analysis to investigate the techno-economic performance of a photovoltaic-diesel-battery hybrid system for a remote area in Jordan. Belmili et al. [34] investigated the techno-economic performance of a stand-alone wind/solar hybrid system by developing a model for optimal system sizing. In that sense, grid-scale storage and demand-side management can provide options for the grid's stability. Kaabeche and Ibtiouen [35] developed an optimization model for determining the configuration of a wind/solar/diesel/battery hybrid system for meeting the electricity demand in a site in Algeria. Their analysis showed that such a hybrid system is more cost-effective than a diesel generator only. Ma et al. [36] used HOMER software to investigate the feasibility of using a wind/solar/battery hybrid system for meeting electricity demand in a remote island. González et al. [37] developed a model for optimal sizing of a grid-connected wind/solar hybrid system. The model's objective was to minimize the system's lifecycle cost with a demand of matching a local need.

Despite the number of models developed for modeling wind/solar/battery hybrid systems, these are still among the most popular systems. They are still a topic of interest in

the area of energy system optimization. The reason for the popularity of these technologies is their untapped potential, declining cost, available technology, and low environmental impacts.

Another topic of interest in the area of renewable energy systems is the design and optimization of energy storage systems. Energy storage systems have been noted in recent years to address the intermittency of renewable energy systems. Andress et al. [38] stated that the cost efficiency of energy storage systems is critical to realizing the potential and advantages of wind and solar energy generation systems. Energy storage systems can increase the security of supply in energy systems with a high share of renewable energies. Beaudin et al. [28] stated that in the high penetration of renewable energies, the development of storage systems might be of higher priority than investment in new generation capacity. Batteries, compressed air, flywheels, pumped hydro and hydrogen are among the known energy storage technologies [39]. Due to its unique characteristics, hydrogen energy storage development has been recognized as a critical storage technology for movement toward 100% clean energy systems.

Hydrogen is an energy carrier that can be used to store energy and has applications in generating heat, power, and fuel in the transportation sector. More investment in renewable energy and producing green power at lower prices makes a great opportunity for low-emission production of hydrogen, a clean alternative for fossil fuels[40]. While fossil fuel-based technologies are dominant for producing hydrogen [40], electrolysis is noted as a technology for using renewable power to generate hydrogen. Andress et al. [38] suggested that wind and solar systems are suitable options for producing hydrogen in developing

countries. Hydrogen production with solar and nuclear power pathways also have the lowest GHG emissions among all hydrogen production pathways [38]. Hydrogen can be used to store large amounts of power for long durations of time [41]. In that sense, hydrogen is an interesting option to be used in renewable energy hybrid systems [42]. Hydrogen has also been suggested as a balancing element for wind and solar electricity systems [43].

Hydrogen can replace fossil fuels in the transportation sector, may be used to generate electricity, and can also be blended with natural gas to form Hydrogen-Enriched Natural Gas (HENG) used in natural gas applications with lower emissions. Hydrogen energy provides the option to use it where we want it, how we want it, and when we want it. This concept is explained in the idea of Power-to-Gas shown in Figure 3-2.
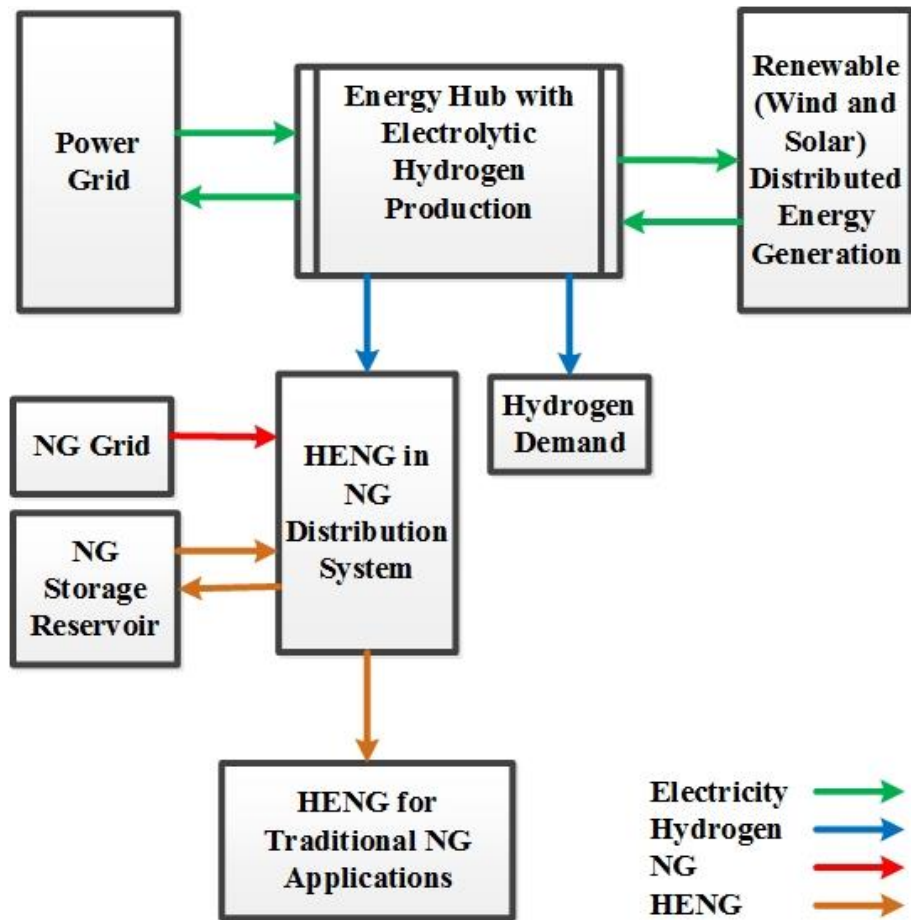
**Figure 3-2. Power-to-Gas block diagram** [44]

In a Power-to-Gas system, hydrogen is generated using surplus grid power or renewable energy. The produced hydrogen is then stored and can be blended with natural gas to form HENG or can be directed to direct hydrogen applications such as fuel cell vehicles. Analysis done by Ameli et al. [45] showed that Power-to-Gas systems are promising options for providing stability to the electricity grid and acting as a link between the natural gas and electricity systems. In that sense, the authors stated that Power-to-Gas could reduce the operating costs of the gas and electricity systems if the capital cost reaches

a threshold of £0.5 million/MW. Hydrogen CHPs are also recognized as promising alternatives for natural gas CHPs for meeting heat and electricity demand while reducing GHG emissions [46]. While research and support policies have been focused on the electricity sector, hydrogen can provide options for reducing GHG emissions in the natural gas sector [46]. Hydrogen has been recognized as a viable alternative for natural gas, particularly in regions with the widespread use of natural gas, which benefit from a developed natural gas infrastructure [46].

As already mentioned, hydrogen is a good match for the wind and solar energy systems. Numerous models can be found in the literature developed to optimize the configuration of hybrid energy systems that use hydrogen as the storage technology. Smaoui et al. [47] developed a mathematical model to find the optimum configuration of a wind/solar/hydrogen hybrid system. The hybrid system is designed to supply the power demand of a desalination unit in Tunisia. Hydrogen was used as a storage technology to control the variations of wind and solar technologies. Kalinci et al. [48] used HOMER to find the optimal configuration of a wind/solar/hydrogen hybrid system for supplying the power demand of an island in Turkey. The optimum configuration of the system was determined using net present cost criteria. Chen et al. [49] developed a multiobjective optimization framework of a wind/solar/hydrogen/battery hybrid system. The objectives considered were cost, electricity efficiency, and energy supply reliability.

The literature compares the cost of battery and hydrogen storage systems; however, it shows a lower cost for a hybrid system that uses battery storage. Al-Sharafi et al. [50] investigated the techno-economic performance of different wind/solar hybrid systems.

Batteries and hydrogen were used as storage to alleviate the intermittency of wind and solar. The results showed that using hydrogen storage instead of batteries doubles the Levelized Cost of Electricity (LCOE) generation. Maleki and Askarzadeh [51] investigated and compared the economic aspects of a wind/solar/battery with a wind/solar/hydrogen hybrid systems for electrification. The authors' findings show that a wind/solar/battery is more cost-effective for electricity generation. Haghi et al. [52] suggested hydrogen and battery storage as complementary technologies in reducing GHG emissions. Mohsin et al. [53] conducted a complete feasibility study for hydrogen production using wind energy. They showed that it is commercially viable to produce hydrogen from wind energy in different sites. Khanmohammadi et al. [54] used the genetic algorithm to optimize a solar-based hydrogen production system. They used exergy efficiency and hydrogen production cost to find the Pareto frontier for such a system. Ishaq et al. [55] modeled a cogeneration system based on producing electricity from wind and hydrogen production. They designed an energy system that can meet the electricity and heat demand for a community of households. An electrolyzer is designed to convert the excess energy into hydrogen which is capable of storing energy for a longer time.

Multiple applications of hydrogen are an essential feature that is tended to be neglected in such analysis. Hydrogen is considered a means for storing power only; meaning surplus power is used to produce hydrogen stored in a tank and then used to generate electricity via a fuel cell. However, the application of hydrogen is not limited to storing electricity. Hydrogen can be used as hydrogen-enriched natural gas (HENG) and fuel for hydrogen vehicles. Hydrogen is particularly suitable for Ontario as it has available surplus

power and extended natural gas transmission infrastructure. Currently, Ontario's surplus power is exported or even curtailed at multiple hours in a year [56]. A report by the Office of the Auditor General of Ontario estimated that around 2 TWh was curtailed in Ontario in 2016 [57]. Walker et al. [58] analyzed using Hydrogen Enriched Natural Gas (HENG) as a way of GHG emission reduction in Ontario. They showed that income generated using HENG is between $100000 to $546000 per year for Ontario. However, with the current capital cost for electrolyzers, such systems are not profitable without governmental help and incentives.

Reviewing the literature concerning the optimal sizing of wind and solar systems shows that the work is focused on finding the optimal configuration of systems for supplying a specific demand. However, the literature lacks work focused on finding the optimal configuration of such systems for reducing GHG emissions. Reviewing the literature on hydrogen energy systems also shows more work is needed for investigating the potential of hydrogen in storing energy and reducing GHG emissions[46][59]. Another critical gap in the literature on energy system optimization topic is the period of modeling. All the reviewed literature has used limited time periods (usually one year) to analyze the system. In other words, models are developed to find the system's optimum configuration based on the system's operation in one year. However, this type of analysis gives minimal insight into the long-term effect of renewable energy development. The developed models found in the literature can provide us with the optimum investment level of hybrid energy systems in the base year. However, if a decision-maker intends to investigate the optimum level of investment in years after the base year, these models will not be helpful anymore. A

configuration optimal for a one-year analysis span may not be optimal anymore if we intend to plan the system for the next 10 or 20 years. A more appropriate model would consider the upcoming years when more and more fossil-fuel-based technologies are replaced with renewable technologies, and GHG emissions reduction targets are more ambitious each year.

In this work, we are developing a mathematical model for finding the optimal configuration of an energy system for reducing GHG emissions in a manufacturing facility. The manufacturing facility uses a natural gas CHP to meet its electricity demand and uses a natural gas burner for its industrial heating demand. Wind, solar, battery, and hydrogen technologies are considered in different scenarios to analyze the cost-effectiveness of renewable technologies in reducing emissions. Considering the facility's energy consumption, wind and solar power can replace fossil fuel-based electricity generation. A battery storage system is supposed to balance the intermittency of these technologies. Wind and solar power and Ontario's surplus power may be used to produce hydrogen, which can be used as HENG or to generate electricity via a fuel cell.

A multi-period optimization model is developed to find the optimum configuration of the system in each period for achieving a specific amount of $CO_2$ emission reduction. The new capacity of each technology added in each period depends on the capacity of technologies in the previous periods and the emission reduction target for future periods. Different scenarios are considered to evaluate the cost-efficiency of technologies in reducing $CO_2$ emissions. The rest of the chapter is organized as follows: Section two describes the model and scenarios developed in this work; Section three presents the results from each

scenario; Section four presents a discussion of the results of different scenarios and compares them. Conclusion and references are presented in sections five and six.

## 3.2 Model description

This section explains the mathematical model used in developing the optimization model. Scenarios considered in this wok are also described in this section.

### 3.2.1 Mathematical Modeling

In this section, the mathematical modeling of the system is described. A detailed linear programming model is implemented to minimize the total cost of the system while meeting the constraints.

#### 3.2.1.1 Objective Function:

The objective function of this problem is to minimize the system's total cost over the periods of planning. The model's outputs would be technology size that leads to the lowest emission reduction cost over all periods of the analysis. The total cost is the sum of capital cost and operation and maintenance (O&M) cost. The capital cost is first distributed through each technology's lifespan. Subsequently, the present value of every single year's capital cost is calculated using cash flow relations. The discount rate and the inflation rate for the cash flow calculations are assumed to be 6% and 2%, respectively. O&M cost includes natural gas, electricity, and operation costs of different technologies.

$$Total\ Cos\ t = \sum_{m,t} Enewcap_{m,t} \times Cap\ Cos\ t_{m,t} \times CRF_m + Electricity\ Cos\ t + NG\ Cos\ t \qquad (3\text{-}1)$$

28

where Enewcap$_{m,t}$ is the new capacity of technology m added in year t, Cap Cos t$_{m,t}$ is the cost of technology m in year t in the form of CAD/kW (which is shown in Table 3-2), CRF$_{m,t}$ is capital recovery factor for technology m and year t, Electricity Cos t is the total cost of electricity and NG Cos t is the total cost of natural gas. The capital recovery factor distributes the capital cost through the lifetime of newly added capacity.

### 3.2.1.2  Constraints

different constraints considered in this work are presented in this section. The first constraint is the demand constraint. Heat and electricity demands must be met through various technologies. The demand, however, doesn't necessarily need to be met with the new capacity. In other words, renewable technologies are added to the already-built technology capacity to reduce GHG emissions. The constraint for supplying the electricity demand is shown below.

$$Eout_{CHP,t,h} + Eout_{wind,t,h} + Eout_{solar,t,h} + Eout_{battery,t,h} \geq D_{electric,t,h} \qquad (3\text{-}2)$$

where Eout$_{CHP,t,h}$, Eout$_{wind, t,h}$, Eout$_{solar, t,h}$, and Eout$_{battery,t,h}$ are the output of electricity from CHP, wind, solar, fuel cell, and battery technologies in year t and hour h, respectively. Also, D$_{electric,t,h}$ is the electricity demand in year t and hour h.

The constraint for supplying the heat demand is calculated using the equation below.

$$Hout_{CHP,NG,t,h} + Hout_{CHP,HENG,t,h} \geq D_{heat,t,h} \qquad (3\text{-}3)$$

where Hout$_{CHP,NG,t,h}$ and Hout$_{CHP,HENG,t,h}$ are the output heat from the CHP using natural gas and HENG in year t and hour h, respectively. D$_{heat,t,h}$ is the industrial heat demand of the facility in year t and hour h.

The emission reduction is calculated as the aggregate of the reduction from supplying electricity and heat demand. In other words, although supplying both heat and electricity demand leads to GHG emissions, the reduction may happen only in one of them or a combination of both, depending on the cost and characteristics of the technologies.

Each technology has a capacity constraint that keeps its outlet less than its capacity. The capacity constraint equation is shown below.

$$Ein_{m,t,h} \times \eta_m \leq Ecap_{m,t} \tag{3-4}$$

where $Ein_{m,t,h}$ is the input of the technology m in year t and hour h, $\eta_m$ is the efficiency of technology m while $Ecap_{m,t}$ is the maximum output capacity of technology m in year t. Table 3-1 shows the input and output for each technology.

**Table 3-1. Inputs and outputs of technologies**

| Technology | Input | Output |
|---|---|---|
| CHP | Natural gas | Electricity |
| Furnace | Natural gas | Heat |
| Wind turbine | Wind flow | Electricity |
| Solar PV panel | Solar radiation | Electricity |
| Electrolyzer | Electricity | Hydrogen |
| Fuel cell | Hydrogen | Electricity |
| Hydrogen tank | Hydrogen | Hydrogen |
| Battery | Electricity | Electricity |

As our model is optimizing the configuration over more than one period, the capacity of each technology can change every year, as shown below.

$$Ecap_{m,t} = Ecap_{m,t-1} + Enewcap_{m,t} \tag{3-5}$$

where $Ecap_{m,t}$ is the capacity of technology m in year t, $Ecap_{m,t-1}$ is the capacity of technology m in year t-1, and $Enewcap_{m,t}$ is the new capacity of technology m added in year t.

The amount of stored energy in storage technology can be calculated using the formula below.

$$Sstored_{s,t,h} = Sstored_{s,t,h-1} + Sin_{s,t,h} \times effStorage_s - Sout_{s,t,h} \tag{3-6}$$

where $Sstored_{s,t,h}$ is the stored electricity or hydrogen in storage technology s in year t and hour h, $Sstored_{s,t-1,h}$ is the stored electricity or hydrogen in battery or hydrogen tank in year h and hour t-1, $Sin_{s,t,h}$ is the input hydrogen or electricity to storage in year t and hour h, $effStorage_s$ is the efficiency of storage s, and $Sout_{s,t,h}$ is the output electricity or hydrogen from storage in year t and hour h.

It should be mentioned that the stored hydrogen or electricity in year t can be used in the next years as well.

The capacity constraint of storage technology is shown below.

$$\sum_{h=1}^{8760} Sin_{s,t,h} - \sum_{h=1}^{8760} Sout_{s,t,h} \leq Scap_{s,t} \tag{3-7}$$

where $Scap_{s,t}$ is the capacity of storage technology s in year t. 8760 is the number of hours in a year.

31

It is assumed that hydrogen can be mixed with natural gas to form HENG. As a technical constraint, the maximum amount of hydrogen that can be added to natural gas is limited to a volume percentage. This constraint is shown below.

$$H_2volume_{m,t,h} \leq HENGlimit \times NGvolume_{m,t,h} \qquad (3\text{-}8)$$

where $H_2volume_{m,t,h}$ is the volume of hydrogen added to the natural gas input in technology m, year t, and hour h ($NGvolume_{m,t,h}$). HENGlimit is the technical limit of the percentage of hydrogen in HENG. The value of $HENGlimit$ is assumed to be 5% in this work, and only up to 5% of the HENG volume can be hydrogen.

The GHG emission from the facility has to be reduced under a specific limit each year, as shown below.

$$Em_t \leq EmLim_t \qquad (3\text{-}9)$$

where $Em_t$ is the total emission of the facility in year t and $EmLim_t$ is the limit of emission in year t. in this work, we assume that the emission should reduce 4.53% each year.

As already mentioned, wind, solar, fuel cell, and battery storage technologies are considered to reduce GHG emissions from the electricity generation section. To achieve GHG emission reduction limit, a share of the electricity demand has to be supplied by these technologies instead of the CHP. However, this share may change at different hours based on the optimal operation of the system. This change leads to a variation in the electricity generation output of the CHP. However, the output of the CHP system can't increase or decrease more than a specific limit compared to the previous hour. To consider the ramp-up constraint of CHP, the constraint shown below is added to the model.

$$Eout_{CHP,t,h} = Eout_{CHP,t,h-1} + RupLim_{CHP} \qquad\qquad (3\text{-}10)$$

Where In $EQout_{CHP,t,h}$ and $Eout_{CHP,t,h-1}$ are the electricity output from CHP in year t and hour h and year t and hour h-1, respectively. Also, $RupLim_{CHP}$ is the ramp-up limit for CHP.

### 3.2.2 Scenarios

This section describes all scenarios modeled and analyzed in this work.

#### 3.2.2.1 Base Case scenario

In this scenario, the industrial manufacturing facility uses a CHP for supplying the electricity demand. Moreover, natural gas is used in a burner to meet the industrial heat demand. Figure 3-3 shows the schematic for the Base Case scenario.
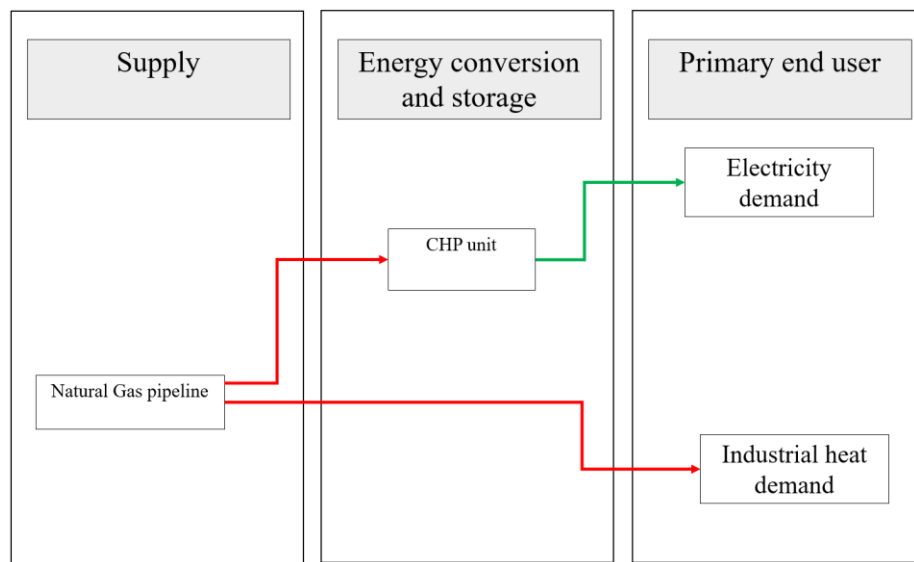


**Figure 3-3. Base Case scenario system configuration**

The hourly electricity demand of the facility is shown in Figure 3-4. The furnace is assumed to be working from 8 AM to 4 PM with a natural gas consumption rate of 4000 m$^3$/hr. The CHP has an output capacity of 4500 kW and a ramp-up rate of 2250kW/hr.
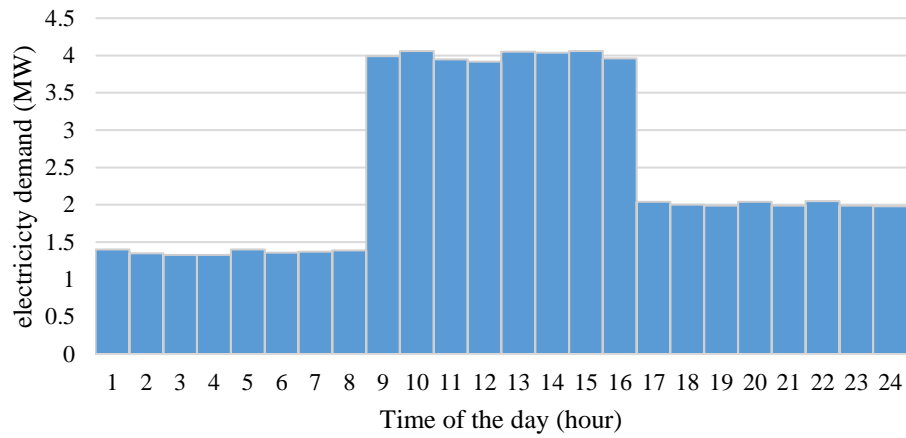
**Figure 3-4. Electricity demand of the facility**

### 3.2.2.2     Scenario 1: Hydrogen

In this scenario, different hydrogen pathways are combined to achieve the annual GHG emission reduction target.

An electrolyzer is used to produce hydrogen using grid power. Produced hydrogen can be added to natural gas to form HENG or go through a fuel cell to generate electricity. Storage tanks are employed to store the generated hydrogen. The system's configuration in this scenario is shown in Figure 3-5.
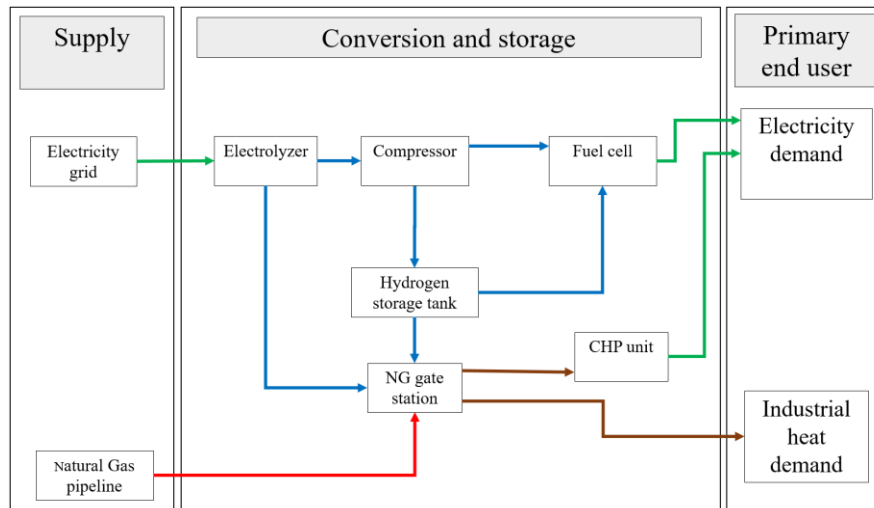
**Figure 3-5. Scenario 1: Hydrogen system configuration**

As can be seen, emission reduction can be achieved by replacing CHP with fuel cell electricity and replacing natural gas in the burner with HENG or a combination of these two.

### 3.2.2.3    Scenario 2: Wind Power

In this scenario, GHG emissions are decreased by replacing a part of CHP electricity generation with wind power. A battery for electricity storage may also be used in the system. In this scenario, the natural gas pipeline supplies all the natural gas demand. Figure 3-6 shows the system configuration for Scenario 2: Wind Power configuration.
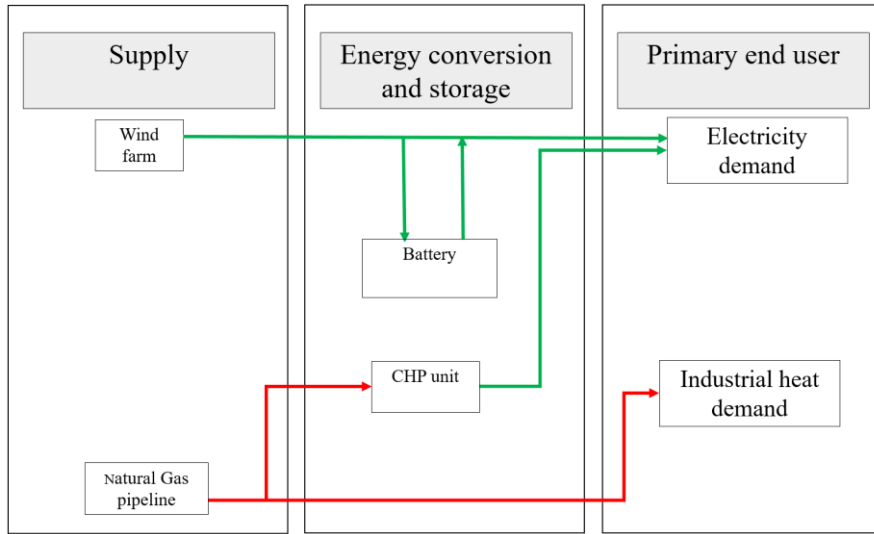
**Figure 3-6. Scenario 2: Wind Power system configuration**

### 3.2.2.4　Scenario 3: Solar power

In this scenario, GHG emissions are decreased by replacing a part of CHP electricity generation with solar power. A battery for electricity storage may also be used in the system. In this scenario, the natural gas pipeline supplies all the natural gas demand. Figure 3-7 shows the system configuration for Scenario 3: Solar power.
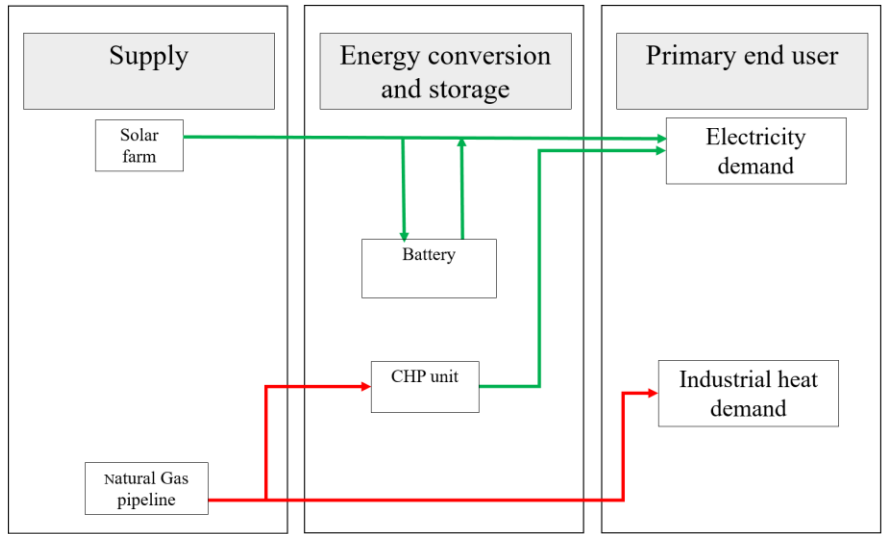
**Figure 3-7. Scenario 3: Solar power system configuration**

### 3.2.2.5    Scenario 4: Wind and Solar power

In this scenario, a combination of solar and wind energy decreases GHG emissions by replacing a part of CHP output power with renewable power. A battery compensates the intermittency of wind and solar energy. Figure 3-8 shows the system configuration for Scenario 4: Wind and Solar power.
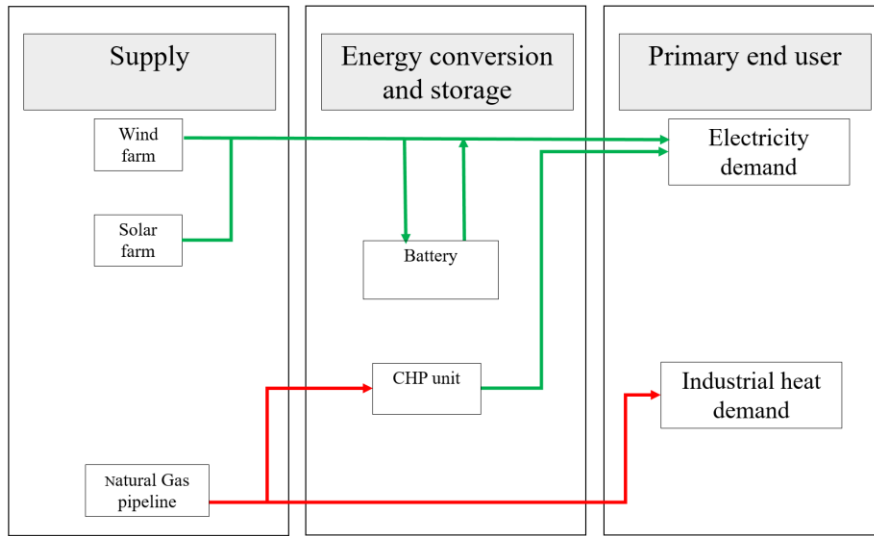
**Figure 3-8. Scenario 4: Wind and Solar power system configuration**

### 3.2.2.6 Scenario 5: Wind, Solar, and Hydrogen

In this scenario, the electricity from CHP is replaced by the electricity from solar panels, wind turbines, or fuel cells. Additionally, electricity can be bought from the grid at HOEP for hydrogen production via electrolyzer. The produced hydrogen can be sent to storage tanks, added to natural gas to form HENG, and used in a fuel cell to generate power. The electricity produced by wind turbines or solar PV can be stored in a battery. Figure 3-9 shows the system configuration for Scenario 5: Wind, Solar, and Hydrogen.
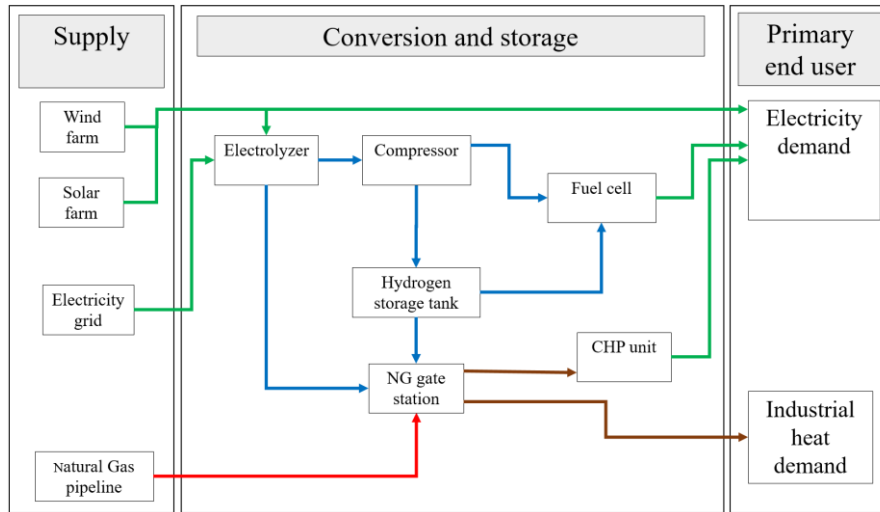
**Figure 3-9. Scenario 5: Wind, Solar, and Hydrogen system configuration**

### 3.2.2.7    Scenario 6: Wind power and grid

In this scenario, it is assumed that electricity from the grid can also replace CHP electricity. However, the global adjustment fees are also considered in the electricity price calculation. Figure 3-10 shows the system configuration for Scenario 5: Wind power and grid.
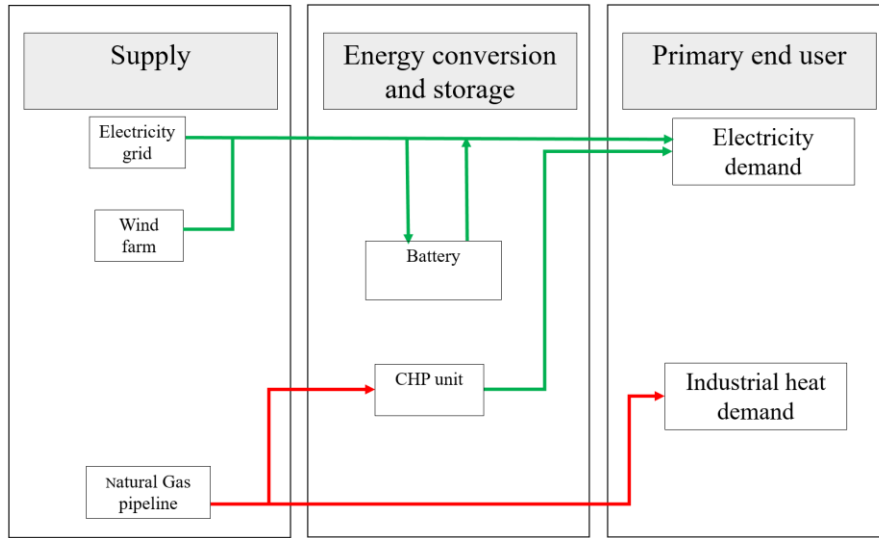
**Figure 3-10. Scenario 6: Wind power and grid system configuration**

It is assumed that in all scenarios, the equipment and machines used in the base scenario are already paid for, and their price is not considered in the cost of emission reduction.

### 3.2.3   Inputs to the model

Table 3-2 shows the cost of technologies considered in this work. All values are in 2017 CAD.

**Table 3-2. Cost of technologies**

| Technology | Capital cost (2017 CAD) | Annual O&M cost |
|---|---|---|
| Alkaline Electrolyzer (CAD/kW) | 1076 [60] | Assumed to be 4% of capital cost |
| Electrolyzer stack replacement | 30% of electrolyzer capital cost | Already included in electrolyzer operation and maintenance cost |
| Wind turbine (CAD/kW) | 1475 [61] | 95 CAD/kW [61] |
| Solar panel (CAD/Wac) | 1.74 [62] | 24 CAD/kW [62] |
| Fuel cell | 4058 [60] | 68 [60] |
| Battery (CAD/ kWh) | 723 [63] | Assumed to be 1% of capital cost |
| Underground storage preparation cost (CAD/m$^3$ Hydrogen) | 0.38 [60] | 0 |
| Compressor | 51605×(Capacity, kg/hr) + 23282 [64] | Assumed to be 4% of capital cost |
| Hydrogen storage tank | 1200 per kg of $H_2$ [64] | Assumed to be 4% of capital cost |

A typical wind data for southwest Ontario is considered for calculating the output of the wind system. The capacity factor of wind power, considering the available data, was estimated to be about 30%. Solar radiation data for Detroit [64] was used to model the solar PV system. The capacity factor of wind power considering that data was calculated to be about 16%. Electricity price is considered in this work has two elements: Hourly Ontario electricity price (HOEP) and global adjustment (GA). Data for HOEP and GA is from the

IESO website [65][66]. The natural gas price is assumed to be 19 cents/m$^3$ based on the values available in [67]. The $CO_2$ emission factor for natural gas is considered to be 0.056 kg/MJ [68].

## 3.3 Results and discussion

This section provides the results of all six scenarios and a comprehensive discussion.

### 3.3.1.1 Results for Scenario 1: Hydrogen

Figure 3-11shows the capacity of energy conversion technologies in each year required in Scenario 1: Hydrogen to achieve the emission reduction target each year.
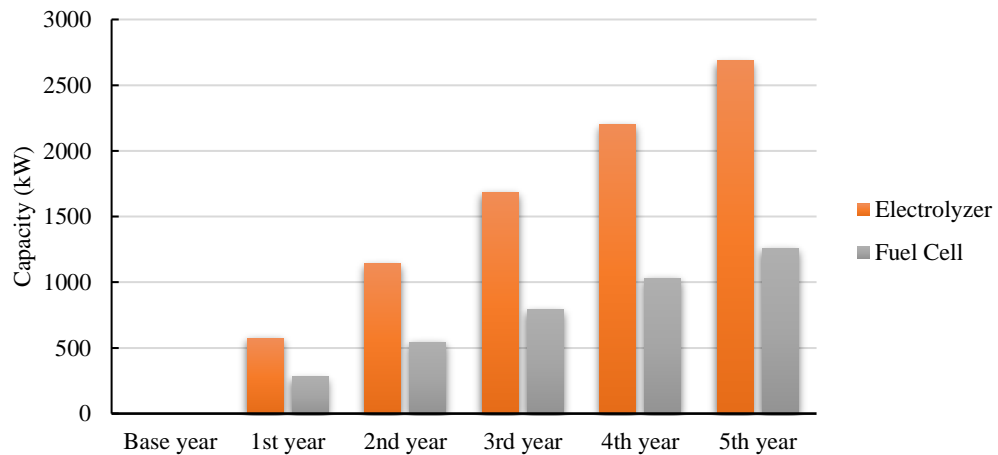


**Figure 3-11. Energy conversion technology capacity for Scenario 1: Hydrogen**

As shown in Figure 3-11, the capacity of both electrolyzer and fuel cell technology increases each year as the emission cap increases. In Scenario 1: Hydrogen, a combination of fuel cell power (to replace CHP power), and HENG are used for reducing GHG emissions. It should be noted that 6-8% of generated hydrogen is added to natural gas each year, and the rest is used in the fuel cell.

Figure 3-12 shows the capacity of energy storage technology (hydrogen storage) in each year required in Scenario 1: Hydrogen to achieve the emission reduction target each year.
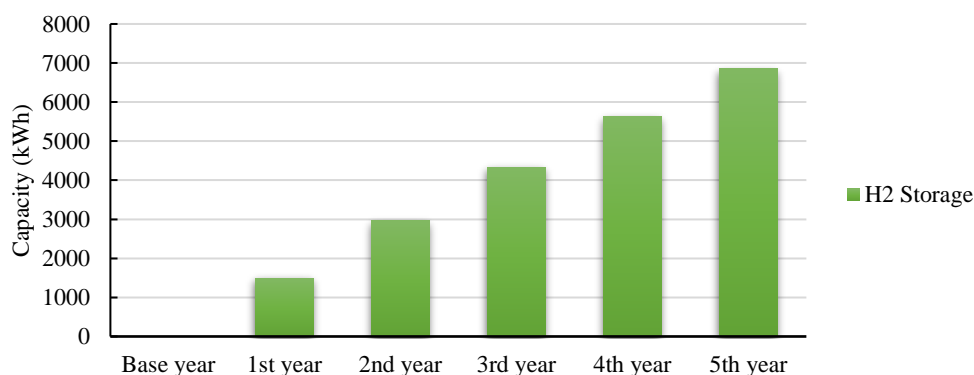


**Figure 3-12. Energy storage technology capacity for Scenario 1: Hydrogen**

Figure 3-12 illustrates the required storage capacity built each year in the 1st scenario. As hydrogen storage is more cost-effective and more efficient, it is preferred compared to batteries.

Table 3-3 shows the emission reduction cost in each year for Scenario 1: Hydrogen. As shown in Table 3-3, the emission reduction cost doesn't increase much from the first year to the 5th year (an increase of 22%). The reason for this small increase is the high potential for using HENG and fuel cell power for replacing CHP output. In other words, the natural gas consumption is so high that replacing each percentage of it with clean power from a fuel cell or HENG needs the same amount of investment. This observation will not exist for wind and solar power generation scenarios as the potential for replacing CHP power output will be limited and needs high energy storage investment. This issue is explained in the following for other scenarios.

The reason for the cost increase in each year in Scenario 1: Hydrogen is then only attributable to the electricity purchase cost. As the need for hydrogen increases, the system needs to buy more power, leading to power purchase at hours with higher prices.

**Table 3-3. Emission reduction cost in each year for Scenario 1: Hydrogen**

| Year | Emission reduction cost (2017 CAD/ tonne of $CO_2$) |
|------|-----------------------------------------------------|
| 1    | 107                                                 |
| 2    | 115                                                 |
| 3    | 120                                                 |
| 4    | 125                                                 |
| 5    | 130                                                 |

Figure 3-13 shows the annual energy cost of the facility in Scenario 1: Hydrogen. The capital cost of the CHP unit is excluded as it is assumed to be built before the study period. It should be mentioned that the costs are in the future value-form, which means annual costs are calculated assuming a discount rate of 8%. Figure 3-13 shows that the fuel cell and electrolyzer are the main contributors to the facility's cost and hydrogen storage has a negligible effect. The utility cost of the facility (electricity and natural gas) has remained constant for the facility over the five years. This means the cost of electricity purchased for producing hydrogen has covered the saved cost from lower natural gas consumption. Comparing Scenario 1: Hydrogen with the base scenario (assuming no capacity addition and an inflation rate of 2%) shows that the total annual cost of the facility increases 5.16%, 10.14%, 14.84%, 19.19%, and 23.22% for year one, two, three, four, and five, respectively.

45
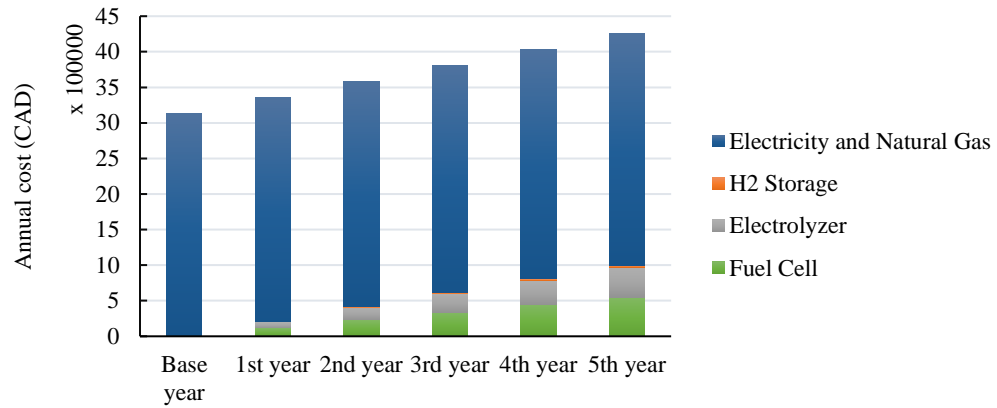
**Figure 3-13. Annual energy cost of the facility in Scenario 1: Hydrogen**

### 3.3.2 Results for Scenario 2: Wind Power

Figure 3-14 shows the Wind power capacity each year for Scenario 2: Wind Power. Figure 3-14 shows that wind power capacity increases with the emission reduction target increase in each year.
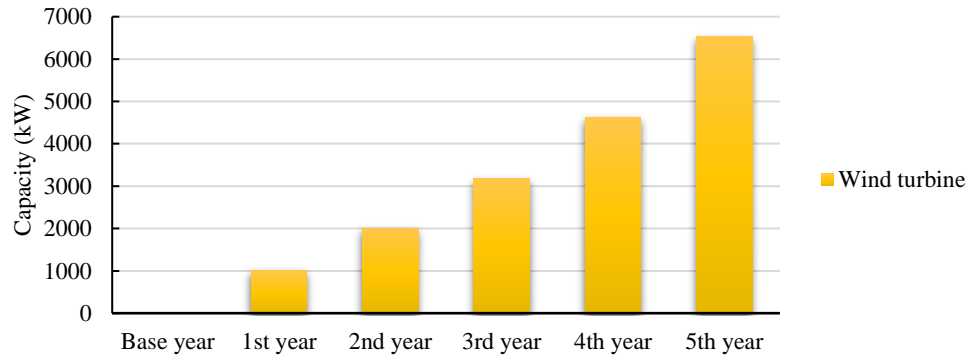


**Figure 3-14. Wind power capacity in each year for Scenario 2: Wind Power**

Another point that can be seen in Figure 3-14 is that the required new capacity in each year increases with time. In other words, to achieve a 4.53% emission reduction in the 1st year, 1003 MW new wind turbine capacity is needed, while in the 5th year, this amount

46

increases to 1916 MW. The reason for this increase can be related to the wind capacity factor. We are assuming that the wind profile stays the same. Generating renewable power to replace CHP power is the only pathway for reducing GHG emissions in this scenario because no hydrogen is blended with natural gas to reduce the emission from the heating demand. As the objective function of the optimization problem is minimizing the cost, the developed wind power capacity is large enough to reduce emissions by generating renewable power at times of high wind speed. However, the emission reduction needs to be reduced each year, and the potential of wind power generation in hours with high-speed wind is already used in previous years. As a result, wind power generation in hours with low-speed wind is required. Generating the same amount of renewable power in low-speed wind hours needs more generating capacity than hours with high-speed wind. As a result, the need for new generation capacity increases each year, although the emission reduction percentage is unchanged.

Figure 3-15 shows the energy storage (battery) capacity in each year for Scenario 2: Wind Power. As shown in Figure 3-15, the developed battery capacity in years 1, 2, 3, and 4 is very small compared to the electricity demand (average of about 2500 kWh). The minimum electricity demand of the energy system is around 1300 MW. In the first year, the required wind capacity is less than the minimum demand, and the electricity produced by the wind turbines at each hour is used to replace CHP output. As the required wind turbine capacity increases in the $2^{nd}$ and $3^{rd}$ years, more storage capacity is added to the system to store the surplus electricity in hours when the generated wind power exceeds the demand. Until the $4^{th}$ year, the wind power capacity is still lower than the CHP capacity (4.5 MW).

47

However, the wind power capacity in year 5 is higher than the CHP capacity and maximum electricity capacity. As a result, there would be hours when the generated wind power would exceed the demand. As a result, there is a drastic increase in the battery storage capacity to store that electricity to reduce the needed new wind power capacity.
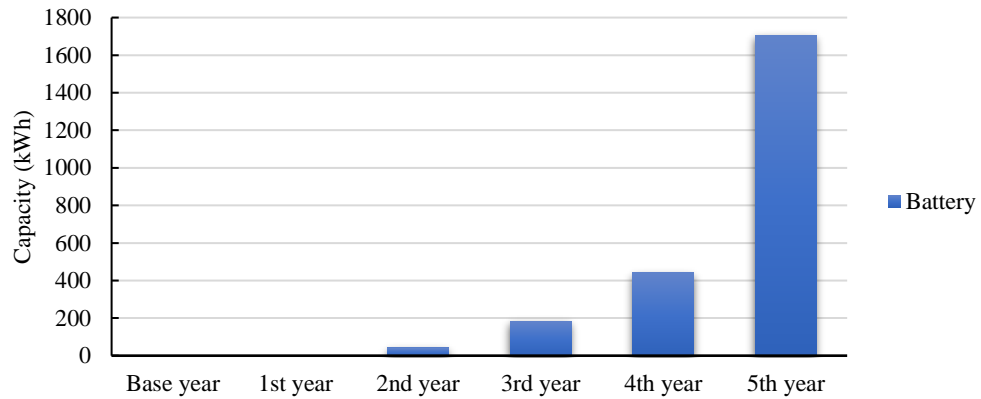


**Figure 3-15. Energy storage (battery) capacity in each year for Scenario 2: Wind Power**

Table 3-4 shows the emission reduction cost each year for Scenario 2: Wind Power. As shown in Table 3-4, the emission reduction cost from year 3 to year 4 and from year 4 to year 5 increases 102% and 85%, respectively. This considerable increase shows the limited potential of wind power for reducing $CO_2$ emissions at low costs. If the emission reduction targets are met with wind power, the price increases drastically when the system requires investing in energy storage capacity (years 4 and 5 in this case).

**Table 3-4. Emission reduction cost in each year for Scenario 2: Wind Power**

| Year | Emission reduction cost (2017 CAD/ tonne of $CO_2$) |
|------|----------------------------------|
| 1    | 44                               |
| 2    | 69                               |
| 3    | 125                              |
| 4    | 253                              |
| 5    | 467                              |

Figure 3-16 shows the annual energy cost of the facility in Scenario 2: Wind Power. Figure 3-16 shows that battery storage costs are minimal compared to wind power costs. The natural cost of the facility decreases each year, as shown in Figure 3-16. The reason for this decrease is replacing CHP power output with wind power. In the 5th year, the facility would pay 21% less on fuel. Figure 16 shows a 2.42%, 4.96%, 9.03%, 15.21%, and 26.82% increase in annual cost compared to the base year in years one, two, three, four, and five, respectively.
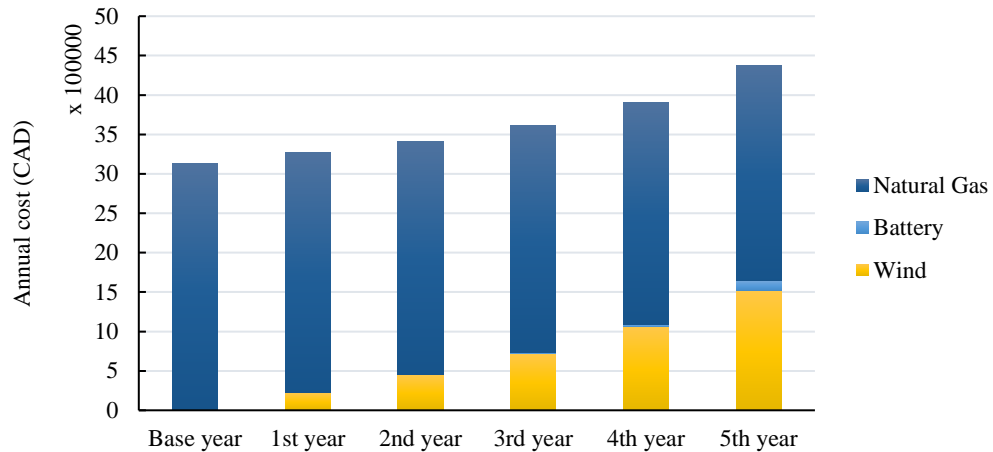
**Figure 3-16. Annual energy cost of the facility in Scenario 2: Wind Power**

### 3.3.3 Results for Scenario 3: Solar power

Figure 3-17 shows the solar power capacity in each year for Scenario 3: Solar Power. As expected, the capacity must be increased to achieve more emission reduction. As can be seen, the required new capacity increases every year except for the 5th year. The reason for this observation can be explained using Figure 3-18.
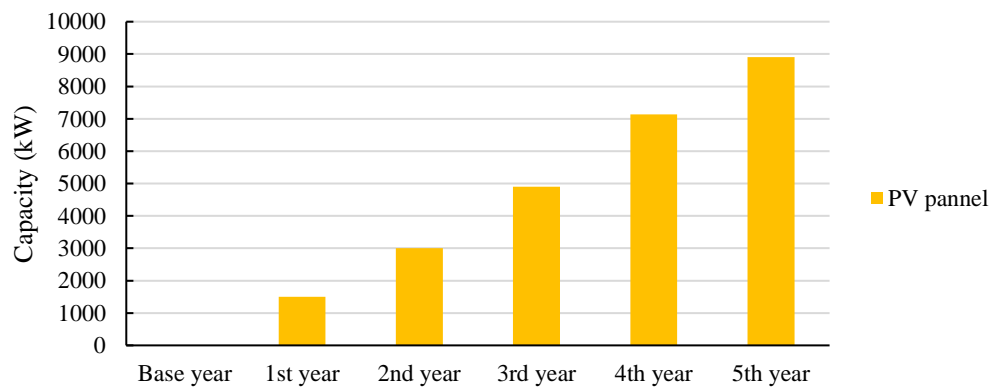


**Figure 3-17. Solar power capacity in each year for Scenario 3: Solar Power**

50

Figure 3-18 shows the energy storage (battery) capacity in each year for Scenario 3: Solar Power.
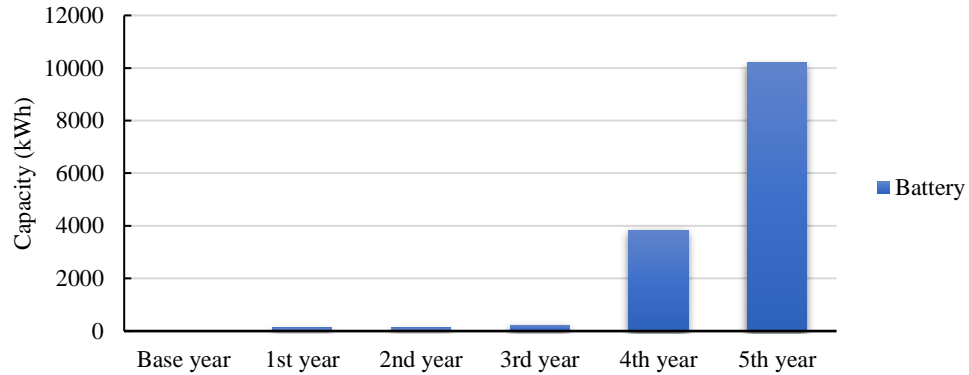


**Figure 3-18. Energy storage (battery) capacity in each year for Scenario 3: Solar Power**

In the first two years, the capacity of PV panels is less than the maximum capacity. Additionally, the maximum demand happens at the same time with maximum solar irradiation (from 8 AM to 4 PM), so there is a low potential for taking advantage of the battery. Even in the 3rd year, the optimum capacity of solar PV panels is not much higher than maximum demand. Therefore, investing in batteries in the $3^{rd}$ year is not rational as solar PV power output can replace enough CHP power output to meet emission reduction limits. In the $4^{th}$ year, however, the emission target dictates renewable power generation to be higher than the maximum irradiation. As a result, a large storage capacity is added this year to store surplus power when the renewable power generation exceeds the demand. The same logic exists for the $5^{th}$ year. When the solar system reaches a capacity of about nine MW, adding more PV panels is not necessary. Instead, the priority would be adding more storage capacity to the system. This can be seen in Figure 3-17 and Figure 3-18, where in the

5<sup>th</sup> year, a large new storage capacity is added to the system while the added solar PV capacity is less than the previous year.

Figure 3-17 and Figure 3-18 show that almost no battery storage capacity is developed before the solar PV capacity has reached the maximum demand. However, a large battery storage capacity is added when the solar capacity reaches the maximum demand. This is different from what is observed in Scenario 2: Wind power when the large storage capacity is developed only when the wind power capacity has exceeded the maximum demand (Figure 3-14 and Figure 3-15).

Table 3-5 shows the emission reduction cost in each year for Scenario 3: Solar Power. Table 3-5 shows the emission cost reduction increases of 126%, 54%, and 14% from year 2 to 3, 3 to 4, and 4 to 5, respectively.

**Table 3-5. Emission reduction cost in each year for Scenario 3: Solar Power**

| Year | Emission reduction cost (2017 CAD/ tonne of $CO_2$) |
|------|------------------------------------------------------|
| 1 | 132 |
| 2 | 173 |
| 3 | 391 |
| 4 | 602 |
| 5 | 689 |

Figure 3-19 shows the annual energy cost of the facility in Scenario 3: Solar Power. Figure 3-19 shows the importance of cost of storage in this scenario. As discussed earlier, solar energy requires more storage capacity than wind as it has more intermittency. Figure

3-19 shows a 6.9%, 13.6%, 23.4%, 43.1%, and 64.8% increase in annual cost compared to the base year for years one, two, three, four, and five, respectively.
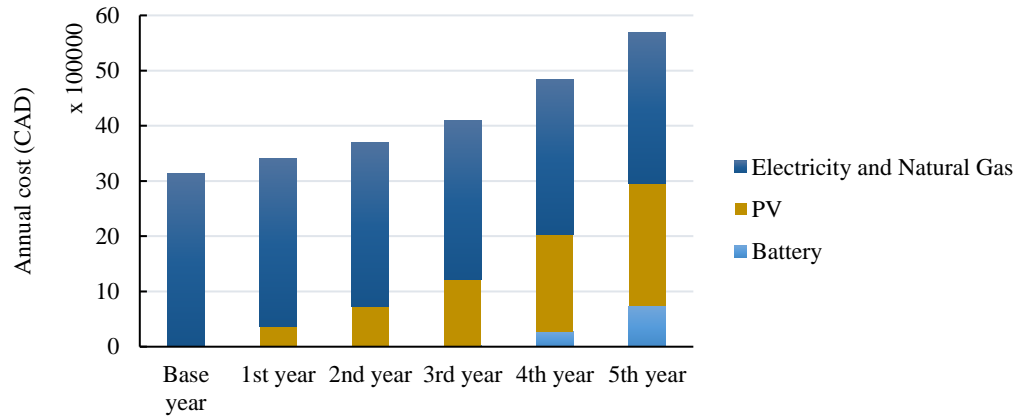


**Figure 3-19. Annual energy cost of the facility in Scenario 3: Solar Power**

### 3.3.4    Results for Scenario 4: Wind and Solar power

Figure 3-20 shows the wind and solar power capacity in different years for Scenario 4: Wind and Solar power. As shown in Figure 3-20, no solar capacity is developed until the 4th year, and all the emission reduction is achieved by replacing CHP output with wind power. The advantage of wind power over solar power is lower investment cost and higher capacity factor in Ontario. The results for Scenario 4: Wind and Solar power are similar to Scenario 2: Wind power in the first three years. As shown in Figure 3-21, the developed energy storage capacity in the first three years is also similar to the values in Scenario 2: Wind power. In the 4th year, the optimum capacity of the wind system capacity reaches around 4000 kW, which is maximum electricity demand. In Scenario 2: Wind power, battery storage capacity was developed at this point instead of more wind power capacity. In other words, storing power in times of surplus renewable power made more economic sense compared to

53

developing more generation capacity. When the wind power capacity reaches 4000 kW in Scenario 4: Wind and Solar power, solar power and battery storage capacity (very small amount) are developed. This observation shows that the development of the solar capacity to capture its high potential is more cost-effective than developing wind capacity to store surplus power.
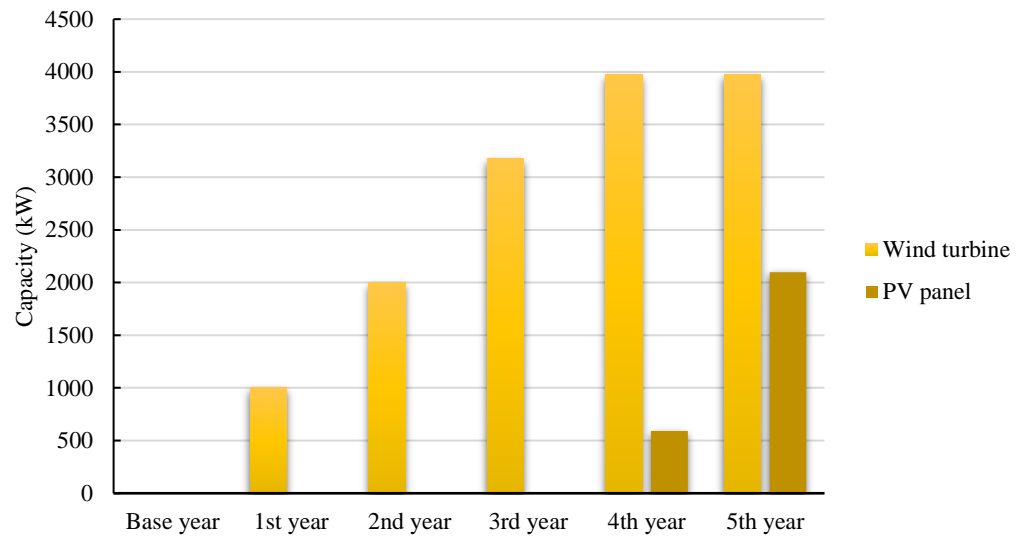


**Figure 3-20. Wind and solar power capacity for Scenario 4: Wind and Solar power**
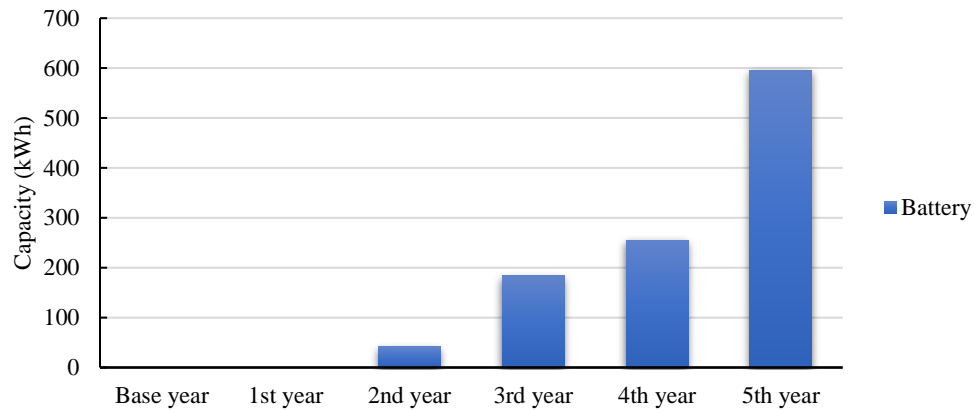
**Figure 3-21. Energy storage (battery) capacity in each year for Scenario 4: Wind and Solar power**

Table 3-6 shows the emission reduction cost in each year for Scenario 4: Wind and Solar power. The emission reduction cost until year 3 is similar to that of Scenario 2: Wind power as the technology selection is the same. However, the emission reduction cost for Scenario 4: Wind and Solar power in years 4 and 5 is lower than scenarios when wind only and solar only technologies were considered (Table 3-4 and Table 3-5).

**Table 3-6. Emission reduction cost in each year for Scenario 4: Wind and Solar power**

| Year | Emission reduction cost (2017 CAD/ tonne of $CO_2$) |
|------|------------------------------------------------------|
| 1 | 44 |
| 2 | 69 |
| 3 | 125 |
| 4 | 199 |
| 5 | 283 |

Figure 3-22 shows the annual energy cost of the facility in Scenario 4: Wind and Solar power. As already stated, the priority is developing wind capacity in the first three years. In $4^{th}$ and $5^{th}$ year, investment in wind turbines stops and solar PV capacity and batteries are added to the system. The increase in annual cost in comparison with the base scenario is 2.4%, 5%, 9%, 14.8%, and 22.4% for years one, two, three, four, and five, respectively.
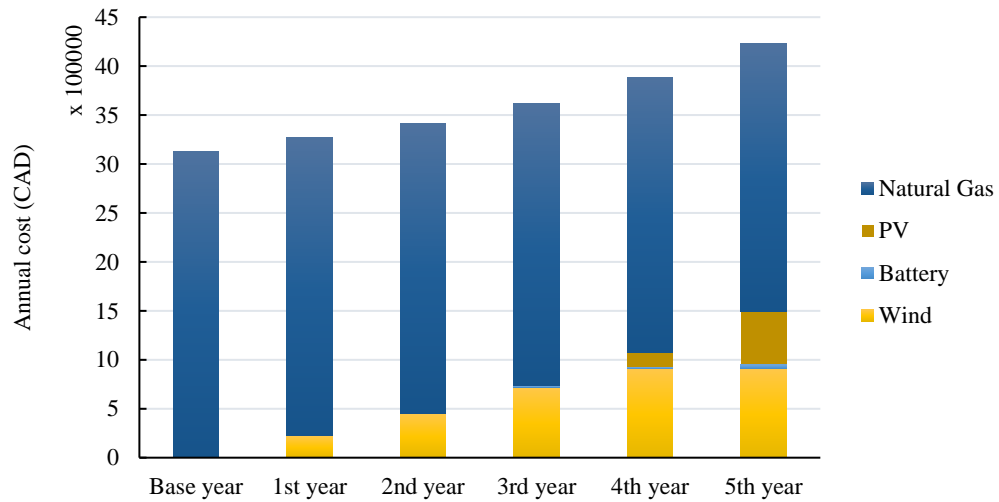


**Figure 3-22. Annual energy cost of the facility in Scenario 4: Wind and Solar power**

### 3.3.5   Results for Scenario 5: Wind, Solar, and Hydrogen

Figure 3-23 shows the energy conversion technology capacity for Scenario 5: Wind, Solar, and Hydrogen.
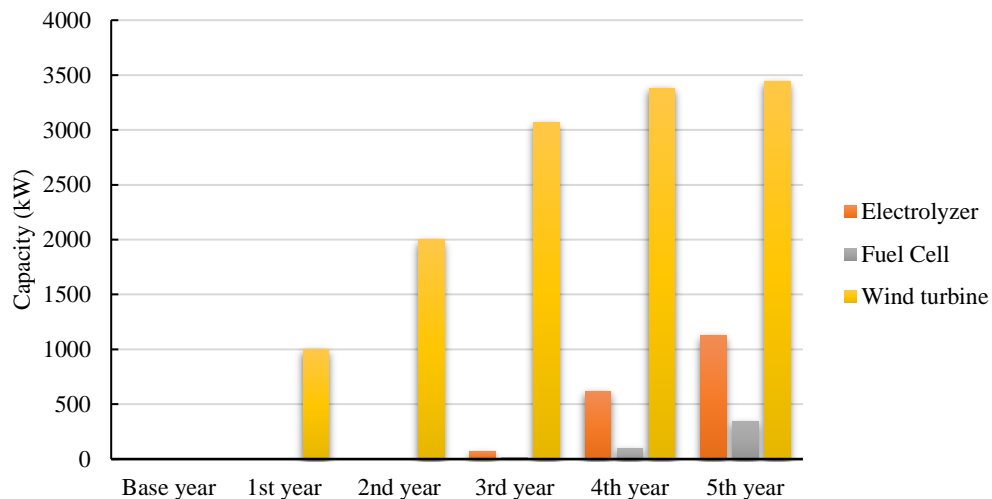
**Figure 3-23. Energy conversion technology capacity for Scenario 5: Wind, Solar, and Hydrogen**

Figure 3-23 shows that almost no hydrogen energy technology is developed until the 3rd year, and a combination of wind turbines and battery storage is utilized for reducing emissions. In the 4th and 5th years, however, the energy system is a combination of wind turbines, an electrolyzer, and a fuel cell.

It should be mentioned that it is supposed that the industrial facility is using a subsidy from the government to buy electricity at the HOEP to produce hydrogen. The electricity bought at this rate is not used directly to replace CHP power output.

Figure 3-24 shows the storage capacity for Scenario 5: Wind, Solar, and Hydrogen. As it can be seen, a high capacity of hydrogen storage should be added to the system to store the hydrogen produced at low electricity price. This hydrogen, then, can be converted to electricity by fuel cells or blended with natural gas to for HENG. In the 5th year, the hydrogen storage would have the capacity of storing eight hours of full-load hydrogen

generation from the electrolyzer. Figure 3-24 shows that the battery storage capacity is negligible compared to hydrogen storage capacity. The system prefers storing energy whether it is inexpensive power from the grid or wind power in the form of hydrogen instead of electricity in a battery.
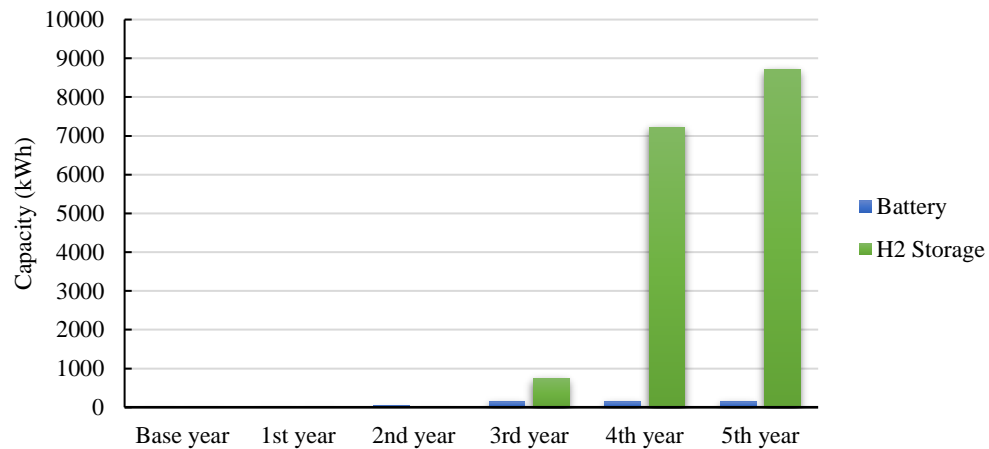


**Figure 3-24. Energy storage capacity for Scenario 5: Wind, Solar, and Hydrogen**

Table 3-7 shows the Emission reduction cost in each year for Scenario 5: Wind, Solar, and Hydrogen. As shown in Figure 3-23, emission reduction is achieved by wind power capacity development in years 1, 2, and 3, and thus the numbers in Table 7 for years 1, 2, and 3 are similar to the costs of emission reduction for Scenario 2: Wind power reported in Table 4 in those years.

**Table 3-7. Emission reduction cost in each year for Scenario 5: Wind, Solar, and Hydrogen**

| Year | Emission reduction cost (2017 CAD/ tonne of $CO_2$) |
|------|------|
| 1 | 44 |
| 2 | 69 |
| 3 | 122 |
| 4 | 135 |
| 5 | 156 |

Figure 3-25 shows the annual energy cost of the facility in Scenario 5: Wind, Solar, and Hydrogen. As shown in Figure 3-25, wind power has the highest share of the cost. But it should be noted that no technology is developed until the 3rd year for emission reduction. To achieve the emission reduction targets in this scenario, annual cost has increased 2.4%, 5%, 9%, 13.6%, and 18.1% in years one, two, three, four, and five compared to the base year.
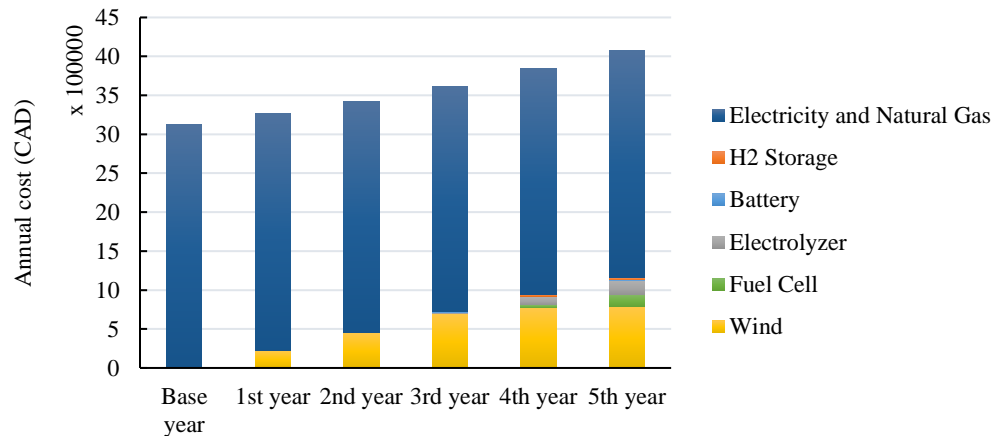


**Figure 3-25. Annual energy cost of the facility in Scenario 5: Wind, Solar, and Hydrogen**

### 3.3.6 Results for Scenario 6: Wind power and grid

Figure 3-26 shows the wind power capacity in Scenario 6: Wind power and grid. In this scenario, grid electricity can be directly utilized to reduce emissions. The grid electricity price is assumed to include global adjustment. Although the facility can buy electricity from the grid to replace its CHP output, wind power capacity is developed to generate renewable power. However, the capacity of wind power generation increases only slightly after the 3rd year staying about 2000 kW. In other words, wind turbines can compete with the electricity grid up to around 2000 kW. After the wind power capacity heats that peak, buying power from the grid is a more cost-effective method of reducing GHG emissions than developing more wind power capacity. No storage capacity is developed in this scenario. The optimum operational strategy for the facility in this scenario is to generate electricity with wind turbine and replace CHP electricity with it and buy electricity at low rates from the grid if there is no wind power available.
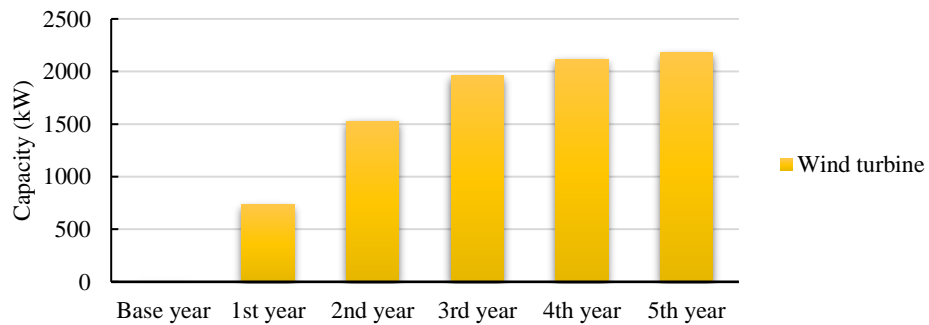


**Figure 3-26. Wind power capacity for Scenario 6: Wind power and grid**

Table 3-8 shows the emission reduction cost in each year for Scenario 6: Wind power and grid. Values in Table 3-8 show that purchasing grid power in combination with

60

developing wind power capacity is more cost-effective in reducing emissions than developing storage technologies or hybrid systems.

**Table 3-8. Emission reduction cost in each year for Scenario 6: Wind power and grid**

| Year | Emission reduction cost (2017 CAD/ tonne of $CO_2$) |
|---|---|
| 1 | 44 |
| 2 | 59 |
| 3 | 74 |
| 4 | 96 |
| 5 | 110 |

Figure 3-27 shows the annual energy cost of the facility in Scenario 6: Wind power and grid. As shown in Figure 3-27, the cost of electricity and natural gas for the facility has increased every year. This increase is due to replacing CHP power output with grid electricity. The cost of the facility increases 2%, 4.3%, 6.9%, 9.8%, and 13.2% in years one, two, three, four, and five compared to the base case, respectively.
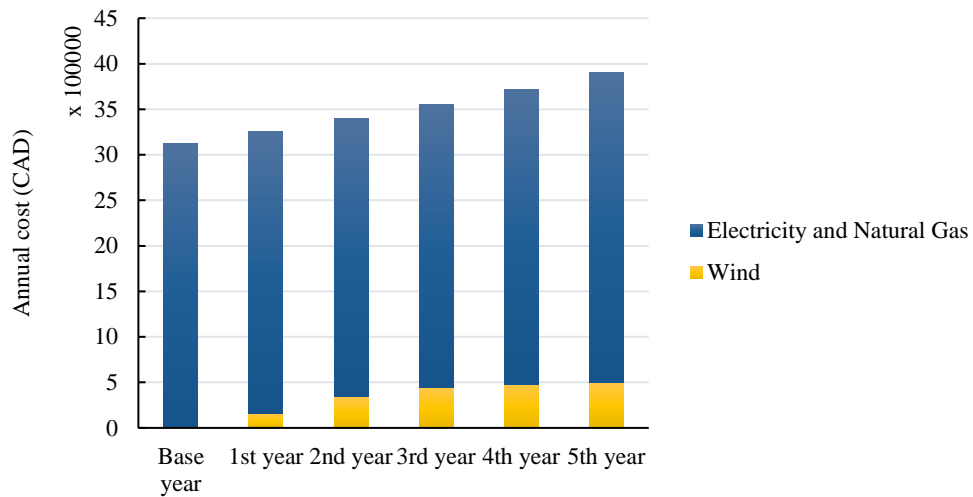
**Figure 3-27. Annual energy cost of the facility in Scenario 6: Wind power and grid**

### 3.3.7 Comparison between different scenarios

This section presents a comparison of the results for different scenarios. Figure 3-28 compares the cost of emission reduction for different scenarios in all years.

Figure 3-28 shows that Scenario 6: Wind power and the grid has the lowest cost among all scenarios. However, this scenario enables the facility to replace its CHP capacity with grid power. While this replacement may seem beneficial for a single facility, widespread replacement of CHP plants with grid electricity may not be viable in a region as it puts too much pressure on the grid and may cause a need to develop new centralized generation capacity.
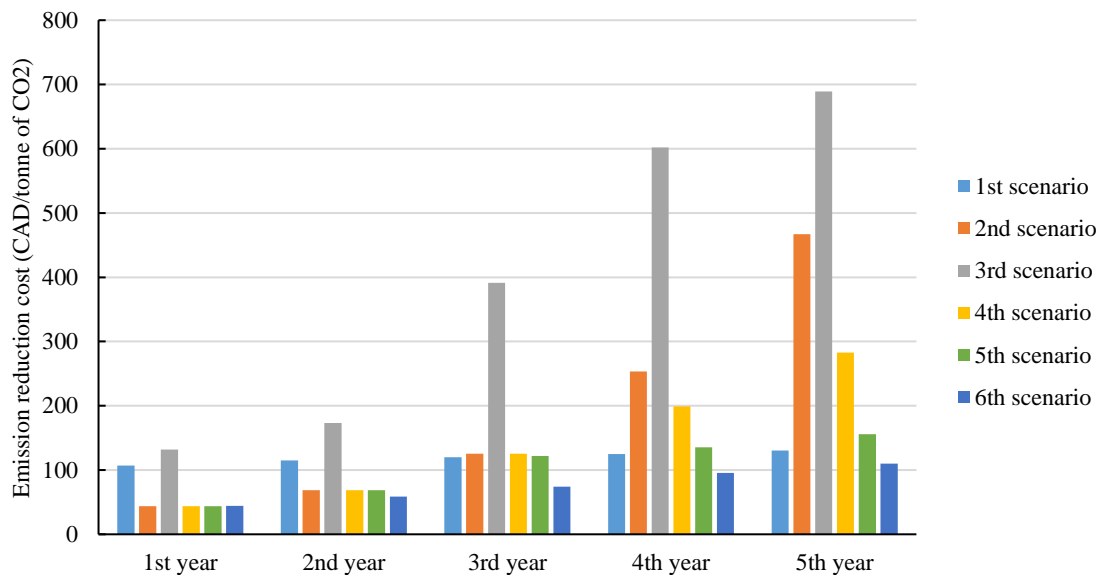
**Figure 3-28. Emission reduction cost of all scenario**

Another point to note is comparing the emission reduction cost for hydrogen and wind technologies. Although the cost of emission reduction with hydrogen only (Scenario 1: Hydrogen) is higher than wind power (Scenario 2: Wind Power) in the first two years, its cost decreases well below the cost of wind power development in the 4th and the 5th year. This decrease shows the potential of wind/hydrogen hybrid systems in reducing GHG emissions in a region.

Figure 3-28 shows that wind power is a more cost-effective technology for reducing emissions in Ontario compared to solar power. Higher capacity factor and lower investment cost have given an advantage to wind power over solar power regarding the cost of emission reduction in Ontario.

Lower required storage capacity is another advantage of wind power systems over solar power systems. In all scenarios, storage has a negligible effect on the annual cost of the

facility except for Scenario 3: Solar power. This means that if a region/country has a grid that can supply the demand and wants to reduce emissions by introducing renewable power to the grid, adding wind power capacity makes more sense than adding solar power capacity. One of the reasons for the advantage of wind power over solar power in our work is the higher wind potential of Ontario compared to the solar potential. This may work the other way in regions with high solar potential.

Wind power looks like a promising option for reducing emissions at a low cost; however, this technology loses its potential after taking the first emission reduction steps. However, the cost of emission reduction using hydrogen technologies doesn't change much through each step. This shows the potential of using hybrid energy systems for reducing GHG emissions. At low emission targets, wind power is a promising option for reducing emissions as it can replace fossil fuel-based electricity generation. On the other hand, hydrogen needs different technologies (electrolyzer, fuel cell, storage) to do that. However, the intermittent nature of wind and solar energy makes them costly technologies for reducing emissions in the long term. Intermittent renewable technologies should be integrated with technologies that can cover their intermittency. Even when two intermittent energy sources are combined (Scenario 4: Wind and Solar power), the emission reduction cost is significantly lower than utilizing single technologies (Scenario 2: Wind Power and Scenario 3: Solar Power).

The review of the literature focused on the development of hydrogen energy systems shows that there is a consensus in the need for financial initiatives for the development of hydrogen energy systems [69][70][71]. This work shows that hydrogen energy systems are

cost-effective in reducing GHG emissions in Ontario as long as industries can receive surplus power at HOEP. In other words, the only incentive hydrogen needs is permission to purchase power at HOEP. It should be noted that the literature has shown that electricity cost has a significant effect on the cost of hydrogen production[44][72][73]. Although some researchers suggest that the penetration of hydrogen in energy systems will be viable in 2030 [59], our analysis indicates that hydrogen is a viable option for reducing GHGs in Ontario right now. This result can be extended to countries/regions that have an extended network of natural gas transmission infrastructure and surplus emission-free power. A vital force in pushing the development of hydrogen technologies is the presence of GHG emission reduction targets [59].

This result can draw policy implications for regions with fossil fuel-based electricity and heat generation infrastructure. If that region is planning to gradually reduce GHG emissions with the least cost, developing wind power plants for the beginning percentages would be the optimal solution.

## 3.4  Conclusion

In this study, a five-year mathematical model for finding the optimal sizing of renewable energy technologies for achieving specific $CO_2$ emission reduction targets is developed. The renewable energy technologies are assumed to be used in an industrial manufacturing facility that uses CHP for electricity generation and natural gas for heating. The optimization model is developed to find the combination of technologies that lead to a 4.53% annual $CO_2$ emission with the lowest cost.

The results derived from the optimization model show that wind power is the most cost-effective technology for reducing emissions in the first and second years, with a cost of 44 and 69 CAD per tonne of $CO_2$, respectively. Hydrogen energy was found to be more cost-effective compared to wind power from the third year on. The cost of $CO_2$ emission reduction doesn't change drastically from the first year to the fifth year as it increases from 107 CAD per tonne of $CO_2$ in the first year to 130 CAD per tonne of $CO_2$ in the fifth year.

Solar power is found to be a considerably more expensive technology compared to wind power for reducing $CO_2$ emissions in all years. The reasons for higher cost of solar power are lower capacity factor (in Ontario), more intermittency (requiring more storage capacity), and higher investment cost. The optimization model showed that a hybrid wind /battery/hydrogen energy system has the lowest emission reduction cost over five years. The emission reduction cost of a wind /battery/hydrogen system increases from 44 CAD per tonne of $CO_2$ in the first year to 156 CAD per tonne of $CO_2$ in the fifth year.

Although developing hydrogen-based energy systems in industry sector can reduce the environmental externalities, the transportation sector has the highest potential of both environmental and health externalities. The next chapters focus more on implementing hydrogen economy in the transportation sector.

# 4. Macro-Level Optimization of Hydrogen Infrastructure and Supply Chain for Zero-emission Vehicles on a Canadian Corridor

## 4.1 Introduction

In recent years, with increased interest, the hydrogen energy storage system has grown widely [74]. Since the beginning of the 20th century, the rapid growth of the economy and industrial revolution globally has brought about the need for more energy resources to cope with the increasing energy demand. A significant portion of current energy resources comes from fossil fuels, which are finite and not environmentally friendly. The use of fossil fuels is a major contributor to climate change, as it causes an excessive increase in anthropogenic greenhouse gas (GHG) emissions [75]. The global emissions from fossil fuel combustion have increased by 90% since the 1970s, reaching over 36.1 Gt in 2014, representing an all-time high emission level [76]. In Canada, reducing GHG inventory has become a national priority, with the target of a 33% reduction in GHG emissions by 2020 and an 80% reduction by 2050 from 2007 levels. The largest contributor to Canadian emissions, accounting for 24%, is the transportation sector. Within this sector, road transportation accounts for 82.5% of national transportation emissions, mainly due to the consumption of fossil fuels [77]. GHG emission is an important issue, but more importantly, the pollution generated from vehicles can negatively impact human health. Lwebuga-Mukasa et al. [78]

found a correlation between traffic volume and the number of asthma patients at the Peace Bridge, a US-Canada border crossing point. Finkelstein et al. [79] used regression to model mortality from natural causes during 1992–2001 concerning chronic pulmonary disease, chronic ischemic heart disease, diabetes, and residence within 50 m of a major urban road or within 100 m of a highway in Ontario, Canada. In this study, it was found the mortality rate advancement period associated with residence near a major road was 2.5 years, while by comparison, the rate advancement periods attributable to chronic pulmonary disease, chronic ischemic heart disease, and diabetes were 3.4 years, 3.1 years, and 4.4 years, respectively. This meant that subjects living close to a major road had an increased risk of mortality. A more recent study by Brauer et al. [80] estimated that there are 21,000 premature deaths attributable to air pollution in Canada each year, nearly nine times higher than the number of deaths due to motor vehicle collisions. The health impact caused by traffic pollution can also cost the government and society a significant amount of money.

There are several cleaner alternatives for energy sources such as wind, solar, geothermal, biomass, and nuclear power. The cost of producing energy from these sources has decreased significantly, making it viable to use widely. However, unlike fossil fuels, the energy produced from these sources would need to be stored in a different form than its source. Batteries and hydrogen Tanks are two promising energy storage systems being focused on currently [81,82]. In the transportation sector, electric vehicles, including battery electric vehicles (BEVs) and fuel cell electric vehicles (FCEVs), play an essential role in reducing emissions and pollution. With a high powertrain energy efficiency, electric vehicles are a promising alternative to conventional internal combustion engine vehicles [83,84]. While

BEVs are penetrating the market for light-duty vehicles with great promise, FCEVs are still not a familiar concept to many consumers [85]. This is largely due to the lack of infrastructure for FCEVs, even though a study has shown that the infrastructure efficiencies of both EV types are very similar [86]. Despite the underdevelopment of FCEV infrastructure, hydrogen fuel cell technologies are promising compared to BEVs, especially for medium and heavy-duty trucks. This is because fuel cell technologies present several advantages such as high driving range due to the much higher energy density by weight of hydrogen, very low refueling time, no battery degradation problems, and the capability of long-term storage of the hydrogen fuel without the hydrogen fuel loss [87]. A large number of truck body types, weight classes, and vocational uses results in a large potential design space [88]. FCEVs also play a significant part in the deployment of the hydrogen economy, a concept that involves the use of hydrogen as a low carbon fuel and has been looked into more recently [89,90].

The deployment of the hydrogen supply infrastructures is a critical step that must be addressed for a successful market transition to FCEVs. Not only must hydrogen refueling infrastructure be constructed, but it must also be commercially viable to encourage the continued expansion of the vehicle market. Even though it is estimated that, by 2030, there will be 15 million FCEVs and 15 thousand Hydrogen Fueling Stations (HFSs) globally [74], the infrastructure for hydrogen refueling is currently still facing many challenges [91]. The infrastructure dilemma is the classic "chicken and egg" conundrum. A refueling infrastructure is required for the mass deployment of FCEVs, but the commercialization of FCEVs is required for investments to be put in refueling stations [92]. Some studies have

69

been conducted on HFS location and infrastructure in various countries. Çabukoglu et al. [93] used a multi-agent, discrete event simulation for HFSs to estimate the number of stations required for different refueling behaviours in Switzerland. Brey et al. [94] analyzed the cost of an initial rollout of FCEVs while considering the perspectives of both the infrastructure investors and the end-users. The authors performed a case study for Seville, Spain, for an initial fleet of 30,000 FCEVs, with a centralized production facility and 10 HFSs. Reuß et al. [95] developed a model to design and analyze all parts of the supply chain, from hydrogen production to refilling, on a nationwide scale in Germany for the year 2050, using a spatial resolution regarding costs, primary energy demand, and $CO_2$ emissions. The authors investigated different scenarios of 25%, 50%, and 75% penetration of FCEVs while considering various technologies such as hydrogen production, storage, transmission, and distribution, to optimize cost and emissions. Liu et al. [96] conducted an economic feasibility analysis of FCEVs in the USA, specifically long-haul trucks, evaluating the total ownership cost. The authors found that for approximately 10% fuel cell truck penetration, they become more competitive in cost and could be economically viable if the vehicle cost and liquefaction cost are reduced to meet the near-term fuel cell technology cost targets. Li et al. [97] conducted a survey on 1072 participants who were asked to select among two FCEVs and one conventional fuel vehicle to calculate the willingness to pay for FCEVs. A range of FCEV configurations was presented and compared to a gasoline vehicle. It was found that the extra value that customers were willing to pay for an FCEV ranged from 20,810 to 95,310 RMB, or approximately 3,000 to 14,000 USD. Hardman and Tal [98] explored the socio-economic profiles, travel patterns, and attitudes of FCEV buyers and

70

compared them to the BEV buyers. It was found that the adopters of BEVs and FCEVs had similarities in gender, level of education, household income, and travel patterns, while their main differences were in age, ownership of previous vehicles, attitudes towards sustainability, and types of home. The results suggested that FCEVs might appeal to consumers who live in homes where they cannot recharge a BEV or install their own charger. Liu et al. [99] studied five scenarios to evaluate the impact of FCEVs on GHG emissions caused by the vehicle fleet in China. They found that, under the best-case scenario, GHG emissions generated by the whole fleet would decrease by 13.9% after introducing FCEVs, and GHG emissions from heavy-duty trucks would decrease by nearly one-fifth.

The North American Superhighway Corridor (NASCO) is one of the most significant corridors in terms of Canada-US-Mexico trade. In Canada, highway (HWY) 401 going from Windsor to Montreal, is a branch of this corridor. There have been some studies on the feasibility of FCEVs in Canada and the logistics of developing hydrogen infrastructures along HWY 401 and in various other parts of Ontario to allow FCEV penetration soon. Hajimiragha et al. [100] developed a comprehensive model to determine robust optimal penetration levels of FCEVs into the transport sector. The authors applied the model to the case study of Ontario, Canada. They found that more than 170,000 FCVs can be introduced into Ontario's transport sector by 2025 while optimizing the technology transitioning cost. Stevens et al. [92] developed a general mixed-integer programming model to optimize the capital cost of hydrogen infrastructure while meeting the demand of a burgeoning hydrogen vehicle market. A case study was conducted, where the model was implemented to develop

an infrastructure across HWY 401 spanning Southern Ontario and Western Quebec, as the number of hydrogen vehicles increases from 10 to 100,000.

Infrastructure logistics is vital at the beginning of the FCEV penetration process. Lin et al. [101] provided a comprehensive review of different HFS location models, including the covering model, the p-median model, the p-center model, and the flow-intercepting model, with each model having different pros and cons. The feasibility of FCEV penetration has been studied thoroughly, but the study of HFS location modeling is still lacking, especially in the case of Ontario, Canada. Motivated by the absence of hydrogen infrastructure studies, this work aims to develop a multi-objective model, based on the p-median model, to determine the optimal sizing and location of the hydrogen infrastructures needed to generate and distribute hydrogen for the HWY 401 corridor in Ontario. Specifically, the Hydrogen Delivery Scenario Analysis Model (HDSAM) is used in this work to estimate the cost of hydrogen delivery and dispensing, and the annual average daily traffic (AADT) is used to estimate the fueling demand based on the number of trucks moving along the corridor. Using the mixed-integer linear programming (MILP) tool in GAMS (General Algebraic Modeling Software), the optimal sizing and location of hydrogen production plants and HFSs along HWY 401 can be determined. Some parameters considered in the model include using electrolyzers as the hydrogen generator, liquid and gaseous hydrogen as fuel, and levels of FCEV penetration being 0.1%, 0.2%, 0.3%, 0.4%, and 1% of the total number of vehicles. The contribution of this chapter is to aid the early-stage transition plan for the conversion of conventional vehicles to hydrogen vehicles in Ontario, particularly along the NASCO, by providing a feasible solution to the infrastructure dilemma posed by the initial

adoption of hydrogen as fuel in the general market. The health benefit cost from pollution reduction is also quantified using MOVES (Motor Vehicle Emission Simulator) to illustrate the potential social and economic incentives of the FCEV market penetration.

## 4.2    Methodology

This chapter develops a mathematical methodology for the primary deployment of a hydrogen supply chain, including hydrogen production plants and refueling stations along highways. Figure 4-1 shows a summary of the methodologies used in this chapter. Our goal is to develop a model for the economic optimization of hydrogen infrastructure; this methodology can be used as a decision-making tool to help stakeholders and investors in hydrogen-related fields. The objective is to minimize hydrogen production and delivery costs to consumers to determine the optimal locations for hydrogen generation plants and HFSs. The information input into the model is a set of possible generation plant and refueling station locations and their capacity levels, variable consumer demand and corresponding locations, and financial data, including the capital, operational, and delivery cost. Since we are building this model for HWY 401 in Ontario, Canada, the hydrogen demand varies for different locations based on the traffic and the number of vehicles.  As explained in the following sections, we estimated the hydrogen demands based on the traffic volume on different parts of HWY 401.
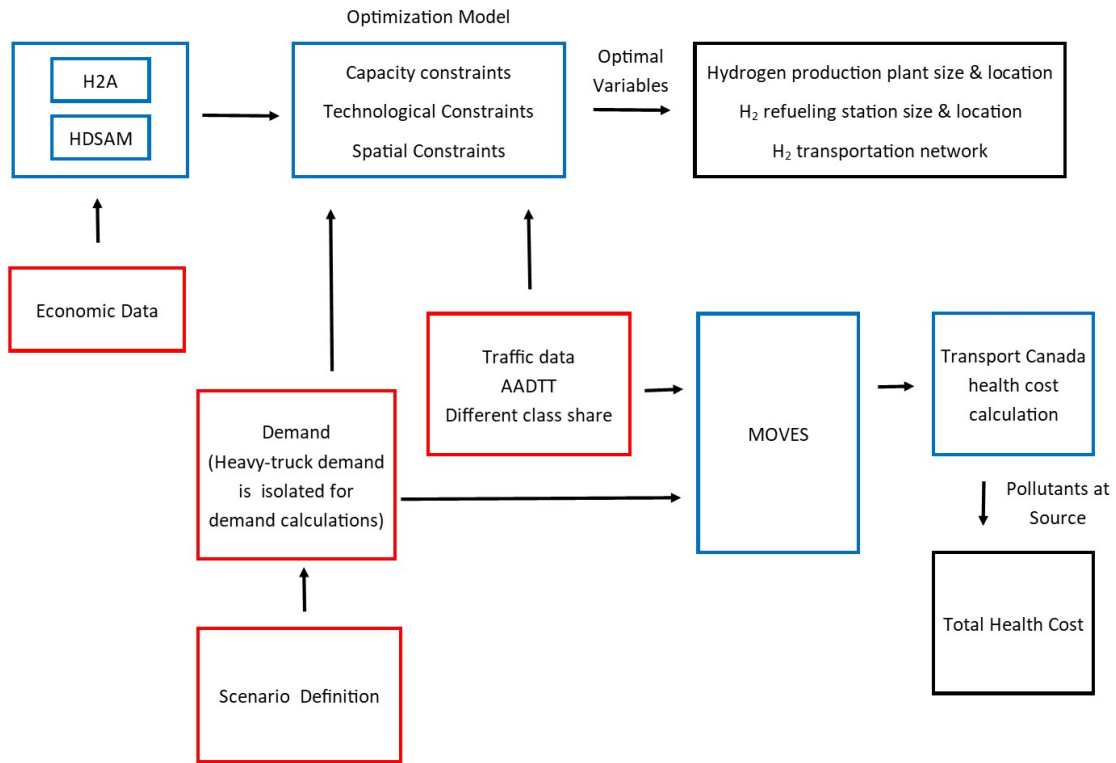
**Figure 4-1. Methodology flowchart of the optimization and selection of node number and locations for hydrogen infrastructure.**

Figure 4-2 presents a very simple overview of the problem. For model development, only electrolysis systems are considered for hydrogen generation. In 2017, around 95% of the Ontario electricity came from non-fossil fuel sources [102]. There is a lot of surplus electricity in off-peak hours due to the high share of intermittent energy sources. These two factors make the electrolysis systems very attractive for hydrogen production. Similarly, all plant-to-station shipments represent compressed hydrogen shipments.

**Figure 4-2. Schematic illustration of problem structure.**

The equation below presents the objective function to minimize hydrogen's delivery and production costs from generation plants to the refueling stations and from refueling stations to the consumers.

$$Min\ Z = Min(\ Production\ cost +\ delivery\ cost)$$

*(4-1)*

Hydrogen delivery cost comprises of the cost of delivering hydrogen from the generation plants to both the station and customers. Hydrogen production cost consists of the capital costs of hydrogen plants and stations, including the investment for electrolyzers, compressors, and storage systems, as shown below.

$$Min\ Z = \sum_i \sum_r cap_{ir}^g.\,\omega_{ir} + \sum_j \sum_q cap_{jq}^s.\,v_{jq} + \sum_i \sum_j C_{ij}\,X_{ij}$$

*(4-2)*

Where X is the hydrogen delivered between plants and stations, and ω and v are the binary variables representing different hydrogen production plants and stations.

There are a set of constraints on capacity and energy balance in the system as follows:

Plant capacity constraint on the delivered hydrogen from plant to station:

$$\sum_{j} X_{ij} \leq \sum_{r} M_{ir} . \omega_{ir} \qquad (4\text{-}3)$$

Station capacity constraint on the delivered hydrogen from station to consumers:

$$\sum_{k} Y_{jk} \leq \sum_{q} V_{jq} . v_{jq} \qquad (4\text{-}4)$$

Energy balance for hydrogen:

$$\sum_{i} X_{ij} \geq \sum_{k} Y_{jk} \qquad (4\text{-}5)$$

Energy demand to be met:

$$\sum_{j} Y_{jk} = D_k \qquad (4\text{-}6)$$

The mathematical modeling is solved using GAMS with CPLEX solver.

### 4.2.1  Corridor demand data

The traffic distribution across the corridor significantly impacts the optimization results. The traffic volumes on HWY 401 are derived from Provincial Highways Traffic Volumes 2016, which provides the annual average daily traffic (AADT), defined as the average twenty-four-hour, two-way traffic for the period January 1st to December 31st [103]. Figure 4-3 shows the average traffic distribution for HWY 401 from Windsor to the Ontario-Quebec border; the blue curve shows the total traffic, and the orange curve represents all truck vehicles (Classes 7, 8, 9, 10) traffic volume.
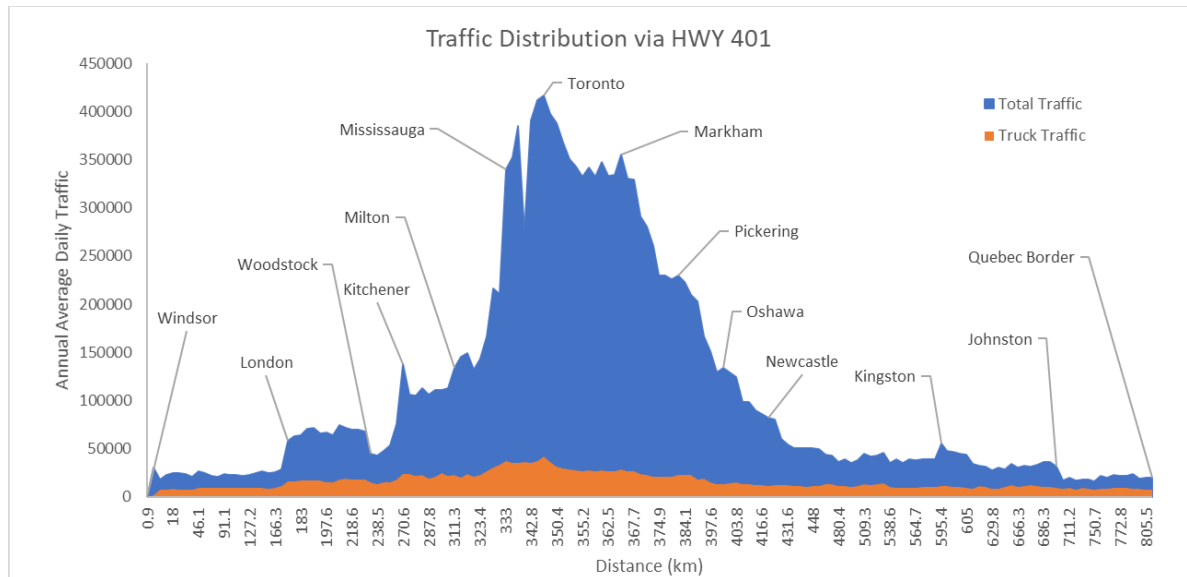
**Figure 4-3. Average daily traffic volume distribution via HWY 401.**

To appropriately estimate the distribution of fuel demand for HWY 401, the traffic volume is estimated within 50 km. Therefore, the total 800 km of HWY 401 is divided into 32-demand zones, each 50 km in length. In other words, the total number of vehicles in each 50 km is aggregated, then the share of heavy trucks is used to estimate the number of trucks in each 50-km zone. Finally, the fuel demand of every 50-km zone is estimated using the average fuel economy of heavy trucks. HFSs are assumed to be at accessible places for drivers on the highway. The ONroute service centers at intervals along HWY 401 are selected as potential places for hydrogen production plants or stations. 'ONroute' is a Canadian commercial operation with a 50-year contract to operate highway rest areas along Highway 400 and Highway 401 in the province of Ontario, with service for fuel stations, rest stations and foodservice operations. The optimization model decides where to build the infrastructure amongst ONroute locations along HWY 401. The company has a long-term

contract and is large enough to invest in the hydrogen economy in the future. This idea is to use private companies' investment rather than government subsidies. Figure 4-4 presents the ONroute locations on HWY 401, which are the possible locations of hydrogen generation plants and refueling stations (ONroute) along the hydrogen corridor.



**Figure 4-4. Possible locations of hydrogen generation plants and refueling stations along the hydrogen corridor.**

### 4.2.2  Hydrogen production data

The majority of the technical and economic information on hydrogen storage and transportation was obtained from various resources related to documents and models from

the Department of Energy (DOE), National Renewable Energy Laboratory (NREL), and Argonne National Lab[104,105]. To assess the financial information of hydrogen production for central and distributed hydrogen plants, we used the Hydrogen Production Analysis model (H2A v3.2018) developed by NREL[106]. Based on the hydrogen demands for trucks, we consider distributed hydrogen production using polymer electrolyte membrane (PEM) electrolyzers. Three distributed hydrogen production cases based on PEM electrolyzers were performed using the H2A v3.2018 model. The information regarding PEM electrolyzers is summarized in Table 4-1.

**Table 4-1. Technical and economic information of the electrolyzer based on the H2A model.**

| Parameter | Value |
|---|---|
| Total Uninstalled Capital (2016$/kW) | 599 |
| Stack Capital Cost (2016$/kW) | 342 |
| Total Electrical Usage (kWh/kg) | 55.8 |
| Effective Electricity Price over Life of Plant (2016¢/kWh) | 7.27 |
| Outlet Pressure from Electrolyser (psi) | 300 |
| Plant Life (years) | 20 |
| Capacity Factor (%) | 97% |

The total hydrogen production costs, including capital, operational, and feedstock costs for different sizes of hydrogen production plants, are summarized in Table 4-2. All numbers are in the 2016 US dollar. The data extracted from H2A and HDSAM are also in the 2016 US dollar.

**Table 4-2. Total production cost of hydrogen for different capacities.**

| Plant size (kg $H_2$ per day) | 500 | 1000 | 1500 |
|---|---|---|---|
| Capital Costs ($ per kg H2) | 0.56 | 0.53 | 0.52 |
| Fixed O&M ($ per kg H2) | 0.91 | 0.67 | 0.57 |
| Feedstock Costs ($ per kg H2) | 4.06 | 4.06 | 4.06 |
| Other Variable Costs ($ per kg H2) | 0.02 | 0.02 | 0.02 |
| Total ($ per kg H2) | 5.56 | 5.28 | 5.18 |

### 4.2.3  Hydrogen storage, delivery, and dispensing data

Figure 4-5 presents hydrogen delivery and storage pathways from hydrogen production plants to refueling stations.
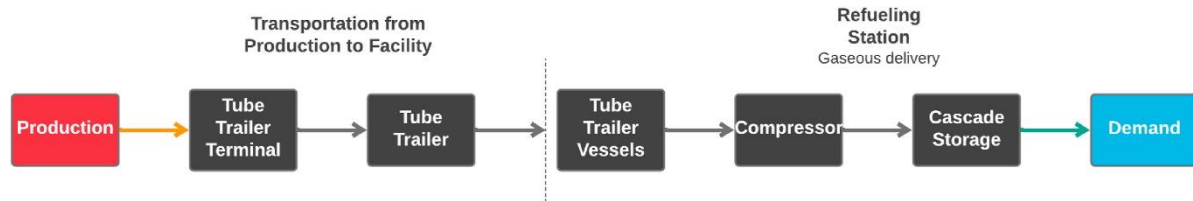


**Figure 4-5. Schematic of hydrogen delivery, storage, and dispensing to the consumers.**

The hydrogen storage, delivery, and dispensing costs are estimated based on the HDSAM developed by Argonne National Lab [107].

Table 4-3 summarizes the key inputs and assumptions that define the scenarios in the HDSAM. Considering tube trailer for hydrogen delivery, cascade storage of gaseous hydrogen, and dispensing pressure of 700 bar, the total cost of storage, delivery, and dispense cost is calculated using HDSAM 3.0 for three different cases as shown in Table 4-4.

**Table 4-3. Hydrogen Delivery Scenario Analysis Model (HDSAM) inputs and assumptions.**

| Parameter | Value |
|---|---|
| $H_2$ Market | Rural |
| Transmission and Distribution mode | Tube-Trailer |
| Storage type | Gaseous Storage |
| Production volume | Low |
| Delivery truck Fuel economy | 6 mpg |
| Useable capacity of individual tube trailer | 1042 kg |
| Number of truck loading compressors | 2 |
| Number of storage compressors | 2 |
| Tube Maximum Operating Pressure | 540 atm |
| Tube Minimum Pressure | 50 atm |
| Vehicle Service Pressure | 700 bar |

**Table 4-4. Hydrogen delivery, storage, and dispensing cost calculation by HDSAM for the capacity of refueling stations.**

| Dispensing Rate (kg H2 per day) | 180 | 350 | 500 |
|---|---|---|---|
| **Compressed Gas H2 Terminal** | **$3.51** | **$3.51** | **$3.51** |
| Compressor | $2.37 | $2.37 | $2.37 |
| Storage | $0.64 | $0.64 | $0.64 |
| Remainder | $0.50 | $0.50 | $0.50 |
| **Compressed H2 Truck** | **$3.66** | **$2.92** | **$2.50** |
| Capital Cost | $3.33 | $2.53 | $2.13 |
| Other O&M | $0.33 | $0.39 | $0.37 |
| **Refueling station** | **$4.84** | **$3.96** | **$3.03** |
| Compressor | $2.26 | $1.83 | $1.50 |
| Storage | $0.51 | $0.52 | $0.36 |
| Dispenser | $0.46 | $0.47 | $0.33 |
| Refrigeration | $0.53 | $0.53 | $0.39 |
| Electrical | $0.25 | $0.14 | $0.10 |
| Controls/Other | $0.82 | $0.47 | $0.34 |
| **Total** | **$12.01** | **$10.39** | **$9.04** |

Instead of assuming a fixed value for the delivery cost, the delivery costs of hydrogen from plants to stations are estimated based on the distance using methodology considered in [92], as shown below.

$$C_{ij} = A \times \text{dist}_{ij} + constant \qquad (4\text{-}7)$$

Where the constant component is the total cost from Table 4-4 and A is calculated based on the gas price, and distance traveled as shown below, and 1042 kg H2/per round is the capacity of a tube-trailer used for hydrogen delivery.

$$A = \frac{(0.75\$/\text{lit}) * (2 \text{ distance/roundtrip})}{(2.6 \text{ km/l}) /(1042\text{kg H}_2/\text{per round})} \qquad (4\text{-}8)$$

## 4.3   Health benefits analysis

To find an estimation of the health benefits from different scenarios, we used MOVES, which was developed by the Environmental Protection Agency (EPA), to assess the amount of emission from on-road and off-road sources. Figure 4-6 shows the inputs and outputs of MOVES model.
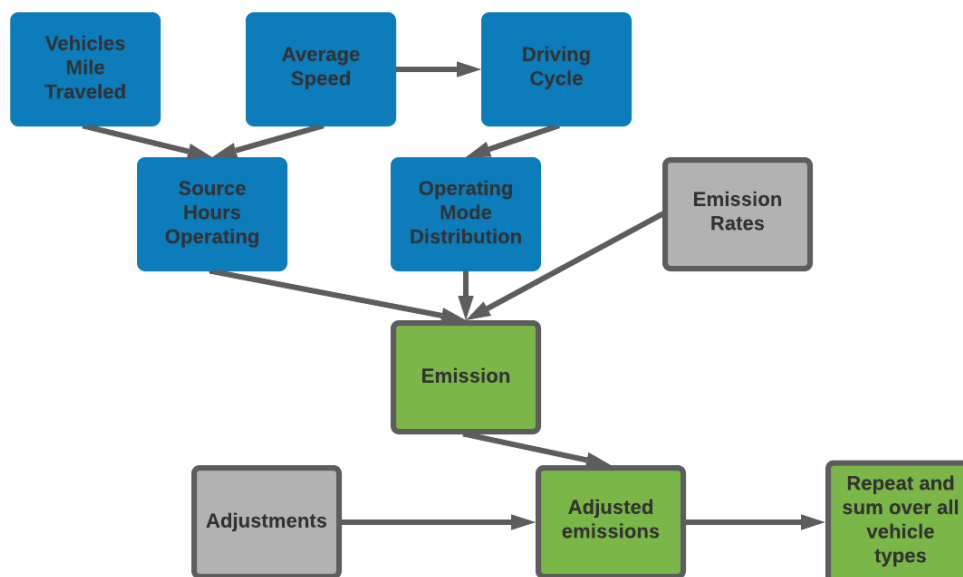


**Figure 4-6 – MOVES inputs and outputs**

As can be seen in Figure 4-6, the inputs for this model are the traffic data driving patterns. The vehicle speed is assumed to be 100 km/h. The traffic count data is extracted from Figure 4-3. Also, the default emission rates and fuel composition for New York, US are used because of the similarity with Toronto weather, fuel, and fleet composition. It should be mention that this assumption might be source of error, and its impact can be investigated in future                                                                                                    works.

To find the impact of all trucks moving along HWY 401 during a year, the number of heavy trucks and the portion of each class are provided to the model. The output of this model, which is the emission of different pollutants, is converted to monetary terms using data from a study conducted by Transport Canada for Ontario territory. The results section will discuss more details of the health benefits analysis.

### 4.3.1 Assumptions and limitations

Some assumptions and limitations of the methodology are outlined as follows:

- Seasonal and hourly changes are not considered.

- The model is not dynamic enough for multiple-year scenarios.

- Electricity price is assumed to be constant. The concept of power-to-gas is based on using surplus electricity at lower costs.

- Storage planning is not modelled because the model is not hourly based.

- The health cost is calculated based on previous pollutant data for all of Ontario, which is an underestimation of health costs due to pollutants. Because HWY 401 passes many high-populated urban and suburban regions, the health cost would be higher than our considerations.

- The vehicles are assumed to move only via HWY 401. This assumption can be true if these trucks are owned by companies transporting goods along the entire HWY 401 corridor.

- As the proposed idea is just for early steps, other transmission modes like liquid H2 and fuel pipeline are not considered.

- BEVs are not considered as they are less competent when it comes to heavy-duty vehicles.

## 4.4 Results and discussion

The optimization model is developed in GAMS. This section includes the output of the model for different scenarios. The location numbers are shown in Figure 4-4. A figure and a table for production capacity and location are provided for each scenario. For all scenarios, tube-trailers are assumed as the transmission mode. Also, the refueling stations utilize a 700-bar cascade dispensing system. There are three options for plant capacity: 500, 100, and 1500 kg/day. Also, there are three options for refueling station capacity: 180, 350, and 500 kg/day. The result of the simulation will be presented for different scenarios.

### 4.4.1 Scenario 1 – 0.1% changeover to fuel cell Class 7, 8, 9, 10 Vehicles

This scenario has 0.1% changeover to fuel cell Class 7, 8, 9, and 10 vehicles from internal engine combustion (ICE) and diesel vehicles. Thus, in this scenario, it is assumed that 0.1% of class 7-10 diesel trucks become hydrogen trucks, which is equivalent to about 8,600 vehicle-kilometres per day. Figure 4-7 and Table 4-5 show the optimal location for scenario 1. According to Figure 4-7 , the output of the optimization model for this scenario shows that for meeting the demand, one production site must be built at location 14. Also, six small size stations should be built at locations 1, 4, 7, 10, 14, and 16. The total demand in this scenario is around 800 kg/day. The dispensing stations are allocated in a way to cover all of HWY 401 without more than 300 km gaps. Also, the production site is located near the midway point of HWY 401, close to Toronto. This allocation reduces transportation costs.

As total demand is less than production and transportation capacity (due to discrete sizing), the capacity factor is less than 100%, leading to a higher overall cost. Also, the dispensing capacity in this scenario is much higher than the dispensing demand because of the 300-km driving range. In other words, constraints make the optimal solution to build more refueling stations to cover the entire highway without gaps of more than 300 kilometers.

**4.4.2  Scenario 2 – 0.2% changeover to fuel cell Class 7, 8, 9, 10 Vehicles**

In this scenario, 0.2% of class 7-10 trucks traveling along HWY 401 become hydrogen trucks. In other words, around 17,000 vehicle-kilometres of transportation demand along HWY 401 depends on hydrogen. The most significant difference between this scenario and the 0.1% Scenario is the production plant location. As shown in Figure 4-7 and Table 4-5, to reduce the transportation cost, it is more economical to build two separate hydrogen production plants with 1000 kg H2/day capacity at locations 4 and 8 and seven refueling stations in small and medium capacities. The hydrogen production capacity factor is equal to that in Scenario 1. Although, in general, the capacity factor increases with an increase in demand, it can be constant in some range because the production sizes are discrete variables. It is worth mentioning that the refueling station capacity factor increases drastically, which reduces the overall cost. Also, utilizing higher station capacity reduces costs due to economies of scale. That is why the overall cost drops drastically compared to the previous scenario.

**4.4.3    Scenario 3 – 0.3% changeover to fuel cell Class 7, 8, 9, 10 Vehicles**

Figure 4-7 and Table 4-5 show the optimal location for the third scenario, in which it is assumed 0.3% of trucks become hydrogen trucks, corresponding to 26,000 vehicle-kilometres of trucks along HWY 401. Two hydrogen production plants at locations 12 and 16 are required to produce the required hydrogen for this scenario. Also, seven refueling stations are required at locations 1, 3, 6, 9, 12, 14 and 16. The highest capacity of refueling stations must be built at location 6. The notable feature of this scenario is supplying one station using two production plants. As can be seen in Figure 4-7, the capacity of west side production is compensated with some of the other production site capacity. This proves the importance of weekly, daily, and hourly planning for the energy network. As expected, the capacity factor increases as the demand increases. In this scenario, both production and refueling stations operate almost in full capacity. In addition, both production and refueling stations utilize higher capacities. This results in a lower overall cost than previous scenarios.

**4.4.4    Scenario 4 – 0.4% changeover to fuel cell Class 7, 8, 9, 10 Vehicles**

Figure 4-7 and Table 4-5 show the results for the scenario in which the target is converting 0.4% of heavy-duty trucks, equivalent to around 34,600 vehicle-kilometres, to hydrogen trucks. The model shows a requirement for building three hydrogen electrolysis plants at locations 1, 8, and 16 in order to meet the demand. Seven refueling stations should be built at locations 1, 5, 6, 8, 12, 13, and 16, from which six stations have the highest defined capacity. The optimal design of this energy network shows an increase in production and dispensing capacity because constructing higher-capacity infrastructures is more economical

due to economies of scale. Compared to the 0.3% Scenario, the hydrogen production, transportation, and dispensing costs drop by a small margin because the capacity factor does not change with an increase in capacity (it has reached the maximum value). The only change in overall cost is due to economies of scale, especially in production; however, the highest share of production cost is related to electricity cost and stack cost, both scaled linearly. In other words, by increasing the capacity, the stack cost and electricity cost per kg of H2 does not change. The balance of plant (BOP) cost is the source of the small change in the overall cost. That said, increasing the market share does not change the per kg cost of dispensed hydrogen unless the production volume of components reaches more significant amounts, which is not achievable in mid-term planning.

**4.4.5    Scenario 5 – 1% changeover to fuel cell Class 7, 8, 9, 10 Vehicles**

As discussed previously, the change in overall cost per hydrogen unit does not change with small increases in market share targets. Therefore, some steps were skipped, and a logical target would be hydrogen trucks reaching 1% of the market share. In the developed model, that means the hydrogen would fulfill 86000 vehicle-kilometres demand in this scenario. The results are shown in Figure 4-7 and Table 4-5. In this scenario, almost all candidate locations are selected to be refueling stations because of high demand. Five 1500-kg $H_2$/day and one 1000-kg H2/day production sites are required to meet the total demand, which is around 8100 kg H2/day. Also, sixteen 500-kg $H_2$/day and one 180-kg $H_2$/day refueling station must be built. This scenario shows close to the maximum demand that can be met using such energy network design. More demand is not feasible with this proposed design

because with building the highest capacity stations (500-kg H2/day stations) in all candidate locations (19 locations), the maximum achievable dispensing capacity is 9500 kg $H_2$/day. Therefore, a 2% target is not achievable unless the number of refueling locations or the maximum refueling station capacity increases. The transmission mode must change for higher dispensing capacity as there are limitations with tube-trailer trucks.

It should be noted that although the tube-trailer is the best transmission mode option in the first stage of hydrogen economy development, it is not practical in high transmission capacities. Our work aims to design a system for the first stage toward establishing a hydrogen economy, so liquid hydrogen trucks are not considered. Also, in most scenarios, some refueling stations are located on the other side of the highway to the production plant. Therefore, although the provided model only considers tube-trailers and not pipelines as a transmission mode, it is likely that implementing a pipeline in such locations would reduce the overall cost.

**Table 4-5. Summary of results for all scenarios. Scenario 1: 0.1% changeover, Scenario 2: 0.2% changeover, Scenario 3: 0.3% changeover, Scenario 4: 0.4% changeover, Scenario 5: 1% changeover**

| Location | Scenario 1 | | Scenario 2 | | Scenario 3 | | Scenario 4 | | Scenario 5 | |
|---|---|---|---|---|---|---|---|---|---|---|
| | Production | Refueling | Production | Refueling | Production | Refueling | Production | Refueling | Production | Refueling |
| 1 | | 180 | | 180 | | 180 | 500 | 500 | | 500 |
| 2 | | | | | | | | | | 500 |
| 3 | | | | | | 350 | | | | |
| 4 | | 180 | 1000 | 350 | | | | | 1500 | 500 |
| 5 | | | | | | | | 500 | | 500 |
| 6 | | | | | | 500 | | 350 | | 500 |
| 7 | | 180 | | 180 | | | | | | 500 |
| 8 | | | 1000 | 180 | | | 1500 | 500 | | 500 |
| 9 | | | | | | 350 | | | | 500 |
| 10 | | 180 | | 180 | | | | | | 500 |
| 11 | | | | | | | | | 1000 | 500 |
| 12 | | | | | 1000 | 350 | | 500 | 1500 | 500 |
| 13 | | | | 350 | | | | 500 | | 500 |
| 14 | 1000 | 180 | | | | 350 | | | 1500 | 500 |
| 15 | | | | | | | | | 1500 | 500 |
| 16 | | 180 | | 350 | 1500 | 350 | 1500 | 500 | | 180 |
| 17 | | | | | | | | | | 500 |
| 18 | | | | | | | | | | |
| 19 | | | | | | | | | 1500 | 500 |
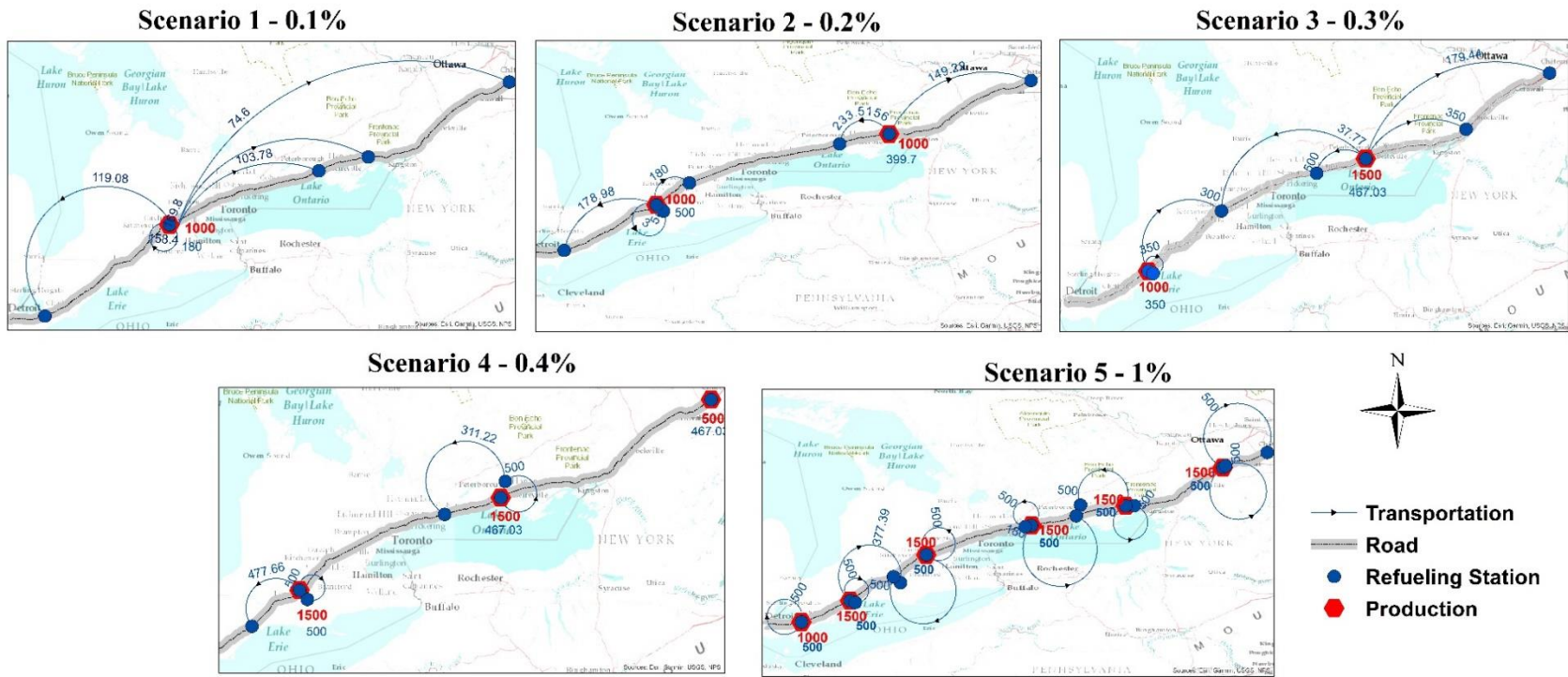
**Figure 4-7. The model output for all market penetration scenarios of Class 7, 8, 9, and 10 vehicles from 0.1% to 1% market share.**

### 4.4.6    Different scenarios comparison

Comparing all scenarios, it can be concluded that allocating production plants and refueling stations depends on the project's market-share goal. For instance, comparing scenarios 1 and 2, one can see that an optimal allocation for the lower market share (scenario 1) is not an optimal location for scenario 2. Specifically, location 14 (ONroute Cambridge South) is optimal for building the production plant and refueling station in scenario 1, but it is not an optimal option in scenario 2. Hence, investors' decisions on the final goal of market-share can change the optimal allocations. Also, there are some similarities in all scenarios. First, the optimal size is always less than the demand, and also as high as possible. That is, to meet a 2500 kg/day demand, the optimal production size would be one 1500 kg/day plant and one 1000 kg/day demand, rather than two 1000 kg/day demand and one 500 kg/day demand. The second similarity between scenarios is full coverage of corridor demand by building multiple refueling stations in all areas from Windsor to Montreal. This is due to the range constraint that is added to the model. And the last similarity is building refueling stations close to all production plant stations. This feature will reduce delivery costs.

### 4.4.7    Total costs analysis

Figure 4-8 shows how the cost of hydrogen production, delivery, and dispensing changes with increasing market share. As discussed before, with an increase in market share up to 0.3%, the cost of 1 kg H2 reduces drastically because of the increase in capacity factor. Achieving 0.3% of the market, the system can be designed with almost maximum capacity factor. Acquiring more market share, the reduction rate decreases. In this share range, the

91

reduction happens because of economies of scale. It should be mentioned that in long-term planning, lower costs would be achievable due to the higher production volume of components. However, in the short term, the only possible source of cost reduction is utilizing surplus power for hydrogen production. Such analysis requires a dynamic hourly-based optimization model [10].
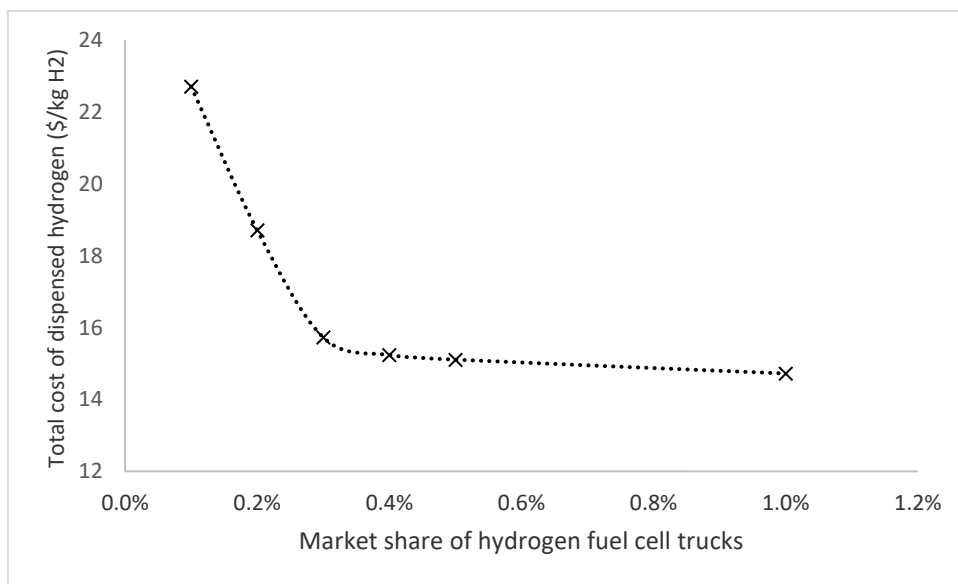


**Figure 4-8. Cost of hydrogen production, delivery, and transportation for different market shares.**

According to[108], the future cost of hydrogen production will reduce to less than $4.5/kg $H_2$ in future central production plants. However, electricity cost with more than 90% share in total production cost will remain a barrier to hydrogen economy development. However, with developing more renewable capacity, there will be a considerable cost reduction potential in mid-term energy plantings. The intermittent characteristics of renewable energy sources will provide some low-cost surplus electricity, which can reduce

the hydrogen cost by $4/kg $H_2$. It means that the hydrogen costs shown in Figure 4-8 have the potential to be reduced by a significant margin just by using surplus electricity. There is surplus electricity in Ontario due to using intermittent renewable energy sources like wind energy and solar energy. This surplus electricity is either exported at a meager price (close to zero) or curtailed in some hours during the year. This surplus electricity can be provided to the hydrogen production plants as an incentive for developing a hydrogen network.

According to Table 4-2, the electricity cost of hydrogen production shown as feedstock cost is more than $4/kg H2. If the incentivized surplus electricity is provided to hydrogen production plants, the production cost will reduce by $4/kg $H_2$. According to Figure 4-8, the total cost of hydrogen production and transportation in Scenario 5 -reaching 1% market share-is $14.7/kg $H_2$ and a $4/kg $H_2$ cost reduction due to surplus energy use would decrease the overall cost to $10.7/kg $H_2$, which is a significant reduction in total cost.

### 4.4.8    Total benefits analysis

Table 4-6 shows the emission from class 7-10 trucks passing along HWY 401 during a year. This data is the output of a model developed in TRAQS, a combined interface for air quality analysis. TRAQS uses a combination of MOVES and AERMOD to simulate the dispersed air pollutants coming from mobile sources.

**Table 4-6. Amount of different pollutants emitted from heavy-duty trucks in HWY 401.**

| Component | Emissions (tonnes/year) |
|---|---|
| CO | 4194 |
| $CO_2$ Equivalent | 3769206 |
| Methane (CH4) | 57 |
| Nitrogen Dioxide ($NO_2$) | 1820 |
| Nitrogen Oxide (NO) | 16190 |
| Oxides of Nitrogen ($NO_x$) | 18155 |
| PM10 | 1865 |
| $PM_{2.5}$ | 1156 |
| Sulfur Dioxide ($SO_2$) | 32 |
| Total Gaseous Hydrocarbons | 852 |
| Total Organic Gases | 959 |
| Volatile Organic Compounds | 886 |

For the current project, only MOVES was utilized as the goal was to find the amount of pollutant emission at the source. The cost per tonne of pollutants in Ontario is calculated using data from [109], which includes personal health impacts, the burden on the health care system, and missed work due to illness. Those costs are converted to 2016 US dollars and are presented in Table 4-7.

**Table 4-7. Cost per tonne of different pollutants in Ontario.**

| Pollutant | Cost per tonne (2016$/year) |
|---|---|
| Oxides of Nitrogen ($NO_x$) | 6000 |
| $PM_{2.5}$ | 29800 |
| Sulfur Dioxide ($SO_2$) | 6700 |
| Volatile Organic Compounds | 900 |

Using amounts from Table 4-6 and Table 4-7, we can estimate the total cost of pollutants due to heavy-duty trucks in a year. This estimation is shown in Table 4-8. It should be noted that the value obtained is a significant underestimation as numbers in Table

4-7 are the estimation for the entire province of Ontario, which includes many unpopulated areas. However, the modeled region is highly populated because it encircles urban and suburban areas. In other words, the health costs presented in Table 4-8 are the minimum amount of health costs due to heavy-duty trucks traveling along HWY 401.

**Table 4-8. Annual health cost from heavy-duty trucks traveling in HWY 401.**

| Pollutant | Cost (million $/year) |
|---|---|
| Oxides of Nitrogen ($NO_x$) | 110 |
| $PM_{2.5}$ | 34 |
| Sulfur Dioxide ($SO_2$) | 0.2 |
| Volatile Organic Compounds | 0.8 |
| **Total** | **145** |

Table 4-9 shows the health benefits for all discussed scenarios. The benefits are calculated assuming linear correlation between the pollution and number of heavy-duty vehicles. In other words, it is assumed that replacing 1% of fossil-fuel heavy-duty vehicles with hydrogen trucks will reduce pollution by 1%. This is an underestimation because the potential trucks for replacement can be chosen amongst high-pollution vehicles. Assuming a linear correlation between the number of vehicles and pollution, it can be seen that the cost-saving increases with the level of market penetration of FCEVs.

**Table 4-9. Health benefits for different scenarios. Scenario 1: 0.1% changeover, Scenario 2: 0.2% changeover, Scenario 3: 0.3% changeover, Scenario 4: 0.4% changeover, Scenario 5: 1% changeover**

| Scenario | Health benefit (thousand $/year) |
|---|---|
| Scenario 1 | 145 |
| Scenario 2 | 290 |
| Scenario 3 | 435 |
| Scenario 4 | 580 |
| Scenario 5 | 1450 |

To calculate the amount of $CO_2$ emitted due to hydrogen production, the annual average emission factor (AEF) is utilized. In 2018, AEF in Ontario was reported to be 31 g $CO_2eq/kWh$ [110]. As shown in Table 4-1, the electricity consumption of hydrogen production is 55.8 kWh/kgH2. Therefore, the hydrogen production emission factor is estimated to be 1.73 kg $CO_2$/kg H2. On the other hand, based on the results from MOVES, every kilogram of hydrogen avoids 12.82 kg $CO_2$. In total, the net benefit of such a system in terms of emission is 11.09 kg $CO_2$/kg H2.

Assuming the social cost of carbon (SCC) to be 50$/tonne $CO_2$ equivalent, the total cost of carbon for heavy-duty trucks along HWY 401 is around $163 million. Avoiding 1% of the emission in Scenario 5 will have a 1630 thousand dollars benefit per year. Comparing health benefits shown in Table 4-9 and SCC shows that pollution is as important as emission. In other words, the results show the importance of bringing health cost analysis into account in order to investigate the drawbacks of current fossil-fuel-based energy systems. Based on the outputs from MOVES, 94% of PM10, 99% of $PM_{2.5}$, and 100% other pollutants are

emitted from vehicles' exhaust. Therefore, substituting diesel trucks with hydrogen trucks will almost make their pollution equal to zero.

## 4.5    Conclusions

Hydrogen is considered to be a cleaner type of fuel and an alternative to traditional fossil fuels and provides energy storage via several power-to-gas (P2G) pathways, including seasonal energy storage. Building some infrastructures for the rollout of heavy-duty fuel cell trucks can act as a catalyst to push the development of the hydrogen economy because heavy-duty trucks have the highest potential amongst other hydrogen applications. Building FCEVs' refueling infrastructure is the first step toward the hydrogen economy and can potentially increase the hydrogen role in the future clean energy system.

This chapter presented a model to optimize the sizes and locations of the hydrogen infrastructures needed to produce and distribute hydrogen for the hydrogen corridor highway (i.e., HWY 401) in Ontario. A novel mathematical modeling and optimization approach has been used to apply to other regions/countries. The methodology involved using the HDSAM tool developed by the H2A Analysis Group and an optimization model built using GAMS. MOVES was also used to quantify the pollution released from conventional vehicles to assist with health cost and benefit calculations. The results showed that the initial development of hydrogen economy and FCEVs could be beneficial despite its high capital cost. The Canadian government should consider it a potential approach to help resolve the climate change problem and improve the quality of public health. Based on our modeling, a 1% share of hydrogen in heavy-duty truck fuel consumption can reduce the environmental

cost by 1.63 million dollars per year and health cost by 1.45 million dollars per year. It is worth mentioning that these costs are an underestimation of real costs and can be investigated more in future works. Also, we demonstrated that despite the current high costs of hydrogen production and delivery, the cost of hydrogen could be minimized using optimal energy planning and higher capacities. Comparing 0.1% and 1% scenarios, the results suggested that the economy of scales could cause a 35% reduction in per kg cost of hydrogen. Analyzing higher capacities and higher market shares requires a deeper look into technology development and future costs, which can be discussed in future works.

# 5. Health Cost Estimation of Traffic-Related Air Pollution and Assessing the Pollution Reduction Potential of Zero-Emission Vehicles in Toronto, Canada

## 5.1 Introduction

Despite Canada having some of the cleanest air globally and ranking amongst the lowest levels of pollution emissions in fine particulate matter ($PM_{2.5}$) concentrations, Health Canada found that approximately 14,600 Canadians died prematurely due to air pollution in 2015 [10]. The trends show that the amount of $PM_{2.5}$ being emitted in Canada is on the rise. The number of Canadians succumbing to poor air quality continues to rise while the air quality is worsening. Action to reduce the amount of pollution in the most affected areas must be taken to prevent the unnecessary loss of life. The air quality is worst in highly populated urban areas, such as the Greater Toronto Area (GTA) [102]. This decrease in air quality can be attributed to fossil-fuel-powered Internal Combustion Engine Vehicles (ICEV) [111]. These ICEVs cause the increased concentration of harmful products in the air, including CO, O3, $NO_2$, and $PM_{2.5}$ which cause acute and chronic medical problems such as asthma, bronchiolitis, and lung cancer [112]. However, the penetration of zero-emission vehicles (ZEVs) into Canada's traffic mix can alleviate this problem by eliminating these harmful exhaust products [11]. This chapter presents an assessment of the impacts of electric

passenger vehicles and hydrogen fuel-cell trucks on human health and greenhouse gas (GHG) emissions in the Toronto 401 corridor.

To determine the total impact on GHG emissions of switching from diesel to hydrogen for semi-trucks and gasoline to electric and hydrogen for passenger cars in Ontario, a well-to-wheels (WTW) life cycle assessment (LCA), as shown in Figure 5-1, is considered. LCA methodology employs a cradle-to-grave approach to assess the environmental impact of a product or service over its life cycle. The processing activity entails extracting raw materials, manufacturing, transportation, recycling, and final disposal. In automotive LCA, vehicle production and vehicle end-of-life are disregarded due to the high uniformity in these processes across fuel types.
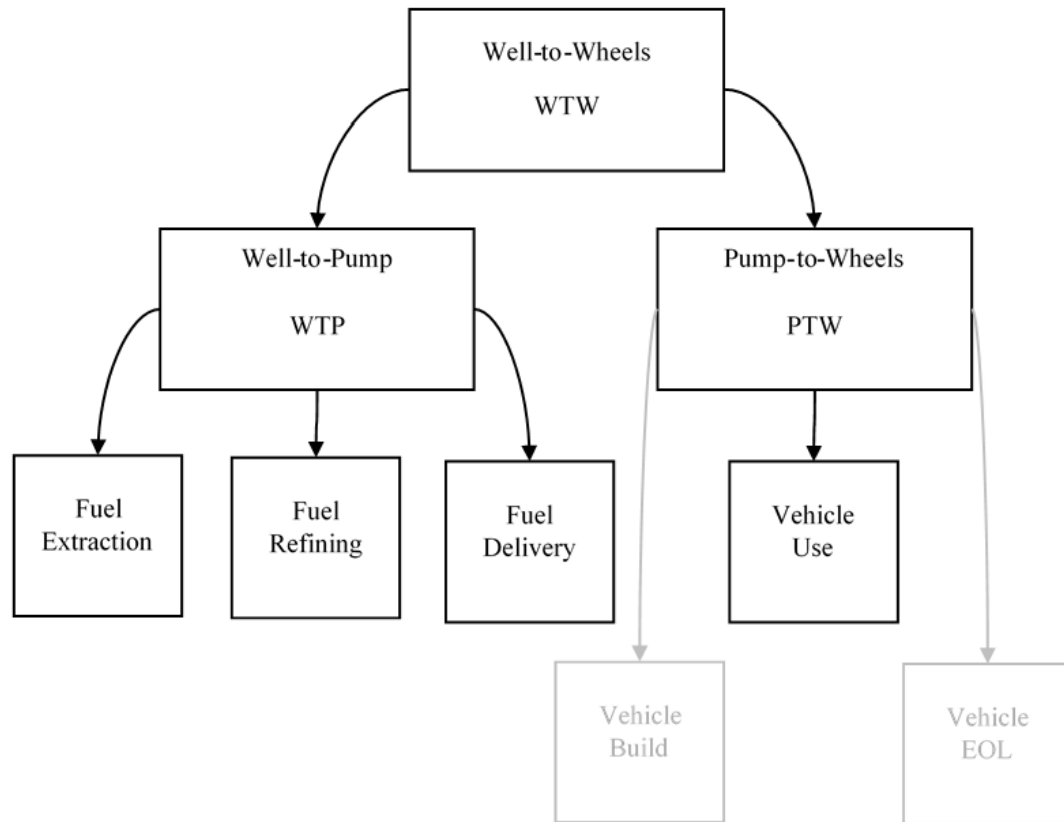
**Figure 5-1. Well-to-Wheels LCA Method Employed in Comparison of Diesel and HFCV Semi-Trucks. (Due to similarity across fuel types, the Vehicle Build and Vehicle EOL are omitted.)**

In addition to the GHG impacts of internal combustion engines, air pollution is a problem that significantly impacts human health. The exhaust emissions from gasoline and diesel vehicles lead to a significant increase in wheezing, coughing, and cases of lung diseases like asthma [113]. There is a substantial increase in the concentration of air pollutants within proximity to US highways, including CO, $NO_2$, $SO_2$, PM, and black carbon (BC)[114]. These pollutants increase the risk of cardiopulmonary mortality in adults and decrease lung function in children between 4 and 8 years of age for those living within 300

meters of the highway. Higher exposure to $NO_2$, NO, and CO is correlated with a higher prevalence of childhood asthma [115]. Further, poor air quality has been strongly linked with poor overall living conditions [116]. Fine particulate air pollution is found to cause 0.8 million deaths and 6.4 million lost life-years globally per year [117].

In Canada, the risk of human health impacts from air pollution is continually increasing. When samples were collected to predict $PM_{2.5}$ and ozone levels in the city of Toronto, along with health data of 2360 subjects, it was found that there was a 17% increase in mortality and a 40% increase in circulatory-related mortality when exposed to 4 ppb $NO_2$ or higher [118]. Further research has examined the relationship between premature mortality and harmful air pollutants across 11 Canadian cities[119]. The findings show that $NO_2$ increased the risk of mortality by 4.1%, followed by ozone (1.8%), $SO_2$ (1.4%), and CO (0.9%). A similar study was conducted by collecting samples of air pollutants over a 16-year period in ten Canadian cities, which also found that $NO_2$ had the strongest association with mortality [120]. A complex relationship exists between the increasing incidence of congestive heart failure and exposure to air pollutants across Canada [121]. Health Canada concluded that in 2019, there was a total of 9,700 premature deaths due to $PM_{2.5}$ chronic exposure, 940 deaths due to $NO_2$ acute exposure, 2,700 deaths due to O3 acute exposure, and 1,300 deaths due to O3 chronic exposure in Canada [122]. Canadians are at an increased risk of health problems due to air pollution. To regulate airborne pollutants and mitigate this risk, the province of Ontario publishes a list of acceptable airborne concentrations of pollutants. On this list, primary pollutants related to the operation of motor vehicles include CO, $NO_2$, $SO_2$, and PM.

A spike in $SO_2$, $NO_2$, and $NH_3$ pollution, which started in the 1950s and peaked in the 1980s, caused a significant increase in acid rain cases [123]. Due to public opposition to the increasing $SO_2$ emissions globally, acid rain has been drastically reduced. In Canada, for example, there was an 80% decrease in $SO_2$ emissions between 1980 and 2015. A spatial analysis between socioeconomic groups and air pollution within three large Canadian cities – Toronto, Vancouver, and Montreal – found that areas with a larger proportion of residents generally had greater exposure to ambient $NO_2$ pollution [124]. Additionally, there is an association between greater $NO_2$ exposure and signs of social deprivation. Another article investigated the change in air quality due to the increasing albedo effect in Montreal. The authors increased the reflectivity of roofs, walls, and roads to decrease the urban heat island (UHI) effect, reducing the overall surface temperature [125]. This temperature increase resulted in a 3% decrease in the 8-hour averaged O3 concentration and a reduction of 1.8 $\mu g/m^3$ in the 24-hour averaged PM$_{2.5}$ concentration [125]. Air quality data collected during the COVID-19 lockdown in Ontario showed no change in PM. However, the average O3, $NO_2$, and NO concentrations were lower than in previous years [126]. It should be noted that during the lockdown in Ontario, there were still many human activities going on in terms of transportation. However, with slightly fewer transportation activities, less pollution was observed, and hence it is evident that air pollutants could be reduced significantly with a lower level of transportation emissions.

Because of the impact of air pollutants on human health, countries are burdened with increasing health costs caused by air pollution. In 1991, the total health costs of pollution from motor vehicles totaled between USD 54.7 billion and USD 672.3 billion [127]. The

103

gross annual damage wrought by air pollution on the US economy in 2002, determined by summing all the public health costs from air pollution, was between USD 71 billion and USD 277 billion [128]. Chronic exposure to $PM_{2.5}$ was found to be the most considerable health burden in 25 European cities, with a calculated yearly monetary gain of around USD 37 billion if the air pollution is reduced to the World Health Organization (WHO) guidelines. The cost of $PM_{2.5}$ air pollution in Skopje was estimated to be between €570 million and €1,470 million in 2012 [129]. Researchers experimented across thirty provinces in China to assess the economic health benefit of decreasing air pollution. The results stated that the total loss from air pollution totaled an estimated ¥346.26 billion, or USD 53 billion, in 2007 [130]. In addition, a similar study focused on the populated urban areas of China found that in 2013, the total health cost caused by air pollution was USD 14.8 to USD 25.3 billion [131].

The public health costs of air pollution in Canada are also high. Analysis of agricultural air pollution in Canada found that 1480 lives could be saved annually by a 50% reduction in agriculture-related air pollution [132]. The economic value of such a reduction in air pollution is estimated between USD 1.66 and USD 9.4 billion [132]. The air pollution removed by urban trees in Canada has both economic and health benefits. In 86 Canadian cities, urban trees removed between 7,500 and 21,100 tonnes of air pollution in 2010, resulting in an annual saving of CAD 52.5-402.6 million [133]. Multiple studies have shown that transportation is one of the primary sources of air pollutions and can lead to significant health costs [11,113–115,127,134]. Examining the impact of vehicle mix on air pollution, having even 1% of the heavy-duty vehicle fleet in Ontario be zero-emission

vehicles has an environmental and health benefit valued at USD 1.63 million per year [11]. The contribution of commercial diesel vehicles to the air quality in the GTA and Hamilton was estimated to be 6-22% for $NO_2$ and BC, and 3% for $PM_{2.5}$ and O3 [134]. The combined emissions of all commercial vehicles were calculated to have a total health impact of 9,810 Years of Life Lost (YLL), corresponding to CAD 3.2 billion.

With the emergence of Power-to-Gas (P2G) technology and infrastructure, the possibility of gradually replacing conventional vehicles with hydrogen Fuel Cell (FC) vehicles has become more achievable. P2G is a method of storing and transporting energy through hydrogen production from renewable and conventional sources. Using P2G, the surplus energy produced from renewable sources can be used to produce hydrogen, which is then stored and used to produce electricity, renewable natural gas, and in other hydrogen applications such as hydrogen FC vehicles. The introduction of more hydrogen FC vehicles, in addition to battery electric vehicles, can potentially improve the air quality and ultimately the living quality in Canada, resulting in various environmental, economic, and health benefits. In this chapter, the costs of the adverse health effects from air pollution and the estimation of the potential monetary benefit that ZEVs will provide in reducing these health costs are determined and compared with the costs of climate change. The study uses the case study of Highway 401 in Ontario within the City of Toronto, one of the busiest highways in North America, as the basis for calculations. The case studies and results found in this chapter can also give a general idea about the benefits of ZEVs in other highways and other countries. The authors use an emission model, an air dispersing model, and a health risk model to find the health costs of traffic-related air pollution near the studied highway. ZEVs'

health and environmental benefits, including FC trucks and electric passenger vehicles, are calculated in different scenarios based on the integrated health cost calculation model and the life-cycle emission model. The results from this chapter show the significant health and environmental effects of traffic-related air pollution on people who are living in the vicinity of major highways in Canada, and to a certain extent, in the vicinity of other major highways in the world, as well as providing a potential solution by showing the benefits of a mass roll-out of ZEVs.

## 5.2 Methodology

### 5.2.1 Climate Change Cost Calculation

The cost of climate change is estimated using an estimated price of GHGs per tonne of carbon dioxide equivalents ($CO_{2e}$). The value of carbon has been estimated to be only USD 2 per tonne globally. In contrast, a higher estimated value of USD 75 per tonne is necessary to entice corporations and individuals into reducing GHG emissions [27]. In this analysis, a value of CAD 40 per tonne of $CO_2$, which is the value of the Canadian carbon tax as of April 2021, is used [28].

### 5.2.2 Health Cost Modeling and Calculation

Figure 5-2 shows the schematic of the integrated models for health cost calculation. A four-step model was built to find the traffic-related health cost of Highway 401. The first step was finding the amount of pollution coming out of diesel trucks in different sections of Highway 401. Next, an air dispersion model was used to find the concentrations of different

pollutants caused by light vehicles and trucks moving along Highway 401. The third step was to investigate the health impacts of air pollution on residents living in the vicinity of Highway 401. Finally, the increased risk of mortality was converted into dollar values in the fourth step. The four steps are described in the following subsections.
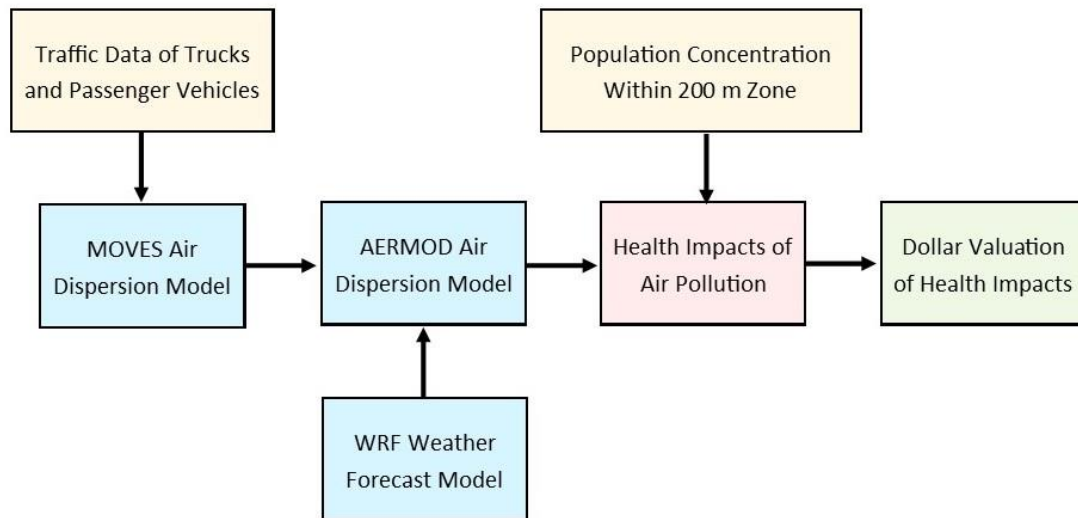


**Figure 5-2. Schematic of the Health Cost Calculation Model.**

#### 5.2.2.1 Total Emissions from Highway 401

To find the total air pollution emissions from diesel trucks traveling along Highway 401, EPA's Motor Vehicle Emission Simulator (MOVES2014b) is used [135] to estimate the pollution emitted from traffic on Highway 401. MOVES2014b is a Windows-based model designed to accurately estimate emissions from motor vehicles. The model performs a series of calculations based on vehicle types, geographic areas, time of the year, road type, and other factors to estimate bulk emissions or emission rates.

The Annual Average Daily Traffic (AADT) data from 2016 was found from Ontario's Ministry of Transportation traffic repository [103]. AADT, seasonal traffic change factor, and hourly traffic change factor were inputted into the MOVES2014b software to find the total emissions of passenger vehicles and trucks along Highway 401. Figure 5-3 shows the AADT along Highway 401, where the x-axis is the distance from the western end of Highway 401 in Toronto. As shown in Figure 3, more vehicles pass in the west part of Highway 401 in Toronto. Therefore, the corridor-related pollution concentration is expected to be higher in the western regions. The numbers in Figure 3, taken from [103], include class 7, 8, 9, and 10 trucks, which are heavy-duty truck classes.
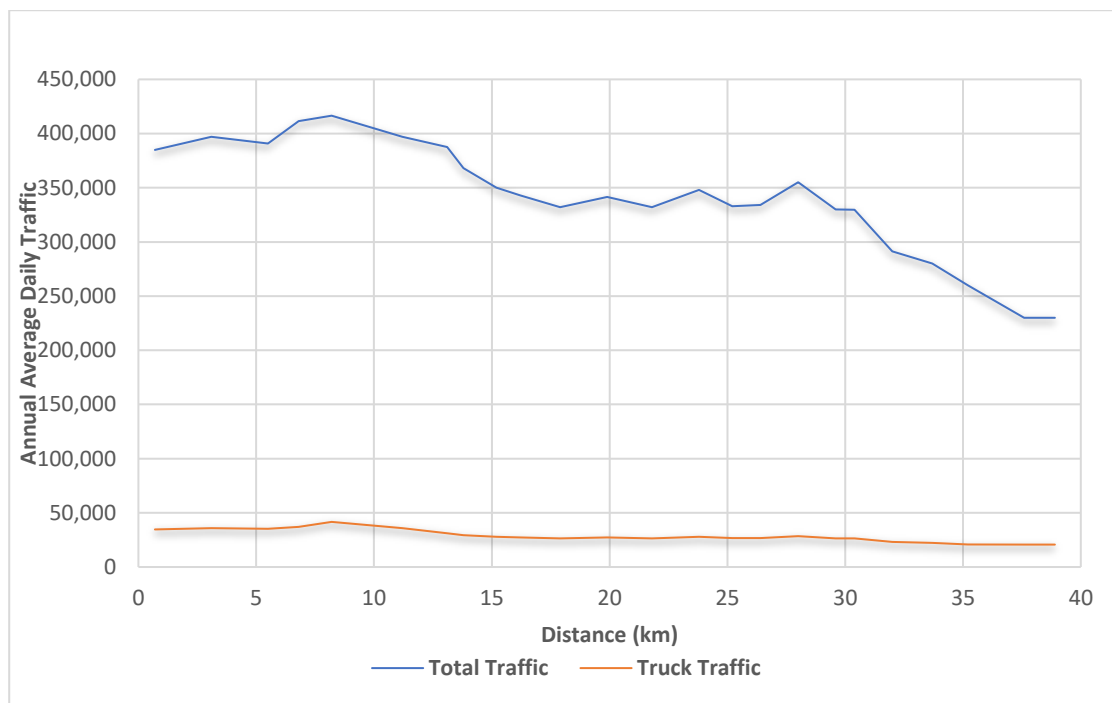


**Figure 5-3. Annual Average Daily Traffic (AADT) along Highway 401.**

Figure 5-4 shows the seasonal-hourly traffic factor. Fall and winter have higher traffic factors. Also, we can see that the PM peak in all seasons is the busiest period in Highway 401. Also, overnight, traffic volume drops, resulting in a drop in air pollution.
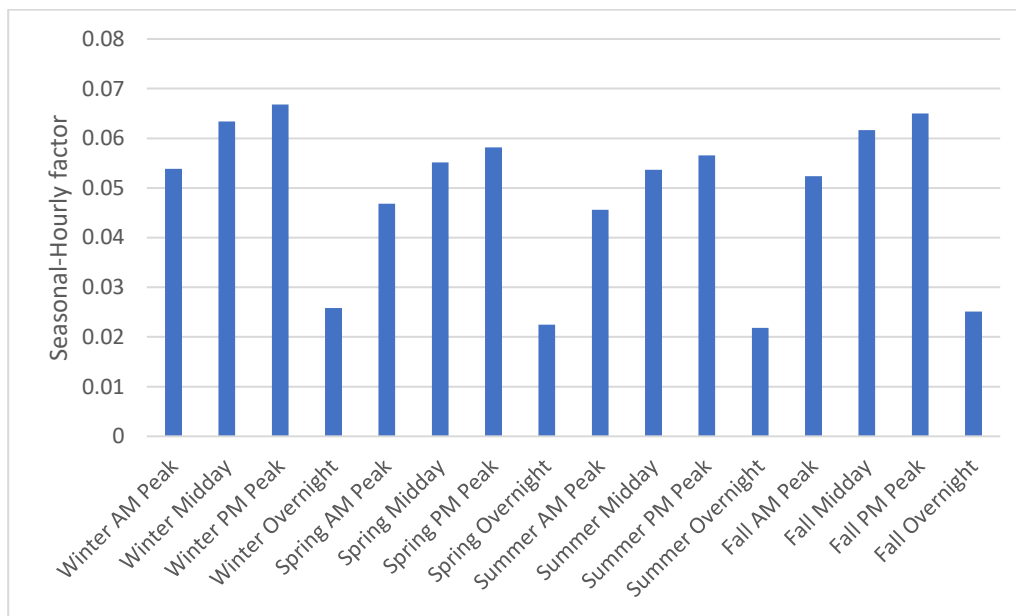


**Figure 5-4. Traffic Seasonal-Hourly Adjustment Factor.**

**5.2.2.2    Dispersion of Air Pollutants along Highway 401**

To find the concentrations of air pollutants in the vicinity of Highway 401, the emission data from the first step as an input to EPA's AERMOD executable version 19191 was used [136]. AERMOD is a steady-state Gaussian plume air dispersion model and is the U.S. EPA preferred dispersion model for near-field impacts (less than 50 Km). The model can handle flat or elevated terrain. Dispersion is conducted as a plume from each source which disperses entirely in the downwind direction. The meteorological preprocessor for AERMOD called AERMET calculates hourly values of advanced turbulence parameters

(e.g., sensible heat flux, convective velocity scale, surface friction velocity, Monin-Obukhov length, etc.). These parameters are used to build the planetary boundary layer for each modeled hour. Table 5-1 shows the features and inputs of the AERMOD model. Highway 401 in Toronto is divided into 71 line sources, which their emission rates are calculated using MOVES2014b. Also, a network of discrete receptors is generated using TRAQS. The Transportation Air Quality System (TRAQS) is an open-source software interface that successfully integrates regulatory mobile emissions models – MOVES or EMFAC with AERMOD. Spacing between receptors is 100 m. Also, the distance between different layers of receptors is 10 m in the vicinity of the highway; however, it increases to 5 km in regions far from the highway.

**Table 5-1. AERMOD inputs.**

| Input | Description |
|-------|-------------|
| MODELOPT | FASTALL |
| AVERTIME | Annual |
| POLLUTID | PM 2.5 and $NO_x$ |
| Source type | Line Sources |
| Receptor type | Discrete Cartesian Receptors |

To generate meteorological data for the AERMOD air dispersion model, the Weather Research and Forecasting (WRF) model was used. WRF is a mesoscale numerical weather prediction system jointly developed by the National Center for Atmospheric Research (NCAR), the National Oceanic and Atmospheric Administration, the U.S. Air Force, and others [137]. The WRF model was used to extract the necessary meteorological data for air dispersion modeling, such as the surface and profile files along Highway 401. The Weather Research & Forecasting model was executed from 2016 to 2020 at 4-kilometer horizontal

grid resolution. The U.S. Environmental Protection Agency's (U.S. EPA) Mesoscale Model Interface Program was used to format output from WRF for use in the AERMOD modeling system. The input data is used from the National Centers for Environmental Prediction (NCEP) Global Forecast System (GFS) 0.5-degree resolution data. The GFS 0.5-deg data is given every 6 hours at 00, 06, 12, and 18Z. The input for the sea surface temperature (SST) data comes from the GFS 0.5-degree data, updated daily as each WRF simulation is done for 24 hours. Details on the setup used to execute the WRF model (Version 4.0) are provided in Table 5-2.

**Table 5-2. WRF setup characteristics.**

| Domain | Resolution (km) | Number of Grid Points in X and Y |
|---|---|---|
| Domain 1 | 27 | 34 x 34 |
| Domain 2 | 9 | 34 x 34 |
| Domain 3 | 3 | 34 x 34 |

Figure 5-5 shows a predominant wind blowing from the North-West direction 13% of the time. The average wind speed for the five years from 2016 to 2020 is 3.32 m/s with 489 hours of calm conditions.
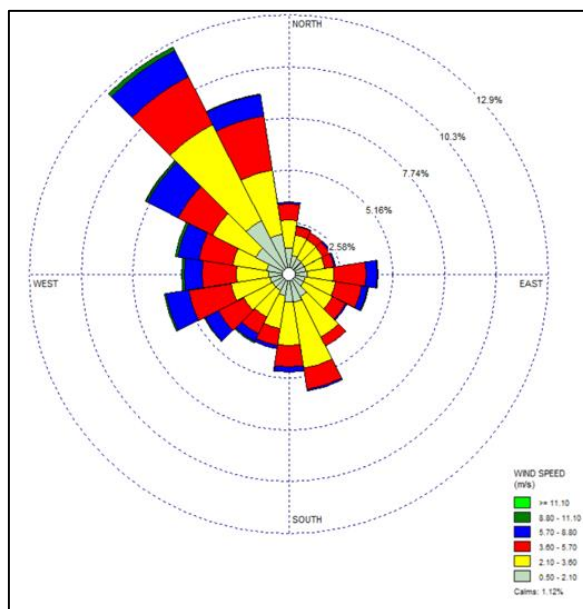
**Figure 5-5. Wind Rose Diagram at Toronto West Air Monitoring Site.**

The metrological data derived from the WRF model was then inputted into the AERMOD air dispersion model to accurately map the dispersion of various air pollutants along Highway 401. Using the AERMOD air dispersion model, the concentrations of air pollutants were found within 10,000 m of Highway 401 at different receptors. A receptor is a location with exact coordinates within the air dispersion model where the concentration is calculated.

### 5.2.2.3    Risk Analysis

Hazard ratios are used to find the increased risk of mortality due to Highway 401 traffic in Toronto [138]. According to [138], mortality increases by 1.04 (95% CI 1.02–1.06) with a rise of 10 $\mu g/m^3$ in annual $NO_2$ concentration. It is assumed that almost all $NO_x$ becomes $NO_2$ in a few minutes, meaning the health risk of $NO_x$ would be relatively equal to the health risk of $NO_2$. It should be noted that the total conversion of $NO_x$ to $NO_2$ is a

112

conservative assumption. To calculate the increased risk of mortality, the current mortality rate must be calculated. According to Statistics Canada, the mortality rate per 1,000 population was 7.3 in 2017 [139]. Combining population data, mortality rate, and increased risk of mortality due to pollution, one can find the increased number of premature death due to Highway 401 traffic pollution.

#### 5.2.2.4    Health Cost Calculation

The Value of Statistical Life (VSL) metric is used to find the pollution's health cost to the economy in monetary units. VSL is the marginal rate of substitution between income and mortality risk was used [140]. According to [141], the mean VSL for Canada is CAD 5.2 million, ranging from a low of CAD 3.1 million to a high of CAD 10.4 million in 1996 CAD. Considering inflation, the mean VSL in 2020 dollars is equal to CAD 8 million.

### 5.2.3   Scenarios

Six scenarios are defined to examine the effect of ZEVs on air pollution as well as pollution costs. In this regard, a specific percentage of passenger vehicles is assumed to have become battery electric vehicles in three scenarios. The other three scenarios assumed the substitution of heavy-duty diesel trucks by hydrogen FC trucks.

Table 5-3 demonstrates the shares of vehicles in the six scenarios.

**Table 5-3. Scenario Definition for Cost Calculation.**

| Scenario | % Electric passenger vehicles | % Fuel Cell Trucks |
|---|---|---|
| 1 – 10% Electric passenger vehicle | 10 | 0 |
| 2 – 10% Fuel cell trucks | 0 | 10 |
| 3 – 50% Electric passenger vehicle | 50 | 0 |
| 4 – 50% Fuel cell trucks | 0 | 50 |
| 5 – 100% Electric passenger vehicle | 100 | 0 |
| 6 – 100% Fuel cell trucks | 0 | 100 |

## 5.3    Results

### 5.3.1    Climate Change Cost

In this analysis, the pump-to-wheels (PTW) emissions are created onsite as vehicles travel through Highway 401 in Toronto. Looking at the 401 Toronto corridor between Dixon Road and Meadowvale Road, there were 1,097,281 vehicle miles driven by semi-trucks and 7,136,138 vehicle miles driven by passenger cars for a total of 11,913,869 vehicle-mile, as tabulated in Table 5-4 [103].

**Table 5-4. Vehicle-kilometers driven by Heavy-duty Trucks and Passenger Cars on 401**

**Toronto (2016)**

| Portion | Diesel Heavy-duty Truck | Gasoline Passenger Vehicle |
|---|---|---|
| Eastern | 183,144 | 1,999,776 |
| Central | 384,083 | 4,416,957 |
| West | 530,054 | 5,497,136 |
| Total | 1,097,281 | 11,913,869 |

Using the GREET (Greenhouse gases, Regulated Emissions, and Energy use in Technologies) transportation LCA tool, the per kilometer emissions results were determined for diesel trucks and gasoline passenger vehicles, as seen in Table 5-5. If hydrogen FC semi-

trucks and electric vehicles are charged using stand-alone solar power, there will be no life-cycle greenhouse gases for either technology.

**Table 5-5. Grams of Greenhouse Gas Emissions ($CO_2e$) per vehicle-kilometer for Diesel Trucks and Gasoline Automobiles**

| Phase | Diesel Heavy-duty Truck | Gasoline Passenger Vehicle |
|---|---|---|
| Well-to-Pump | 9.8 | 13.5 |
| Pump-to-Wheels | 348.4 | 270.0 |
| Well-to-Wheels | 358.2 | 283.5 |

Combining the information, it is possible to estimate the total current greenhouse gas emissions from traffic in this section of Toronto. Additionally, it is possible to determine the impacts of different traffic composition mixes on the overall amount of $CO_2e$. Table 5-6 shows the total emissions in tonnes of $CO_2e$, in addition to the total reductions, for six different scenarios.

**Table 5-6. Thousands of Metric Tons of CO₂e Produced Annually on 401 Toronto Under**

**Different Traffic Profiles.**

| Scenario | LCA Type | | |
|---|---|---|---|
| | Well-to-Pump | Pump-to-Wheels | Well-to-Wheels |
| Scenario 1 (10% EV) | 57 | 1,196 | 1,253 |
| Scenario 2 (10% FC Trucks) | 62 | 1300 | 1,361 |
| Scenario 3 (50% EV) | 33 | 727 | 760 |
| Scenario 4 (50% FC trucks) | 61 | 1244 | 1,305 |
| Scenario 5 (100% EV) | 4 | 140 | 144 |
| Scenario 6 (100% FC trucks) | 59 | 1174 | 1,233 |
| 2016 GHG emission | 63 | 1314 | 1,376 |

As shown in Table 5-6, a more significant reduction in GHG emissions is possible by converting passenger vehicles from gasoline to renewable electric or hydrogen. However, this is primarily due to the substantial size of the passenger vehicle fleet and the high number of kilometers driven by passenger cars on Highway 401. Using the Canadian carbon price of CAD 40 per tonne of GHG, the monetary value of climate change can be determined. Based on this traffic corridor, the cost of carbon emissions in 2016 is CAD 55,053,332. The GHG costs of 100% green semi-trucks and passenger cars are shown in Table 5-7.

**Table 5-7. Component Costs of GHG Emissions Produced Annually on 401 Toronto Under**

**Different Traffic Profiles.**

| | GHG Cost 2016 | GHG Cost of 100% HFCV Semi-Trucks | GHG Cost of 100% Electrified Passenger Cars |
|---|---|---|---|
| Well-to-Pump | CAD 2,510,946 | CAD 2,353,362 | CAD 157,584 |
| Pump-to-Wheels | CAD 52,542,386 | CAD 46,960,153 | CAD 5,582,233 |
| Well-to-Wheels | CAD 55,053,332 | CAD 49,313,515 | CAD 5,739,817 |

### 5.3.2 Health Cost

As shown in Figure 5-6, traffic-related pollution affects areas in the range of 500 m from the highway. However, a more substantial effect of traffic-related air pollution can be seen in the range of 200 m from the highway. An air pollution monitoring station is located close to Highway 401, whose data can be used for model verification.
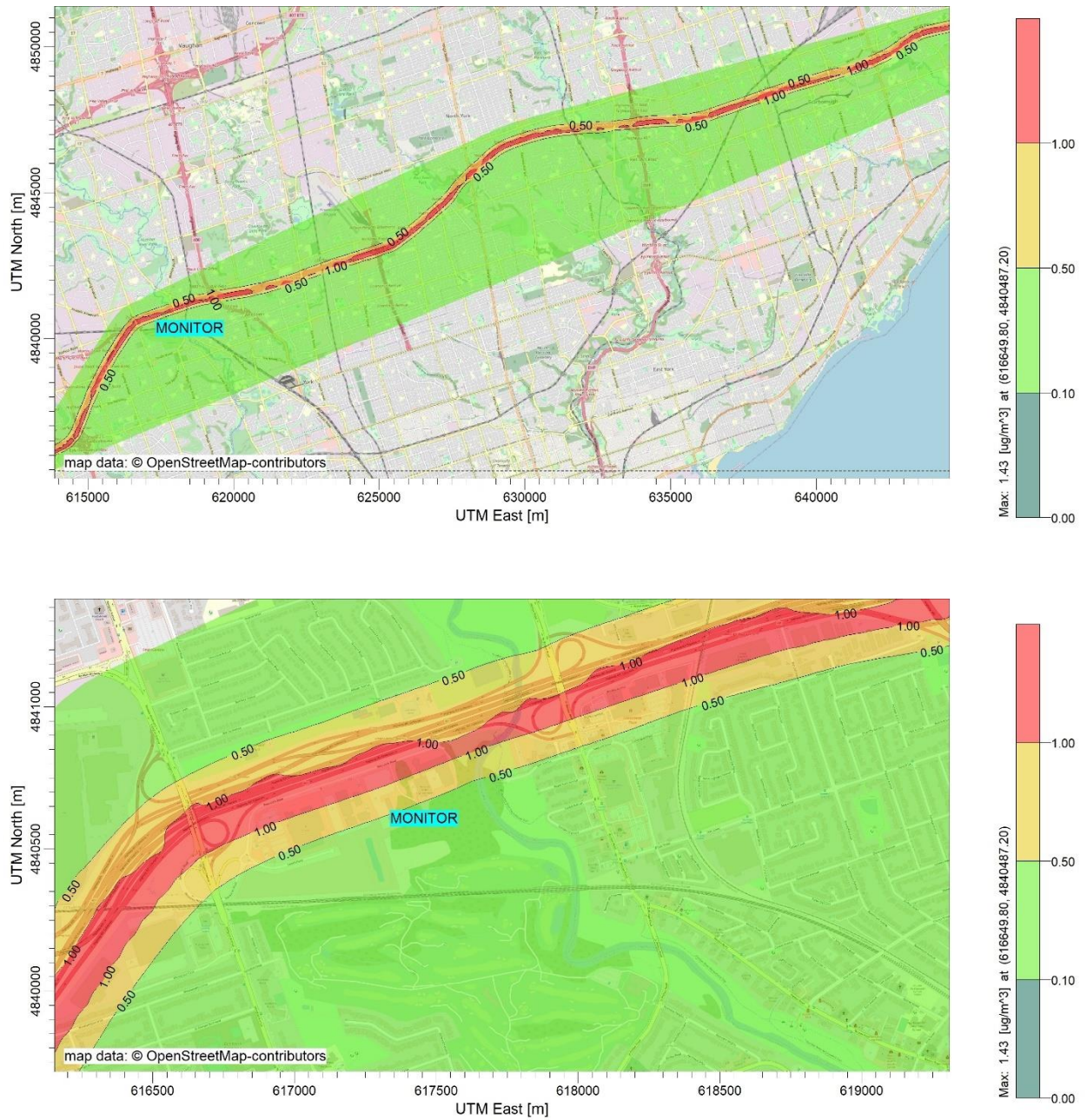
**Figure 5-6. Annual average PM$_{2.5}$ Concentration (µg/m$^3$) due to traffic in 2017 along Highway 401 (top) and near the Air Monitoring Site (bottom).**

There are four air pollution monitoring stations in Toronto. The only station located in the vicinity of Highway 401 is the Toronto West station. The other three stations are located in areas far from highways. The annual average $PM_{2.5}$ concentration in Toronto West and Toronto North monitoring station are 7.4 and 7.35 $\mu g/m^3$, respectively. So, the results from monitoring stations do not show a significant difference between Toronto West station and the other three stations in Toronto in terms of $PM_{2.5}$. The results from the model also show a small $PM_{2.5}$ concentration due to Highway 401 traffic. It should be mentioned that AERMOD is not capable calculating secondary $PM_{2.5}$ formation. According to [142], sulfates, nitrates, ammonium, and organic carbon are major contributors to the ambient $PM_{2.5}$ concentration levels. Calculating the total health cost due to $PM_{2.5}$ requires using chemical transport models. Exclusion of secondary $PM_{2.5}$ will lead to underestimation of the traffic-related health impacts [143]. As the current model is not capable of calculating secondary $PM_{2.5}$, no conclusion can be made about $PM_{2.5}$ health cost. It should be mentioned that, as one can see in Figure 5-7, in some hours, the traffic can increase the primary $PM_{2.5}$ concentration by more than 4 $\mu g/m^3$.
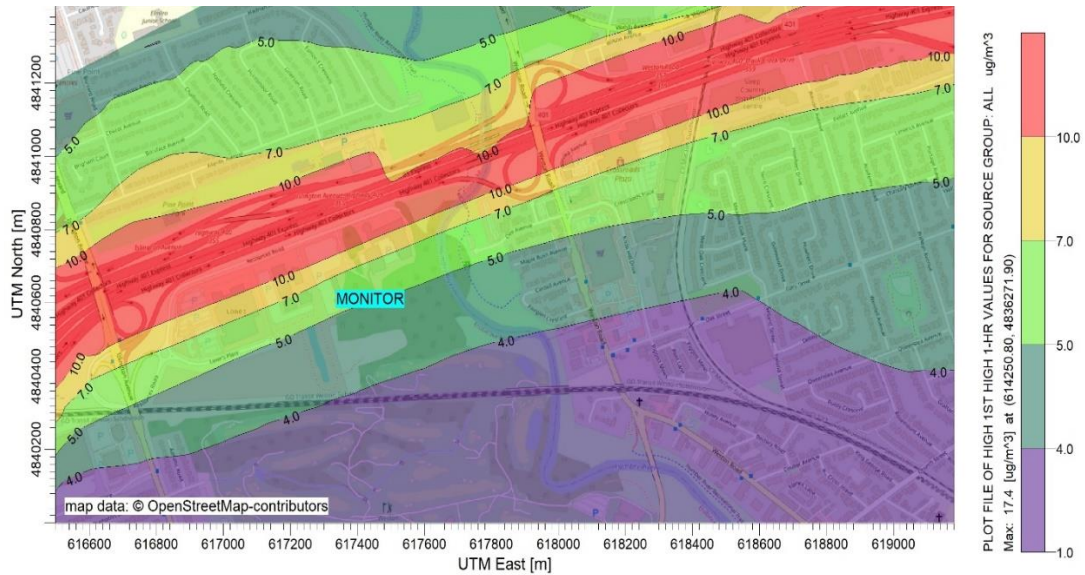
**Figure 5-7. Highest Pollution concentration of PM$_{2.5}$ due to traffic in 2017 in the West Toronto Station (μg/m$^3$).**

On the other hand, the pollution monitoring data show a significant difference in the average concentration of NO$_x$. Especially, measurements from Toronto West, the station located near highway 401, show a higher NO$_x$ concentration. The annual average concentrations of NO$_x$ in Toronto West and Toronto Downtown stations are 22.66 and 15.69 ppb, respectively. NO$_2$ Concentration in Toronto West and Toronto Downtown stations are 14.96 and 12.99 ppb, respectively. Comparing these numbers, it can be concluded that a lower share of NO$_x$ concentration is related to NO$_2$ in the Toronto West station. In other words, a high concentration of NO is measured in the Toronto West station. The higher share of NO/NO$_x$ in Toronto West station is because of proximity to Highway 401. Figure 5-8 shows the hourly changes in NO$_x$ concentration in the two stations. It can be concluded that Highway 401 traffic has a higher effect in terms of NO$_x$ rather than PM$_{2.5}$.

120
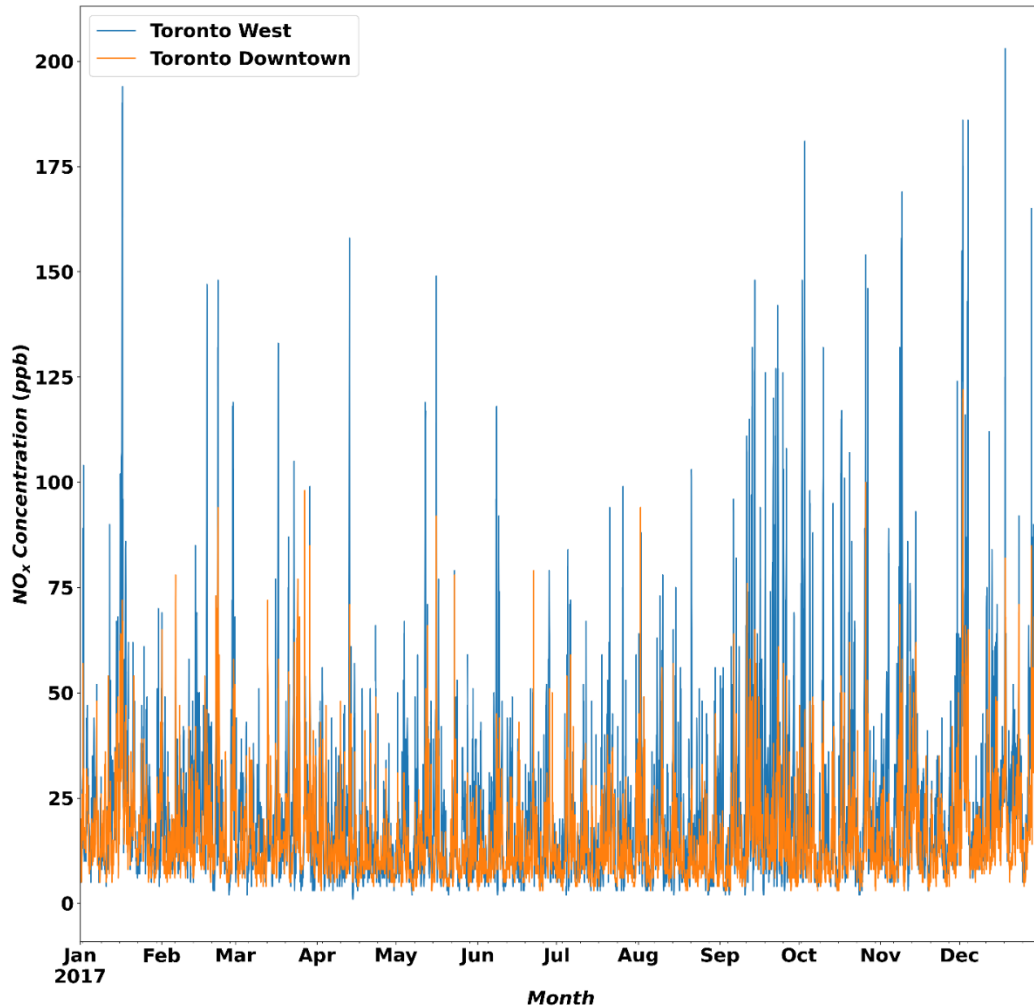
**Figure 5-8. Hourly NO$_x$ Concentration in the Toronto West and Toronto Downtown Air Pollution Monitoring Stations in 2017 (ppb).**

Figure 5-9 and Figure 5-10 show the annual average of NO$_x$ concentration due to Highway 401 traffic in 2017. The annual average concentration of NO$_x$ at the Toronto West station is 7.19 μg/m$^3$. To validate the output from AERMOD, it is assumed that the difference between NO$_x$ annual average concentration in Toronto West station and Toronto Downtown station is due to NO$_x$ pollution coming out of Highway 401. The annual average concentrations of NO$_x$ in Toronto West and Toronto Downtown stations are 39.53 and 29.21

μg/m³, respectively. The difference between these annual average concentrations, which is assumed to be related to Highway $NO_x$ pollution, is 10.32 μg/m³. As the output from AERMOD shows 7.19 μg/m³ of $NO_x$ concentration, the modeling result has a 30.3% error, which is acceptable in air pollution modeling.

Figure 5-9 and Figure 5-10 show that at distances further than 2,000 m, the annual average $NO_x$ concentration due to Highway 401 traffic is less than 1 μg/m³. In contrast, the average concentration is higher than 5 μg/m³ at distances less than 200 m. As shown in Figure 5-9, the concentration of $NO_x$ is higher in the western parts of Highway 401. The reason is the higher traffic count in those regions.
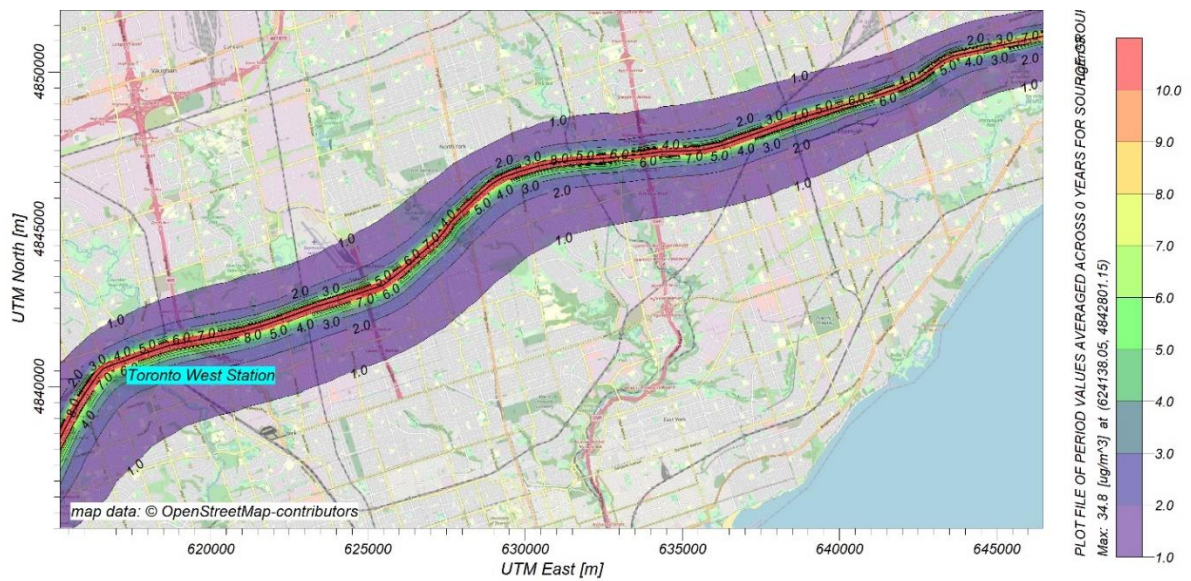


**Figure 5-9. Annual Average $NO_x$ Concentration due to traffic in 2017 in Vicinity of Highway 401 (μg/m³).**
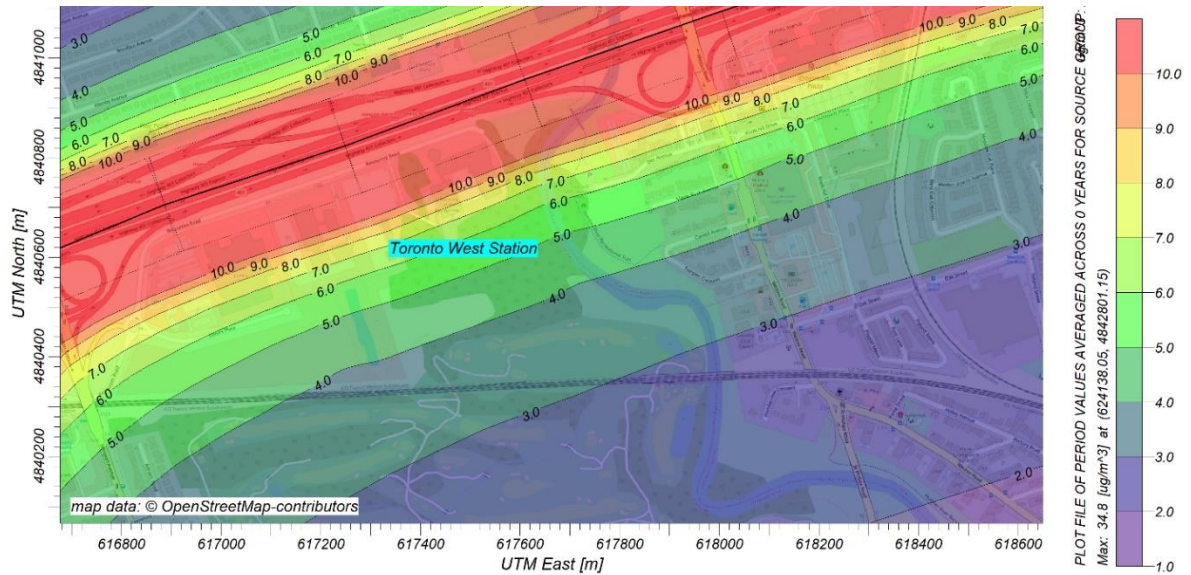
**Figure 5-10. Annual Average NO$_x$ Concentration due to traffic in 2017 in Vicinity of West Toronto Air Pollution Monitoring Station (µg/m$^3$).**

The maximum concentration due to traffic is plotted in Figure 5-11 and equals 101 µg/m$^3$ at the Toronto West station. The annual average and peak concentrations show a significant amount of NO$_x$, which can cause chronic and acute health problems.
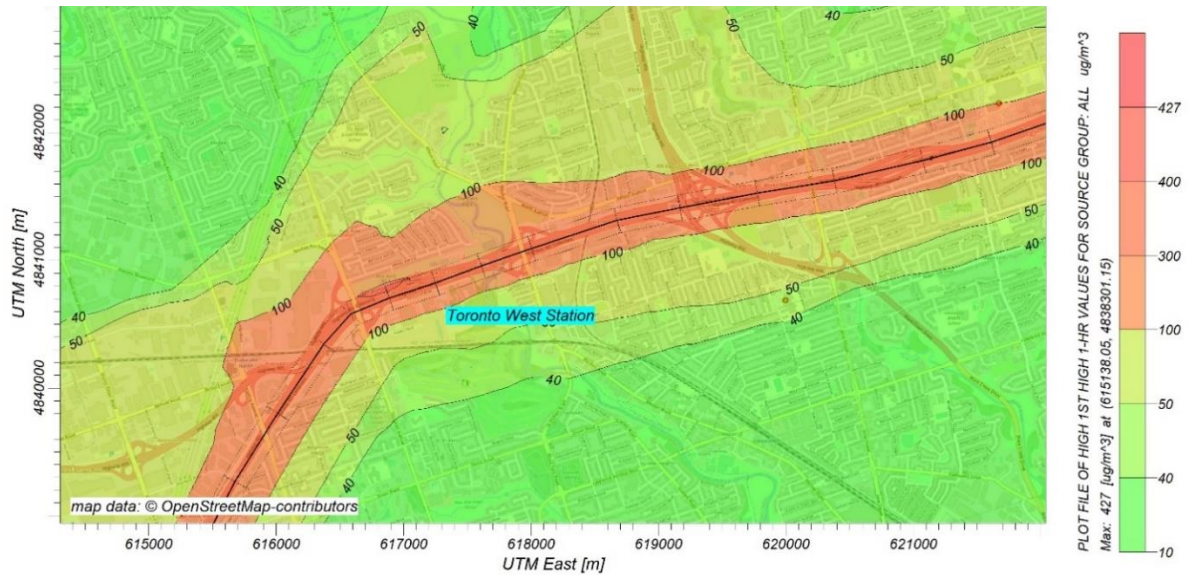
**Figure 5-11. Maximum NO$_x$ Concentration due to traffic in 2017 in Vicinity of West Toronto Air Pollution Monitoring Station (μg/m$^3$).**

Figure 5-12 shows the population density in Toronto. It can be seen that although most of the high-populated areas are located in Downtown Toronto, there are some neighborhoods with a high population close to Highway 401.
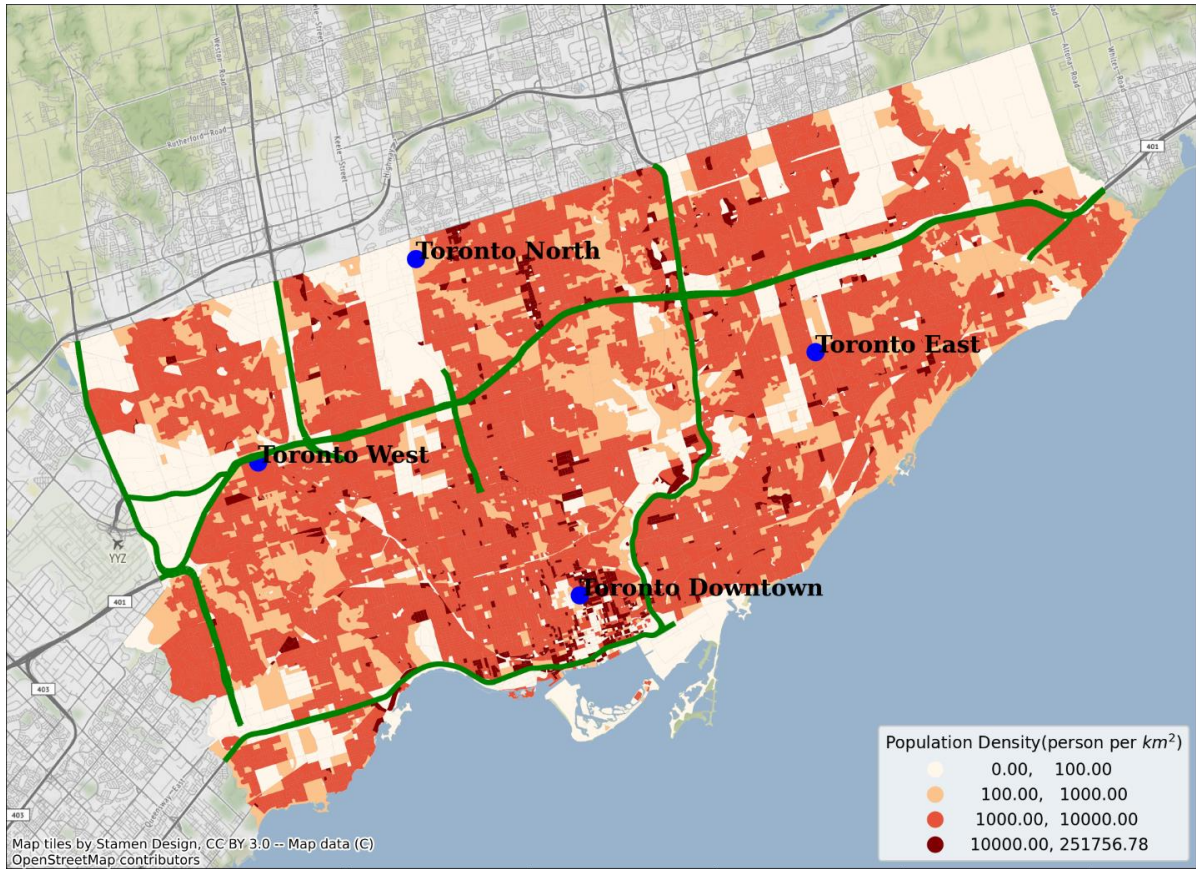
**Figure 5-12. Population Density in Toronto in 2016 (person per km2).**

Combining the results from Figure 5-9 and Figure 5-12, one can find the dissemination areas with higher $NO_x$ concentration due to Highway 401 traffic, shown in Figure 5-13. Analyzing Figure 5-12 and Figure 5-13 together, it can be seen that there are some dissemination areas with low population and high $NO_x$ concentration close to Highway 401, and some dissemination areas with high population and less $NO_x$ concentration far from Highway 401. These two types of dissemination areas are important in terms of health cost calculation. Although the health risk in far regions is lower, the high population increases

125

the number of events. On the other hand, although the population is low near the corridor, the higher concentration increases the health risk.
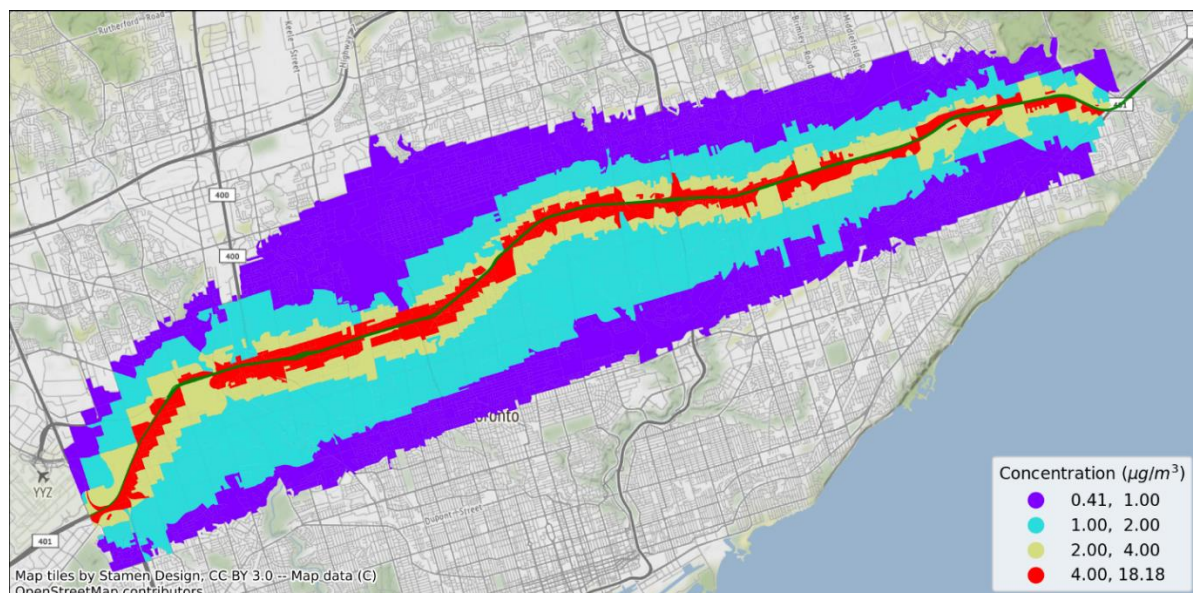


**Figure 5-13. Dissemination Areas with Higher Corridor-Related NO$_x$ Concentration (µg/m$^3$).**

Combining the population, NO$_x$ concentration, mortality rate, and increased risk of mortality, Figure 5-14 can be generated. The total increase in premature deaths due to Highway 401 traffic is 52 (95% CI 26–78). Using the mean VSL, the total cost of premature deaths due to Highway 401 NO$_x$ concentration equals CAD 416 million per year. In comparison to Chapter 4, in which the health cost of heavy-duty truck pollution along Highway 401 from Windsor to Montreal was estimated, the previous estimation was found to be much lower than the current estimation [11]. In Chapter 4, the health cost for all pollutants in all regions around Highway 401 from Windsor to Montreal was found to be around CAD 100 million per year. As stated in that study, estimating the health cost in urban areas using the national health cost average would considerably be underestimating. Table

5-8 shows the premature deaths prevented in different scenarios and the monetary benefits

of ZEVs in terms of health cost in each of these scenarios.
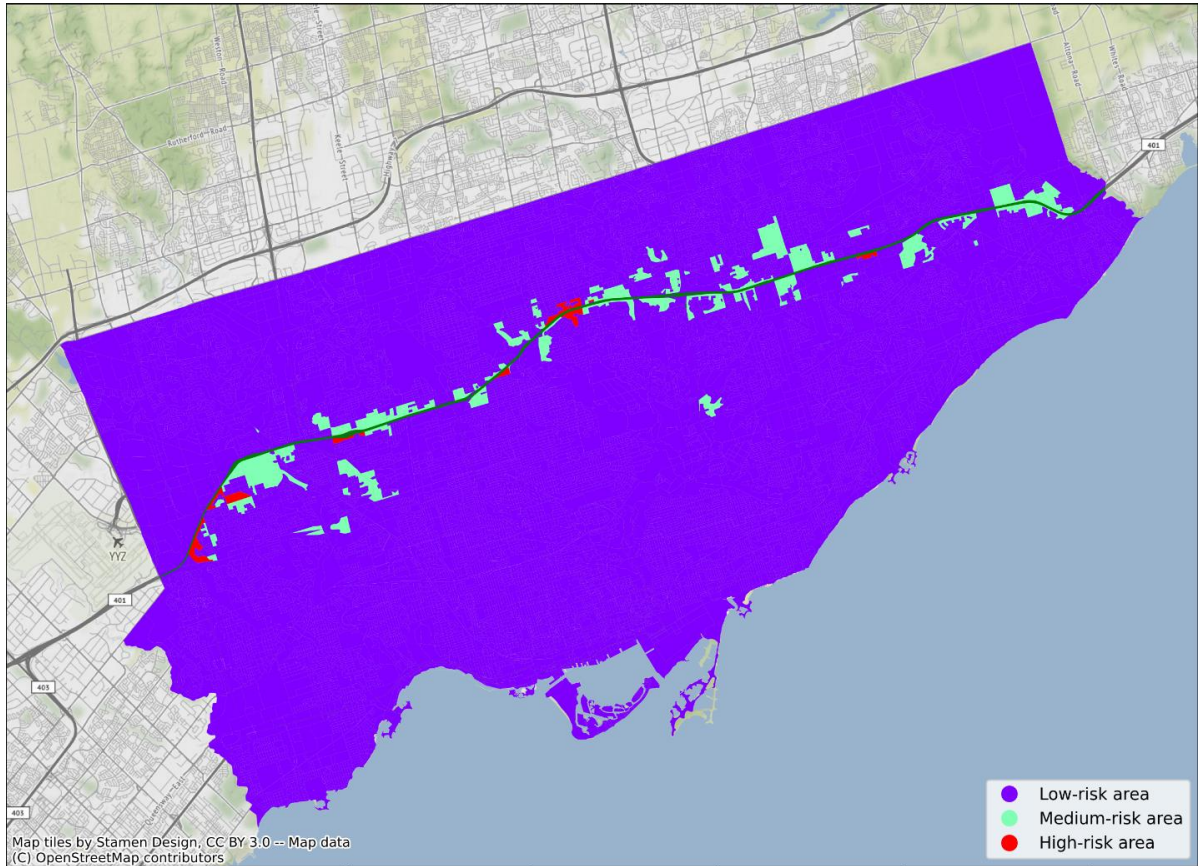


**Figure 5-14. Different Health-Risk Zones in Vicinity of Highway 401 due to Corridor-related**

**NO$_x$ pollution.**

**Table 5-8. Annual Health Benefit Under Different Traffic Profiles.**

| Scenario | Prevented death per year | Prevention of Mortality (CAD million/year) |
|---|---|---|
| Scenario 1 (10% EV) | 3 (95% CI 2–4) | 24 |
| Scenario 2 (10% FC Trucks) | 3 (95% CI 2–4) | 24 |
| Scenario 3 (50% EV) | 12 (95% CI 6–18) | 96 |
| Scenario 4 (50% FC trucks) | 14 (95% CI 7–21) | 112 |
| Scenario 5 (100% EV) | 24 (95% CI 12–36) | 192 |
| Scenario 6 (100% FC trucks) | 28 (95% CI 14–42) | 224 |

Figure 5-15 shows the comparison of the $NO_x$ concentration between all six scenarios. As can be seen, the annual average of highway traffic-related $NO_x$ pollution decreases by more than 50% in Scenario 6, in which all heavy-duty trucks become FC trucks. In other words, although heavy-duty trucks have less than 10% of the traffic count share, they are responsible for more than 50% of Highway 401 $NO_x$ pollution.
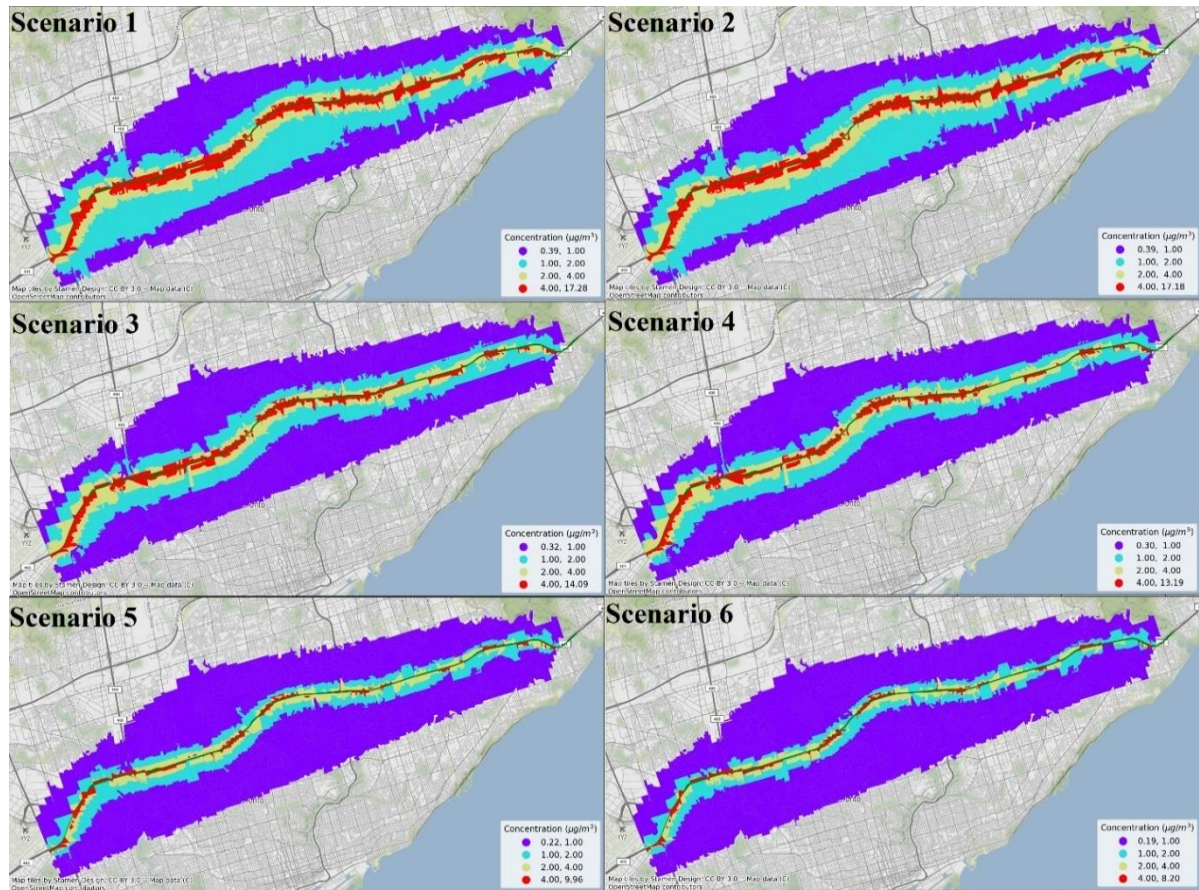
**Figure 5-15. Annual Average Corridor-related NO$_x$ Concentration in all scenarios (μg/m$^3$).**

Comparing the results from Table 5-7 and Table 5-8 one can see that the health cost of traffic for Highway 401 is much higher than the environmental cost. For instance, the health and environmental benefit of Scenario 6 (100% FC trucks) are CAD 224 million and CAD 5.7 million per year, respectively. In total, Scenarios 5 and 6 have the benefit of around CAD 241 million and CAD 230 million per year, respectively.

The results also show that despite a lower share of heavy-duty trucks in Highway 401 traffic, they have almost the same significance as passenger vehicles regarding total environmental and health costs. In other words, although reaching 100% FC trucks scenario

129

is more accessible than achieving 100% electric passenger vehicles in terms of effort and money, 100% FC trucks scenario has almost the same benefit as 100% electric passenger vehicles.

## 5.4   Conclusion

The transportation sector has the highest potential for environmental and health cost reduction amongst other energy-related sectors such as commercial, industrial, and residential. Specifically, pollutants such as PM, $O_3$, SOx, and $NO_x$ emitted from major highways significantly impact people's life expectancy. Also, these high-traffic highways have a significant role in producing GHG emissions. Substitution of passenger vehicles and heavy-duty trucks with ZEVs can reduce the negative impact of transportation on GHG emissions and health costs.

This chapter presented a model to investigate the environmental and health costs related to Highway 401, the busiest highway in Canada. An integrated model was built to calculate the health benefit of the substitution of fossil-fuel vehicles with ZEVs. A combination of MOVES2014b, WRF model, and AERMOD were used to calculate the concentrations of $PM_{2.5}$ and $NO_x$ in the vicinity of Highway 401. Then, the mortality risk of $NO_x$ was calculated using hazard ratios from the literature. The health cost of $NO_x$ in six scenarios was calculated using VSL. Also, GREET was used to assess life cycle $CO_2$ emission from heavy-duty trucks and passenger vehicles in six different scenarios. Then, the environmental cost was calculated by multiplying the total $CO_2$ emission in different scenarios by the Canadian carbon tax, which is CAD 40 per tonne of $CO_2$.

130

The results show that $NO_x$ has the highest impact on the mortality rate. Other pollutants are less likely to have high impacts on human health because of their lower concentration or lower hazard risk. Also, the health impact due to trucks pollution is higher than passenger vehicles, despite their lower traffic share. It can be concluded that investing in trucks pollution reduction is more rational. Also, the environmental cost of Highway 401 traffic is calculated to be CAD 55 million per year, which can be reduced to less than CAD 6 million per year by converting passenger vehicles to zero-emission electric vehicles. Also, converting all trucks to FC trucks can reduce the environmental cost to CAD 49 million per year. Finally, it was concluded that investing in FC trucks has a higher priority than investing in electric passenger vehicles. Despite a lower share in Highway 401 traffic, the economic benefit of the 100% FC truck scenario is almost the same as the 100% electric passenger vehicle scenario.

# 6. Traffic air pollution prediction and health cost estimation using machine learning: A case study of Toronto, Canada

## 6.1 Introduction

The transportation sector is one of the most energy-consuming economic sectors in the world. In 2018, about 50% of the world's oil consumption was used for road transportation [144]. Additionally, transportation is an essential contributor to economic development and social growth and this sector is expected to grow with population and economic growth. The utilization of this sector has risen over the years, with the number of passenger kilometers increasing by 260% in the Organisation for Economic Co-operation and Development (OECD) countries between 1970 and 2008[145]. [145]. However, since most automobiles use fossil fuels such as gasoline and diesel, the transportation sector negatively affects society through air pollution and greenhouse gas (GHG) emissions. In Canada, the transportation sector accounts for 24% of total annual emissions, with road transportation accounting for 82.5% of the transportation sector [77]. GHG emissions from the transportation sector are from  fossil fuel combustion in internal combustion engine vehicles (ICEVs) that provide transportation services. The GHG emissions and contribution to climate change are not the only externality of using fossil fuels in the transportation sector. Air pollution is the largest environmental cause of diseases and premature death in the world with an estimated 9 million premature deaths caused by pollution in 2015 accounting for 16%

of all deaths worldwide [146]. In some countries, pollution can be the cause of more than 25% of all deaths. In Canada, it was estimated that there were, on average, about 21,000 premature deaths caused by air pollution during the 2000s [80]. Some of the most common pollutants released from ICEVs include nitrogen oxides ($NO_x$), sulfur oxides ($SO_x$), and particulate matters ($PM_{2.5}$ or $PM_{10}$), all of which have negative effects on human health [147]. $NO_x$, $SO_x$, and particulate matters ($PM_{2.5}$ or $PM_{10)}$ air pollutants have been found to be a factor in causing serious diseases such as chronic obstructive pulmonary disease, chronic ischemic heart disease, diabetes, strokes, and tracheal, bronchial, and lung cancers [148].

Due to the negative effects on climate change and human health of traffic-related air pollution, governments around the world have started to focus more on cleaner transportation solutions [10]. Electric vehicles (EVs) are an excellent alternative to conventional vehicles because they are zero-emission vehicles (ZEVs) and do not release any harmful pollutants while on the road [112]. EVs can use batteries [111,149] or hydrogen fuel cells [88] as energy storage systems. Batteries are better suited for light-duty and passenger vehicles while hydrogen fuel cells are more fitted to be used in medium and heavy-duty trucks. Since heavy-duty trucks release more air pollutants than passenger vehicles, the use of hydrogen fuel cells in vehicles is more promising regarding the reduction of traffic-related air pollution [11].

Despite the advantages of EV deployment such as reducing air pollution and GHG emissions from the transportation sector, the transition from conventional vehicles to alternative options has been facing major challenges. The cost of infrastructure including

generation capacity, transmission lines, and charging/refueling infrastructure to support EVs, for instance, is a major roadblock to their mass rollout. As a result, the transition to EV utilization in the transportation sector, as in any sociotechnical system, must occur gradually and logically to ensure optimal outcomes in terms of socioeconomic benefits [150].

In recent years, many researchers have been working on investigating the benefits of EVs and their effect on the reduction of traffic-related air pollution and its negative health impact. Schneidemesser et al. [151], conducted a study to quantify the air pollution from vehicle use in urban areas. The authors in considered the effect of environment, density traffic, and vehicle type (buses, trucks, personal cars) on the particle concentrations. The focus of the analysis done in was to assess the cyclists exposure to pollutants and is was assessed by analyzing tracks with accompanying video footage. Ventura et al. [152], assessed the effect of vehicle inspection and maintenance programs on air pollution. The authors analyzed the available data from 2014 to 2017 in Rio de Janeiro state, Brazil. The conclusion of the analysis done in showed that lack of maintenance leads to the increase of CO and hydrocarbon emission from vehicle use up to 5 times compared to national limits. Ke et al. [153] developed a model to estimate energy consumption, GHG emissions, and pollutant emissions from different light-duty passenger vehicles. Each vehicle type emission was estimated using the assumed vehicle emission factors of various vehicle technologies. The emission factors for VOCs, $NO_x$, and PM2.5 for: multiport fuel injection (MPFI) vehicles, gasoline direct injection (GDI) vehicles, and hybrid electric vehicles (HEVs). The results of the analysis performed by Ke et al. [153], showed that while battery electric vehicles (BEVs) have a high potential in reducing pollution. The reduction of $NO_x$ from vehicle use, however,

depends on the source of electricity and will drop if the share of non-fossil electricity in imported power reaches 30%. Some researchers have used empirical data collection to assess the pollutant emissions from different types of vehicles. Kebede et al. [154], for instance, used random roadside testing of different public transport vehicles to analyze the standard compatibility of on-road vehicles. The analysis was done by collecting data from random roadside inspections of diesel-fueled vehicles in in Addis Ababa, Ethiopia. The authors tested 358 vehicles manufactured between 1960 and 2017 including minibuses, mid-sized bus, and large buses.

The limits of traditional methods have made machine learning a popular tool in recent years for air pollution modelling. Machine learning is used to refer to a wide range of techniques that use available data to gain knowledge about the correlation of different parameters and enable forecasting. Bougoudis et al. [155], developed a machine learning model to forecast the air pollutant concentration in the Attica area, Greece. The model developed used clustered datasets that shared similar characteristics including pollutant concentration, day, hour, month, temperature, and relative humidity. In this way, the model gained the knowledge on the correlation of the different factors on pollutant concentration. The model then used the knowledge to forecast pollutant concentration based on contributing factors. Lautenschlager et al. [156] developed a machine learning for air pollution modeling that could work based on openly available data source OpenStreetMap. Sinnott and Guan [157] assessed the potential of linear regression models, artificial neural network (ANN) and long, short term memory (LSTM) models in PM2.5 pollution prediction. The results of the analysis done in showed LSTM forecasted the PM2.5 concentration with

the highest accuracy. Both linear regression and ANN models did not perform well in forecasting high PM2.5 concentration values.

Air pollution modeling is used in the literature to quantify the reduction of air pollution by mass EV rollout. A common approach to model the spatial distribution and concentration of traffic-related air pollution is the land use regression model [158].

Wen et al.[159] developed a novel spatiotemporal convolutional long short-term memory (LSTM) neural network to predict air pollution concentration. The model inputs were the delay between PM2.5 concentrations from monitoring stations as well as some meteorological and aerosol data such as humidity, temperature, wind speed, planetary boundary layer height, and aerosol optical depth (AOD) near the stations. PM2.5 concentration data from over 1000 air quality monitoring stations in China were used to validate the model [152]. The use of meteorological and aerosol data was found to improve the accuracy of the proposed model significantly. Tong et al. [160], proposed a deep learning spatiotemporal model combining LSTM and recurrent neural network to predict the daily concentration of PM2.5. Due to the lack of data, only three features were used, which were longitude, latitude, and time. The model was validated using ground PM2.5 data from the US Environmental Protection Agency (EPA) 's Air Quality System (AQS) and was found to have acceptable accuracy. Adding more features such as AOD, land use, roads, emissions, elevation, and weather conditions could improve the accuracy of the model, as it was determined that the temporal correlation was superior to the spatial correlation. Huang et al. [161], predicted the PM2.5 concentration in the air in Beijing and Shanghai using a deep neural network model which was the combination of LSTM and convolutional neural

network. The input features used in the model included $NO_x$ concentration, accumulated wind speed, and accumulated hours of rain. Results showed that the overall accuracy of the model was verified with low average mean absolute error (MAE) and root mean square error (RMSE) from the model outputs. Fan et al. [162], presented a spatiotemporal prediction framework using a deep recurrent neural network consisting of LSTM layers and fully connected layers. This model was able to handle missing data in the time series. The model was trained using real-world air quality and meteorological datasets in the Jingjinji area of China, and it was found to have a high accuracy in predicting sudden heavy pollution events and average patterns. Qin et al. [163], were able to forecast the PM2.5 concentrations in some regions of China as a time series. A convolutional neural network was used as the base layer to extract input features, which were meteorological data and pollutant concentrations in their air pollution prediction model. An LSTM network was also used to extract the time-series features for the input data. This approach performed well in predicting PM2.5 concentrations, but it could be improved by adding more factors such as geomorphic conditions. Šimić et al. [164], compared the performance of five different machine learning regressors in regards to predicting PM10 and NO2 concentrations in the city of Zagreb, Croatia, and found that Lasso regression was the best performing algorithm. Additionally, it was shown that seasonal weather conditions and traffic locations affected the concentrations significantly. Li et al. [165], used machine learning algorithms to determine hourly street-level PM2.5 and $NO_x$ concentrations. Random forest was determined to the best-performing algorithms out of the six that were utilized and evaluated. It was also found that non-emission factors, like non-local pollution and temperature, accounted for a significant

137

amount of pollution concentration predictions, while the rest came from direct emission contributors like vehicles.

The review of the air pollution modeling literature shows that the research is mainly focused on analyzing PM2.5 emission. However, $NO_x$ emission modeling has not be thoroughly investigated in the literature, although $NO_x$ is a harmful pollutant is released in large quantities by diesel vehicles which are very common in the transportation sector. $NO_x$ is the cause of many health concerns, including serious respiratory diseases[166]. About 10,000 premature deaths in Europe in the year 2013 can be attributed to high $NO_x$ emissions from light-duty diesel vehicles[167]. In that sense, it is crucial to use machine learning methods to investigate and predict $NO_x$ concentration from fossil fuel consumption and to quantify the health benefits of $NO_x$ reduction via the transport electrification.

In this work, $NO_x$ concentration in Toronto is predicted using an LSTM model that is trained based on previous timestep data. The Keras module in Python is utilized to develop the model. LSTM is a recurrent neural network model that uses a sequence of data to predict the outcomes in the future. It is widely used to predict energy consumption, weather forecast, traffic forecast, or air pollution concentration [163,168–172]. The neural network undergoes a sensitivity analysis to determine the best network parameters. A long-term prediction is then presented using the developed model. Finally, the health and economic benefits of ZEVs are estimated using the results from the machine learning air pollution prediction model.

Air pollution concentration in an area is a function of pollutant sources and weather conditions. Traffic-related air pollution, HVAC (heating, ventilation, and air conditioning)

system air pollution, and out-of-Toronto air pollution are critical sources of pollutant emissions in the city of Toronto. Weather parameters including temperature, wind, humidity, precipitation, and solar radiation are also factors that can affect pollution concentrations in different areas.

This research contributes to the literature by:

• Using a machine learning model to predict air pollution in the city of Toronto;

• Using traffic data, in addition to air pollution data and weather data, as an input to the LSTM model that is used to predict air pollution centration in different areas of Toronto; and

• Estimates monetized health impacts from pollution emission base on the concentration predicted by the model.

## 6.2 Methodology

This section provides an overview of the methodology and assumption used for modeling $NO_x$ emission in this work. Figure 6-1 shows the methodology used to estimate the health cost caused by traffic-related air pollution in Toronto.
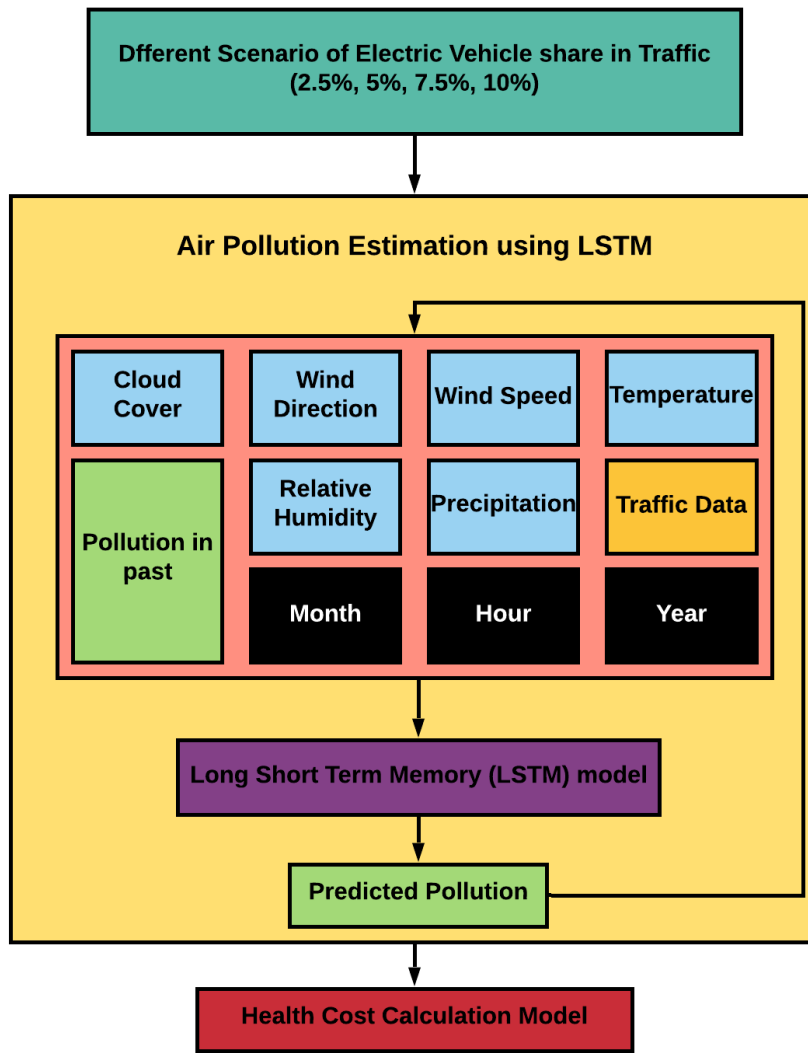
**Figure 6-1. Methodology used to estimate the health benefit of increasing EV share in Toronto**

In the model developed in this work, Long Short-Term Memory (LSTM) model is first developed using features including weather data and time of the day as shown in Figure 6-1. The objective of the LSTM model is to predict the $NO_x$ pollution based on the weather, time, traffic count, and $NO_x$ pollution from previous timesteps. The developed model is then used

to estimate annual average $NO_x$ concentration in four different locations in the city of Toronto in four different scenarios. The annual average $NO_x$ concentration in Toronto's Dissemination Areas (DA) is estimated using nearest, linear, and cubic interpolation methods. Based on the estimated pollution reduction and population data, the decrease in mortality rates is calculated using Hazard Ratio (HR). Finally, the prevented deaths in all scenarios are converted to monetary values using Value of Statistic Life (VSL) [140].

Figure 6-2 shows the features used to predict the $NO_x$ concentration in Toronto. There are four air pollution monitoring stations in Toronto: Toronto Downtown, Toronto East, Toronto North, and Toronto West. The hourly concentration of different pollutants in these four stations is available online [173]. Also, the hourly traffic count data in forty stations were used to input the LSTM model [174]. The other input to the LSTM model is the weather data as it has a significant effect on pollution dispersion. Time data, including year, month, day of the week, and hour of the day are used to consider the temporal effects on $NO_x$ concentration.
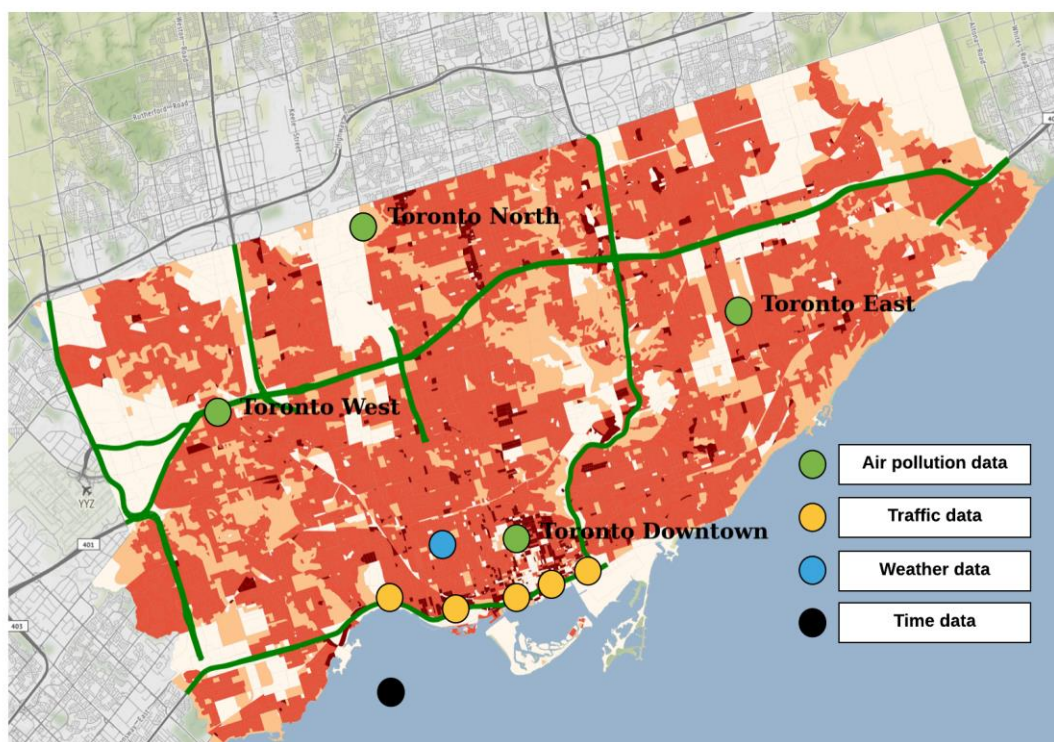
**Figure 6-2. Schematic of features used in the LSTM model.**

The details of different inputs to the model are described below.

### 6.2.1   Weather data

The hourly weather data in the Toronto City Centre station is extracted for the 2015-2017 interval [175]. It includes temperature, relative humidity, wind direction, and wind speed. To shed light on the weather properties in this chapter, a brief explanation is represented below.

### 6.2.2 Temperature

Figure 6-3 shows the monthly average temperature changes. shows the hourly average temperature for each month in the city of Toronto. As can be seen in Figure 6-3 the temperature drops to a minimum in the early morning and has a maximum in the afternoon in all months. A comparison of Figure 6-3 and Figure 6-8 shows the idea that an increase in the temperature on the ground has a significant impact on the amount of $NO_x$ concentration.
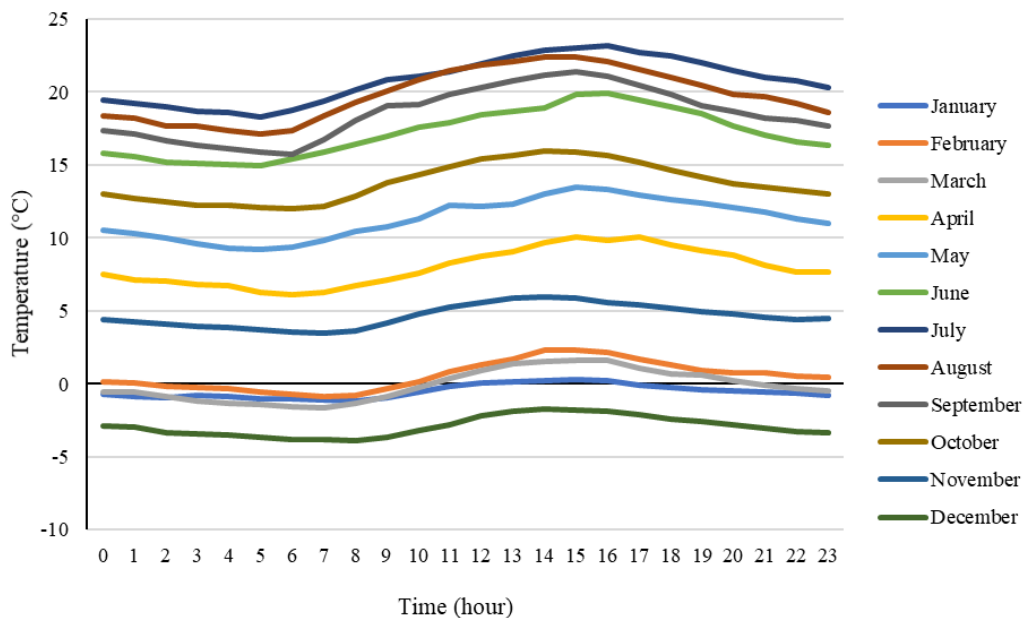


**Figure 6-3. Temperature monthly average during a day for different months.**

### 6.2.3 Wind Speed

Figure 6-4 shows the hourly average wind speed changes during the day for each month. Except for December and January, the wind speed profile shows a vast difference between morning and afternoon wind speed. Also, it can be seen that the wind speed is higher in

colder months. Wind speed not only affects the dispersion of the pollutants, but also can influence the amount of pollutants coming from other regions.
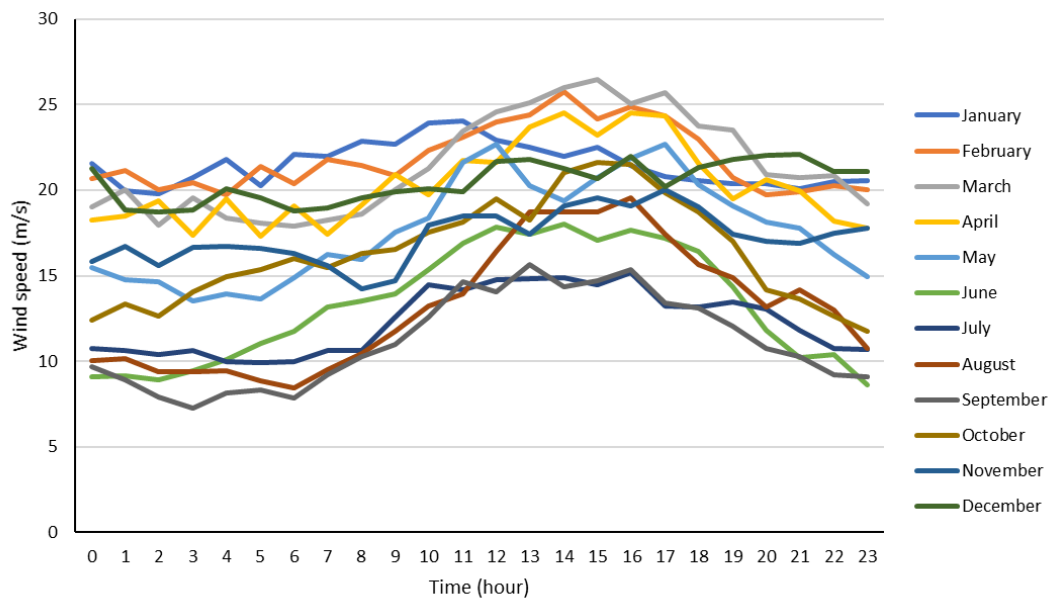


**Figure 6-4. Monthly average of Wind Speed during a day.**

### 6.2.4 Precipitation

The hourly data for precipitation could not be found on the web; however, the number of days with precipitation depicted in the figure below can show the importance of such a dataset. Figure 6-5 shows the number of days with precipitation (rain or snow) in each hour during a year. Instead of precipitation quantity, the weather condition is used as a feature to train the machine learning model. In this regard, three weather conditions are considered: No precipitation, Rainy, and Snowy.

144
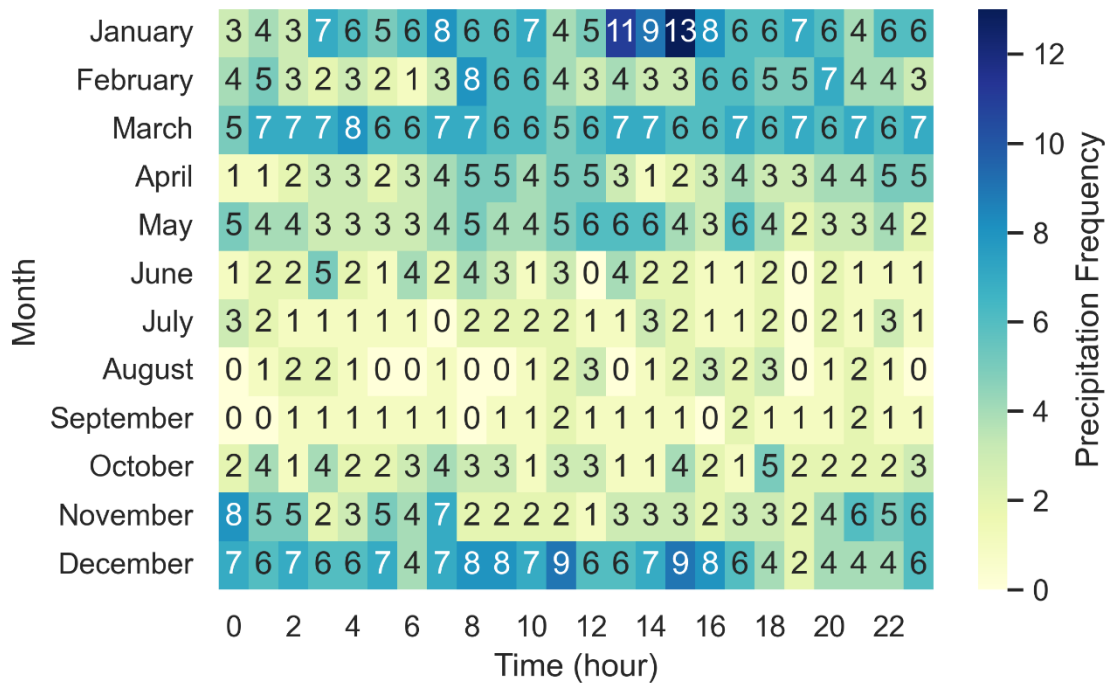
**Figure 6-5. Number of days with precipitation in each single hour.**

### 6.2.5 Traffic count data

Figure 6-6 and Figure 6-7 show the traffic count distribution over a year for a single location (Lake Shore Blvd, East Bound, West of Oarsman Dr) in the city of Toronto is shown [174]. The number of vehicles on weekdays is higher than on weekends. Also, the traffic pattern is different for weekdays and weekends because of work commuters during weekdays. As a result, the day of the week is chosen to be an input feature to the LSTM model for predicting air pollution.
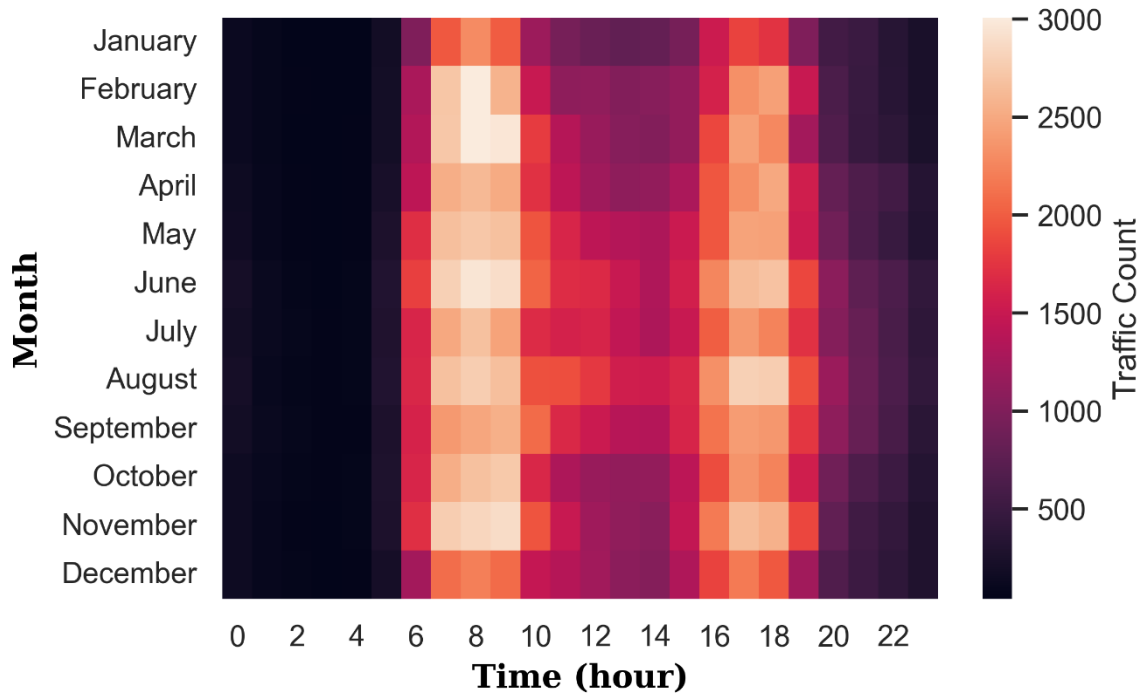


**Figure 6-6. Monthly average traffic count data (Weekdays).**
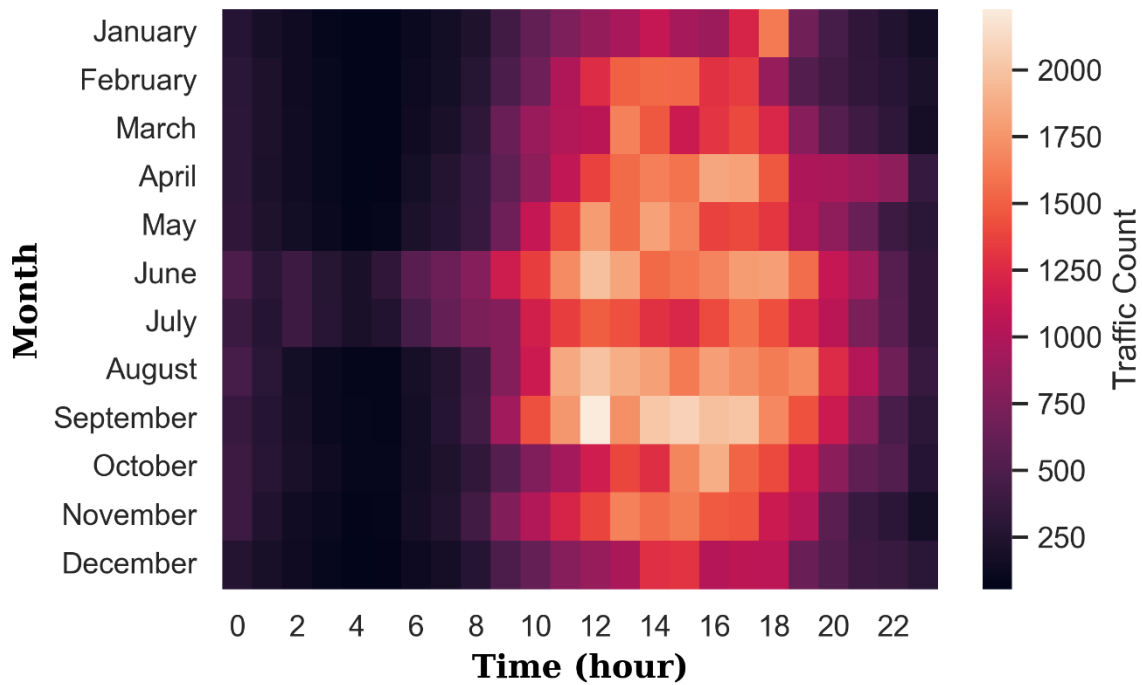
**Figure 6-7. Monthly average traffic count data (Weekends)**

### 6.2.6 Air pollution data

Figure 6-8 shows the monthly average $NO_x$ concentration at the Toronto Downtown air pollution measurement station. The minimum amount of air pollution, at this station, happens in the months of May through July, during the Spring and early Summer. The main reasons for this pattern are the higher use of heating systems and variation of sunlight in Winter and Summer.
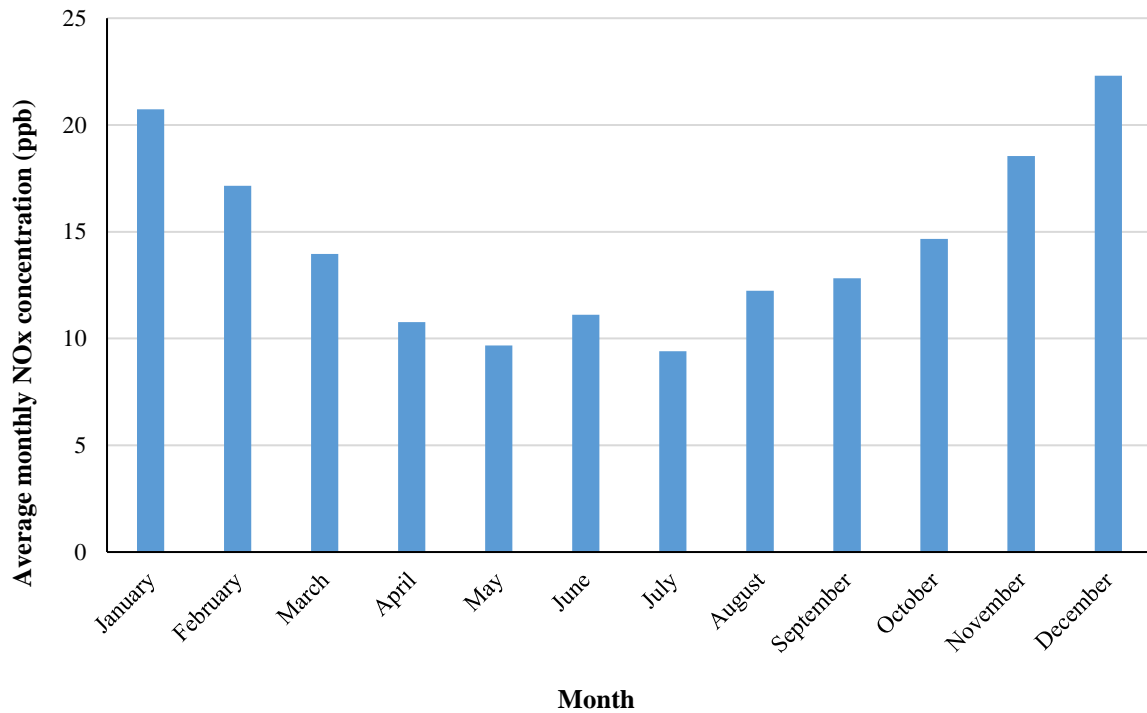
**Figure 6-8. Monthly average NO$_x$ concentration- Toronto Downtown station.**

Figure 6-9 shows the hourly average NO$_x$ concentration during a day in 3 different months. As can be seen, NO$_x$ concentration has a consistent pattern during the day for all three months. It reaches a maximum in the early morning as many people commute to work, so the number of vehicles is a key factor in the morning. Also, after sunset, the pollution starts to increase again. This happens because the sun heats the ground during the day, which results in more air movement during the day.
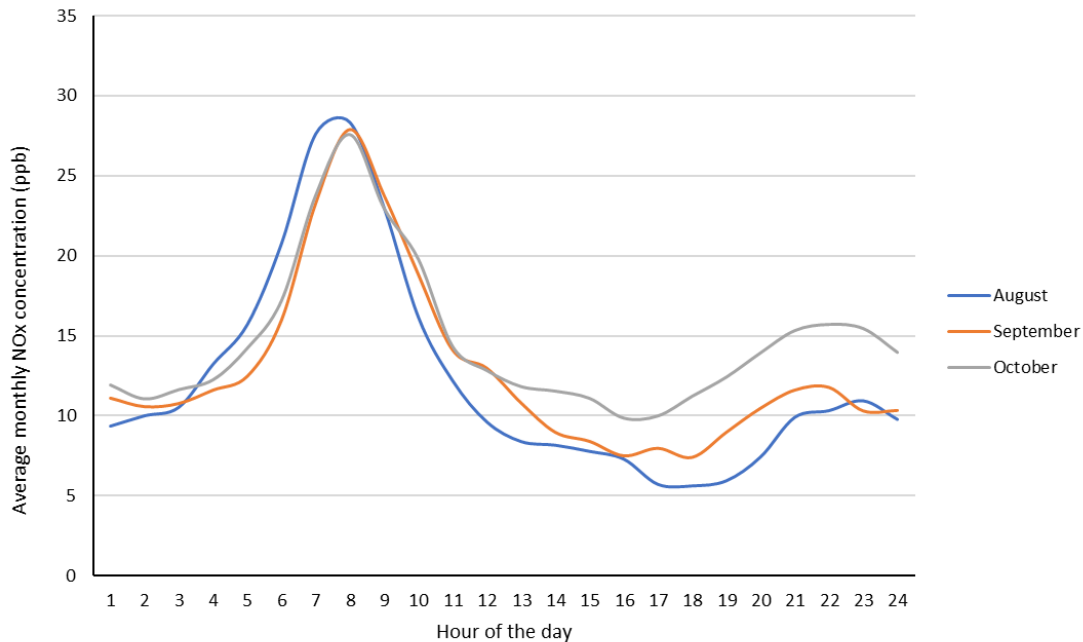
**Figure 6-9. Monthly average of NO$_x$ concentration during a day in August, September, and October.**

### 6.2.7    Air Pollution Estimation Model

To estimate the air pollution at four locations in the city of Toronto, a Long Short-Term Memory (LSTM) model is used. LSTM models are a type of recurrent neural network for learning sequence prediction problems. Keras library is being used in this problem to build the deep learning model. Keras is an open-source library which acts as an interface for TensorFlow library which is a machine learning and artificial intelligence library.  Figure 6-10 shows the features used to learn the LSTM model. The features include weather, traffic count, time, and pollution from past timesteps. To prepare the data, it was found that there are missing values, especially among the 40 traffic count station data. To increase the number of datapoints, the traffic count stations with many missing values are disregarded.

This decreases the number of stations used in the analysis from more than 40 stations to 8 stations. Also, to overcome the complexity of the model, the number of traffic count stations at the input to the model is reduced from 40 to 3. In other words, the 3 traffic count locations that have the largest impact on air pollution are kept, and the other 37 locations' data is disregarded. MinMaxScaler function is used to scale all the features into [0,1]. This will help to find the importance of each feature while disregarding its order of magnitude. The maximum epoch is considered high enough to make sure that the model is learned completely. Also, an early stopping function is added to the model to avoid overfitting. In this regard, if the amount of validation loss does not get better in 50 epochs, the learning process will stop, and the weights are extracted from the best validation loss epoch.
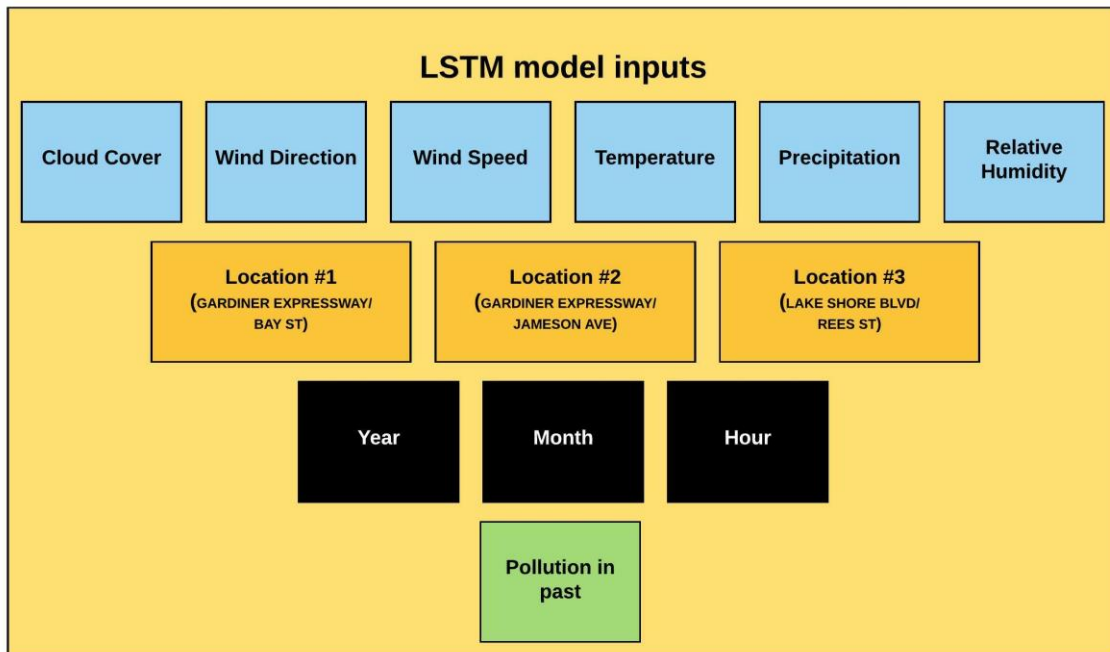


**Figure 6-10. Input features for LSTM NO$_x$ concentration prediction model.**

A sensitivity analysis is conducted to find the best model parameters such as number of timesteps, number of layers, number of nodes in each layer, loss function, optimizer, and etc. The final structure of the neural network is shown in Figure 6-11. Also, the learning model parameters are shown in Table 6-1.

| lstm_1_input: InputLayer | input: | (None, 2, 13) |
|---|---|---|
| | output: | (None, 2, 13) |

| lstm_1: LSTM | input: | (None, 2, 13) |
|---|---|---|
| | output: | (None, 2, 13) |

| lstm_2: LSTM | input: | (None, 2, 13) |
|---|---|---|
| | output: | (None, 2) |

| dense_1: Dense | input: | (None, 2) |
|---|---|---|
| | output: | (None, 1) |
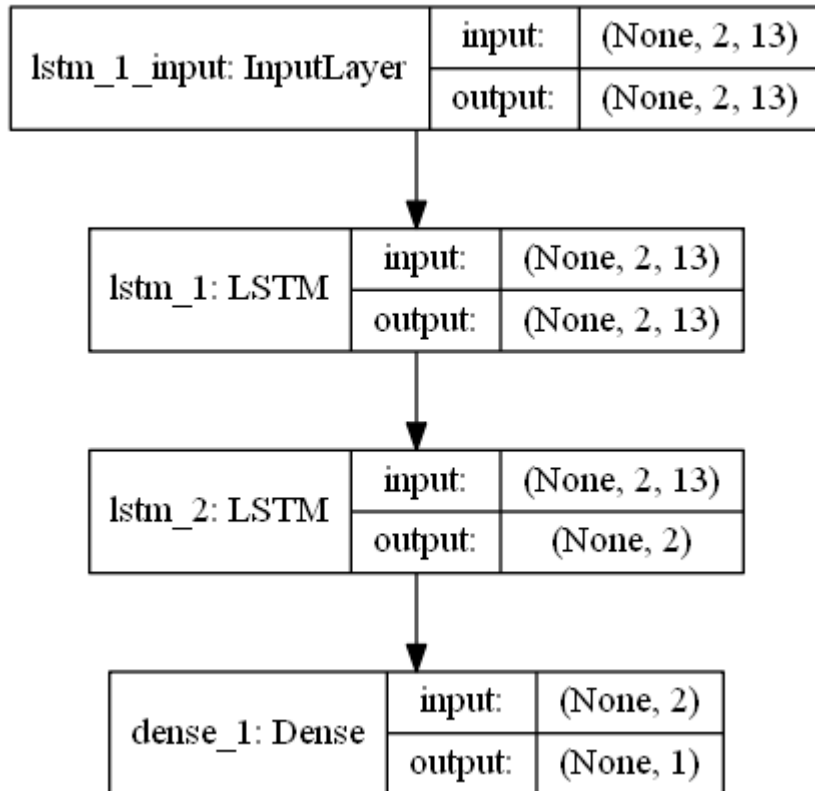
**Figure 6-11. LSTM neural network structure.**

**Table 6-1. LSTM parameters.**

| Parameter | Value |
|---|---|
| Loss function | Mean squared logarithmic error |
| Optimizer | adam |
| Batch Size | 32 |
| Early Stopping Patience | 50 |
| Number of hidden layers | 2 |
| Number of timesteps | 2 |
| Scale function | MinMaxScaler function |
| K-Fold cross-validation | K=5 |

5-fold cross-validation is utilized to find the effect of timestep number in predicting $NO_x$ concentration. K-fold cross validation is a method for finding best evaluation of a machine learning model. In this method, the dataset is randomly partitioned into k subsamples. The model error, then, is calculated by utilizing k-1 subsample as training data, and the last subsample as the validation data. The mean-squared error is calculated for different timesteps and different air monitoring stations. The result is shown in Table 6-2. As can be seen, except for one station, the mean-squared error is lower when assuming two timesteps to predict the $NO_x$ concentration.

**Table 6-2. Mean-Squared error for different timesteps and different locations.**

| Number of timesteps | Toronto Downtown | Toronto East | Toronto West | Toronto North |
|---|---|---|---|---|
| 1 | 5.5176 | 6.9964 | 9.364 | 6.1298 |
| 2 | 5.4924 | 6.812 | 9.3108 | 6.0052 |
| 4 | 5.5172 | 6.8026 | 9.3168 | 6.006 |

One of the challenges of forecasting air pollution using LSTM is long-term prediction is not possible. In other words, it is less challenging when the objective of the problem is to predict the pollution concentration in time t using data from time t-1, t-2, t-3, …, t-n; however, it is more difficult to forecast more steps in the future.

As the aim of the current study is to calculate the impact of changing the share of EVs, it is assumed that all features except traffic count data stay unchanged between each scenario. Then, by changing the traffic counts based on different scenarios, the effect of EVs and ICEVs on pollutant concentration can be estimated. The challenging part is that $NO_x$ concentration at time t heavily depends on concentration at times t-1, t-2, .., t-n, where n is the number of timesteps in the LSTM model. In other words, $NO_x$ concentration at previous timesteps not only affects the concentration at time t but also has an impact on concentration at future timesteps. To overcome this problem, the predicted values of $NO_x$ concentration are used as an input to the model. In other words, assuming timestep=2, the $NO_x$ concentration at time t=3 is predicted using the actual data at time t=1 and t=2; however, the $NO_x$ concentration at time t=4 is predicted using actual concentration at time=2 and predicted concentration at t=3. Also, pollution at t=5 is predicted using predicted values of pollution at t=3 and t=4. It is worth mentioning that the actual values of other inputs such as weather and time data are used in all timesteps. Following this method, air pollution data is provided to the model just for the first two steps. As a result, a higher prediction error is seen due to error propagation. However, this method makes the LSTM model predict $NO_x$ concentration in the long term, which makes the model capable of finding the effect of traffic count on long-term $NO_x$ concentration.

### 6.2.8 Health Cost Calculation

Figure 6-12 shows the model used to calculate the health benefit from increasing EV market share. First, the traffic count from different scenarios is imported to the learned LSTM model. The LSTM model, which is previously learned using current data, is capable of predicting hourly $NO_x$ concentration in different scenarios. An annual average of $NO_x$ concentration is then calculated in four air monitoring stations. To acquire the annual average $NO_x$ concentration in all dissemination areas, three different interpolation methods are used: Linear, cubic, and nearest method. Using Hazard Ratios (HRs) from [176], the risk of mortality in all scenarios is calculated. Having population, current average mortality rate, and decreased risk of mortality, the annual prevented deaths in all DAs are calculated. Finally, the annual deaths prevented are converted into monetary values using the Value of Statistical Life (VSL) in Canada.
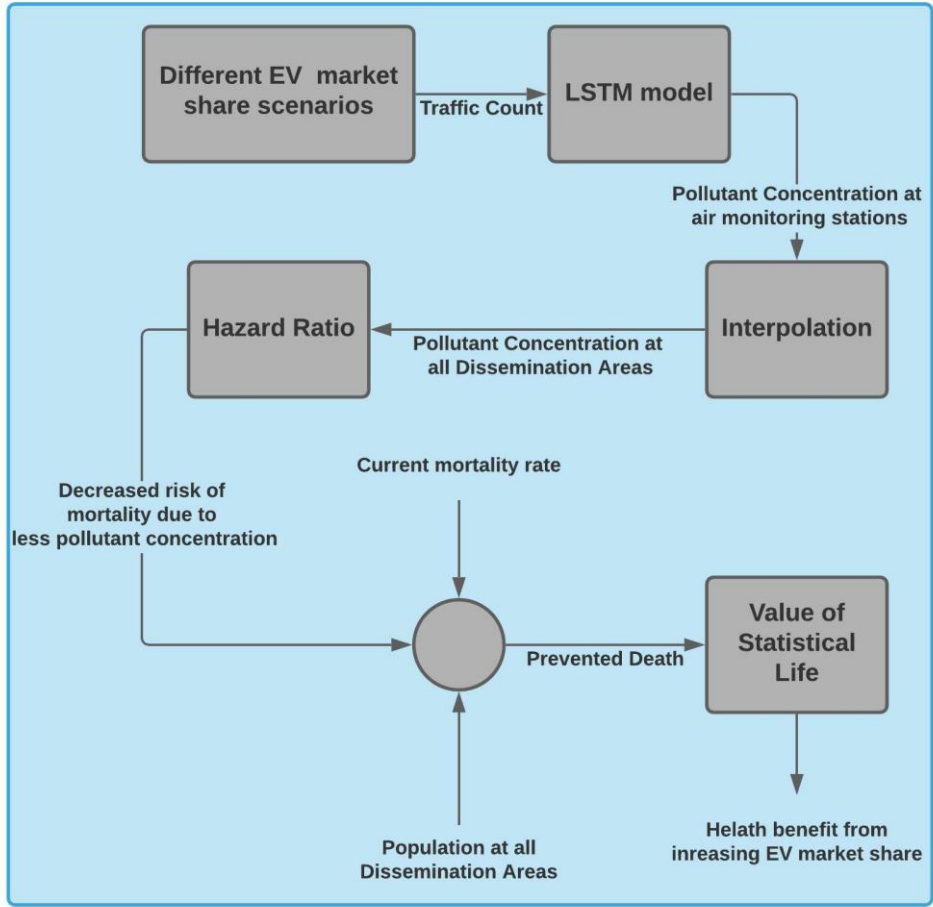
**Figure 6-12. Calculation Process of health benefit due to increased market share of EV.**

Different reductions in traffic count in different scenarios are shown in Table 6-3. Different scenarios are considered to investigate the performance of the model on different inputs. Also, to avoid major errors, significant EV market share increase is not considered, because it might negatively affect the accuracy of air pollution prediction.

**Table 6-3. Reduction in traffic count in different scenarios**

| Scenario | Reduction in Traffic |
|----------|---------------------|
| 1 | 2.5% |
| 2 | 5% |
| 3 | 7.5% |
| 4 | 10% |

## 6.3 Results

Figure 6-13 shows the comparison between the predicted and actual amount of $NO_x$ concentration in Downtown Toronto station using different methods of implementing the LSTM model. In the original LSTM model, during the whole time series, the actual pollution is used to predict future pollution. However, in the alternative method of implementing the LSTM model, a prediction is made based on the previously predicted data. As can be seen in Figure 6-13, the error in the original method is less than the error in the modified method. The mean-squared error in the original method and the modified method are 5.31 ppb and 8.82 ppb, respectively. The annual average of the predicted $NO_x$ concentration in the Toronto Downton air pollution monitoring station is 15.83 ppb and 13.92 ppb using the original and modified method, respectively, where the actual annual average of $NO_x$ concentration in this station is 16.36 ppb. The results show that although the error in the modified method is higher than the original method, the model can still make a reasonable prediction. The reason is that although pollution is predicted based on previous predicted pollutions, actual data are used for other features such as weather, time, and traffic count data. Also, as noted before, using the modified version provides the ability to make long-term predictions, which is the necessity of the current research.

157
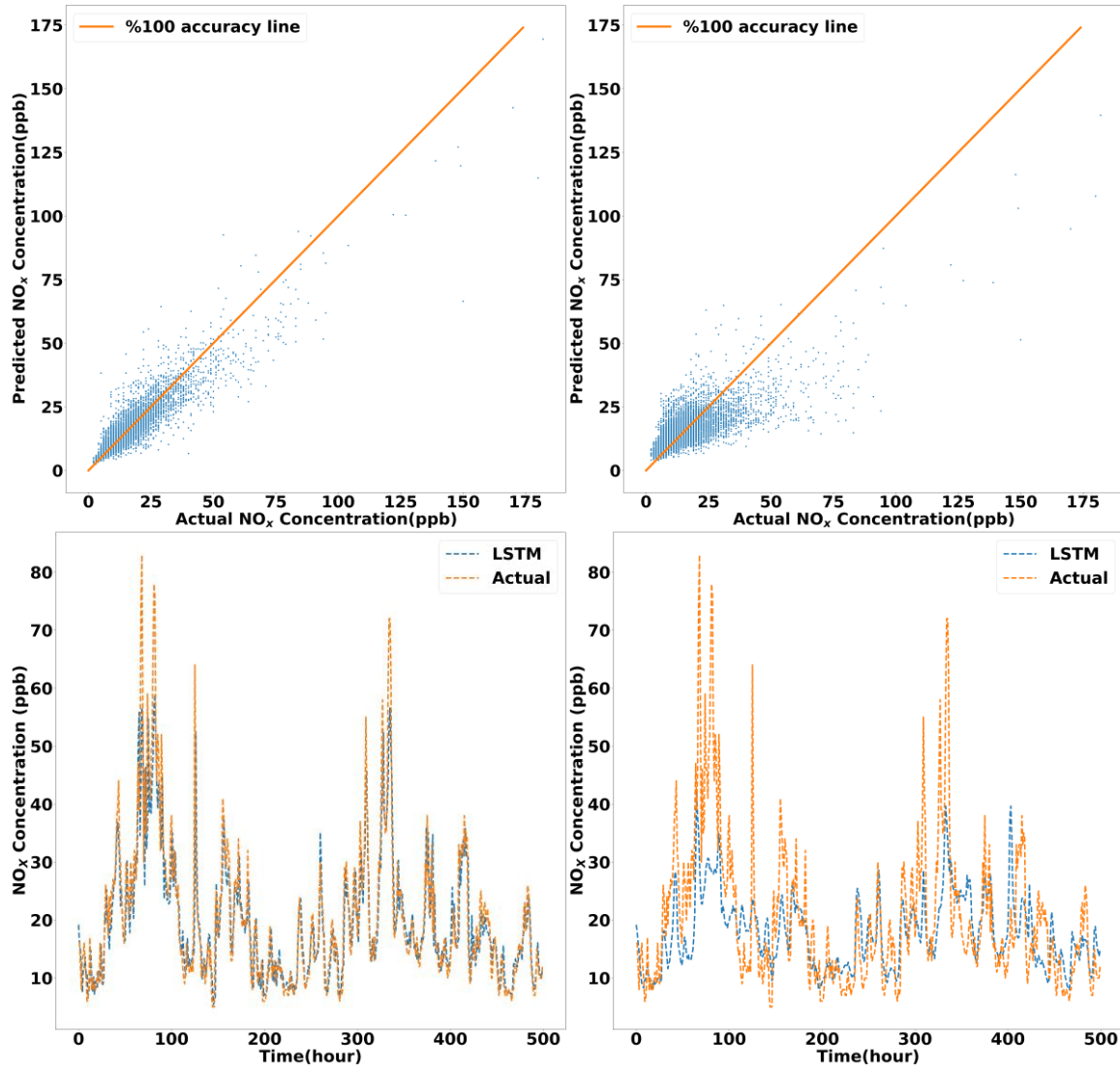
**Figure 6-13. Toronto Downtown NO$_x$ concentration prediction using LSTM and modified LSTM model**
(Top left) Comparison between predicted and actual NO$_x$ concentration using LSTM model.
(Top right) Comparison between predicted and actual NO$_x$ concentration using modified LSTM model.
(Bottom left) First 500 hours of predicted and actual NO$_x$ concentration using LSTM model.
(Bottom right) First 500 hours of predicted and actual NO$_x$ concentration using modified LSTM model.

Due to the stochastic nature of the algorithm or evaluation procedure, or differences in numerical precision, the output of the model may be different every time the learning procedure is conducted. In order to overcome this issue, the training process is applied five times for each location. Then, the Mean-Square Error (MSE) and the annual average error are calculated as an average of the different learned models. The results are shown in Table 6-4.

**Table 6-4. LSTM model error.**

| Parameter | Toronto Downtown | Toronto East | Toronto North | Toronto West |
|---|---|---|---|---|
| **Actual NO$_x$ concentration annual average (ppb)** | 17.3281 | 18.57291 | 16.25966 | 24.64313 |
| **Predicted NO$_x$ concentration annual average (ppb)** | 16.35 | 18.03422 | 15.96259 | 24.6445 |
| **Annual average prediction error (%)** | 5.98% | 2.99% | 1.86% | 0.01% |
| **Mean-Squared Error** | 8.690333 | 13.72669 | 11.54073 | 18.61467 |

As can be seen, the model is highly accurate for all locations. The MSE is lower in the Toronto Downtown station. The reason could be due to the proximity of the Toronto Downtown monitoring station and traffic count locations. Due to the lack of data, almost all traffic stations are located in downtown Toronto. This could result in higher MSE in other locations. Nevertheless, the model shows a high accuracy in predicting annual average NO$_x$ concentration in all stations, which is required for health cost calculations.

The models are next utilized to calculate NO$_x$ concentration in different scenarios as mentioned in Table 6-3. Again, to overcome the stochastic nature of the model, calculations are made five times for each location and each scenario. The results of these analyses are shown in Table 6-5.

159

**Table 6-5. Annual average NO$_x$ reduction in different scenarios (ppb)**

| Scenario | Toronto Downtown | Toronto East | Toronto North | Toronto West |
|---|---|---|---|---|
| Scenario 1 (2.5% reduction in traffic count) | 0.17 | 0.27 | 0.31 | 0.34 |
| Scenario 2 (5% reduction in traffic count) | 0.34 | 0.55 | 0.60 | 0.67 |
| Scenario 3 (7.5% reduction in traffic count) | 0.51 | 0.84 | 0.88 | 1.01 |
| Scenario 4 (10% reduction in traffic count) | 0.68 | 1.11 | 1.14 | 1.34 |

As can be seen in Table 6-5, the highest NO$_x$ reduction can be achieved in Toronto West station. There are two explanations for this possible reduction. First, Toronto West station is in the vicinity of Highway 401, which is one of the busiest highways in North America, thus, the pollution at the Toronto West station is more dependent upon traffic volume. Secondly, the average NO$_x$ concentration is higher in the western regions of Toronto, so the change in traffic volume can have a higher impact on NO$_x$ reduction. The lowest reduction happens in the Toronto Downtown station that is due to low average concentrations and its location near Lake Ontario.

To find the annual average NO$_x$ concentration reduction in all locations in Toronto, three different methods of interpolation are used: linear interpolation, cubic interpolation, and nearest interpolation. For the regions outside the quadrilaterals in between four air monitoring stations, the nearest method is used. The results of interpolation in different scenarios and different interpolation methods are shown in Figure 6-14.
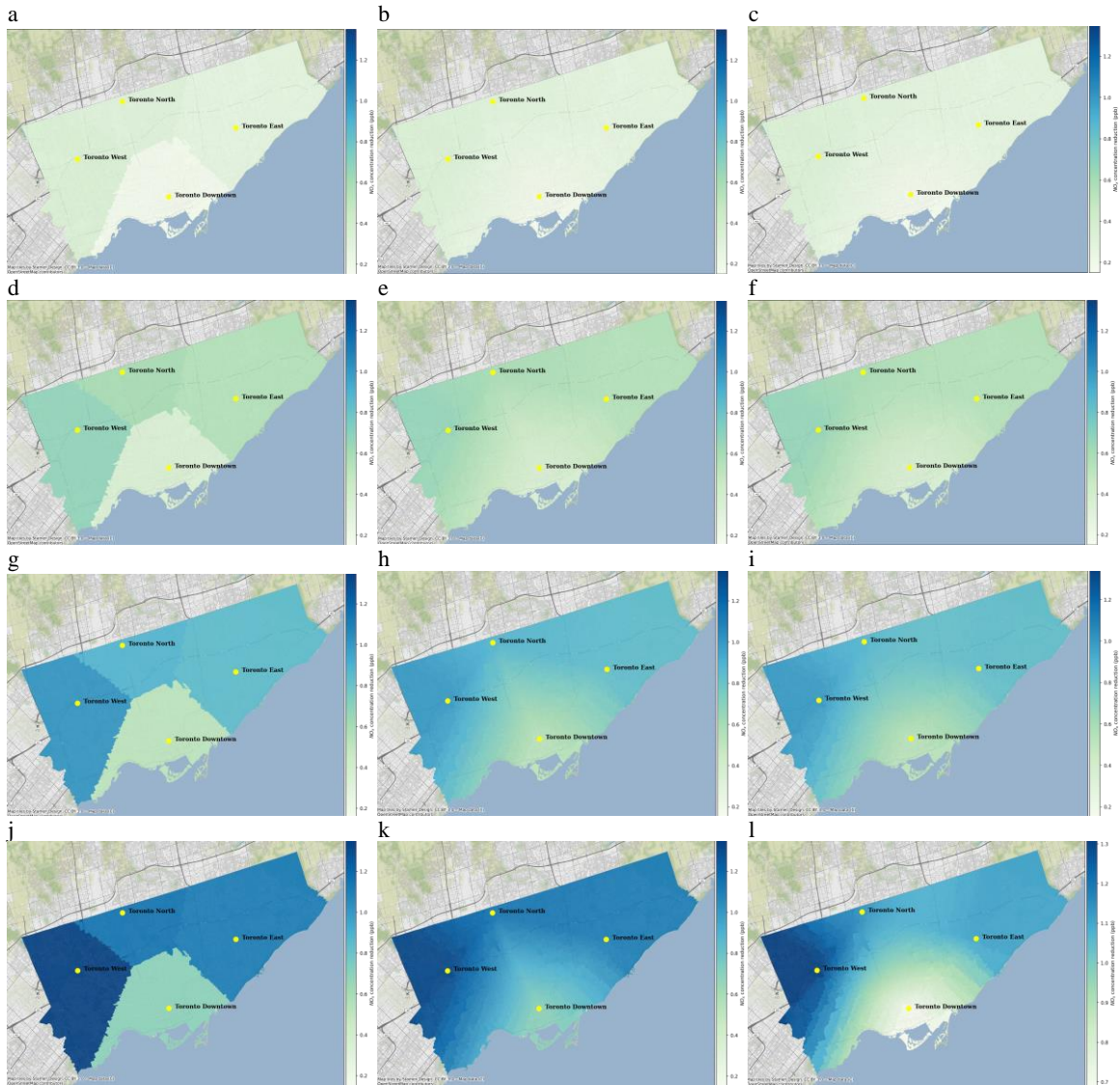
**Figure 6-14. NO$_x$ concentration reduction in different scenarios and different interpolation methods.**
(a) Scenario 1, Nearest interpolation method, (b) Scenario 1, Linear interpolation method,
(c) Scenario 1, Cubic interpolation method, (d) Scenario 2, Nearest interpolation method,
(e) Scenario 2, Linear interpolation method, (f) Scenario 2, Cubic interpolation method,
(g) Scenario 3, Nearest interpolation method, (h) Scenario 3, Linear interpolation method,
(i) Scenario 3, Cubic interpolation method, (j) Scenario 4, Nearest interpolation method,
(k) Scenario 4, Linear interpolation method, (l) Scenario 4, Cubic interpolation method.

As can be seen in Figure 6-14, linear interpolation and cubic interpolation show a very slight difference. As stated before, the highest $NO_x$ reduction occurs in the western regions of Toronto, and the lowest reduction occurs in southern regions. Scenario 4, which is reducing fossil fuel vehicles by 10%, has the highest pollution reduction as expected. It is worth mentioning that interpolation causes possible inaccuracy in $NO_x$ reduction estimation; however, with more air monitoring locations, the model will become more accurate. In other words, the higher number of pollution monitoring stations, the higher accuracy can be achieved. Although the small number of pollution monitoring stations causes estimation errors, especially near highways, it will still give a good estimation of the pollution reduction.

Figure 6-15 shows the reduced mortality in Scenario 4 using cubic interpolation. As can be seen, the reduction in mortality depends on the population and $NO_x$ concentration reduction in different regions. For instance, although the pollution reduction is significant in Pearson International airport because of the low population density in that area, the mortality reduction is not high.
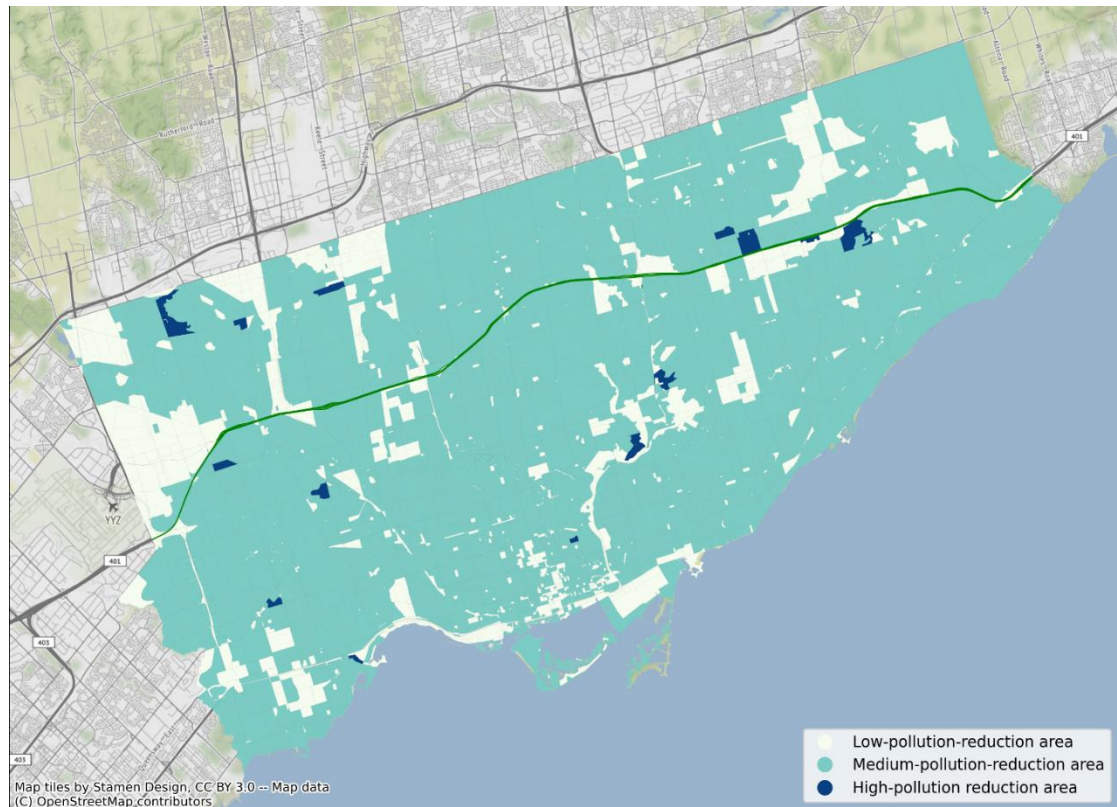
**Figure 6-15. Mortality decrease by area.**

Calculating the mortality reduction in different scenarios using different interpolation methods, it was found that the interpolation method does not impact the total annual death prevented each year. The total prevented death in different scenarios is shown in Table 6-6. As can be seen, more than CAD 500 million per year can be saved in terms of health benefits from reducing $NO_x$ concentration in Scenario 4. The results show a linear reduction, which is mostly because of the linear output of the LSTM model.

**Table 6-6. Prevented mortality and health benefit of different scenarios.**

| Scenario | Annual Prevented Mortality | Health benefit (CAD million/Year) |
|---|---|---|
| Scenario 1 (2.5% reduction in traffic count) | 18 | 144 |
| Scenario 2 (5% reduction in traffic count) | 35 | 280 |
| Scenario 3 (7.5% reduction in traffic count) | 53 | 424 |
| Scenario 4 (10% reduction in traffic count) | 70 | 560 |

## 6.4 Conclusion

Air pollution has a significant effect of human's health condition. Different pollutants such as $PM_{.25}$, $NO_x$, CO, $O_3$ cause lots of premature death and diseases. The aim of this chapter was to estimate the health cost of fossil-fuel-based transportation system. Having the current transportation system's health cost, the benefit of replacing the fossil-fuel vehicle by EV can be investigated. To forecast the air pollution, a machine learning method called Long-Short Term Memory (LSTM) is used to predict the air pollution based on traffic data, weather condition and previous air pollution data. The developed model, then, is used to estimate the $NO_x$ concentration in different scenarios of EV penetration in the market. Using hazard ratio, the impact of reducing number of fossil-fuel vehicles is investigated. Finally, having the population concentration in different neighborhood, the total number of prevented death in each scenario is evaluated. Finally, using Value of Statistical Life (VSL), the health benefit of different EV penetration scenario is calculated.

The results show that highest $NO_x$ reduction occurs in Toronto West. Also, the $NO_x$ concentration reduces linearly as share of fossil-Fuel vehicle decreases. The reduction in

mortality heavily depends on the air pollution reduction as well as population concentration. Finally, the 10% reduction in fossil-fuel vehicle can save 70 people's lives just due to reduction in $NO_x$. In monetary unit, this can benefit the economy by saving CAD 560 million/year.

# 7. Conclusions and Future Work

## 7.1 Summary and Conclusions

In the present thesis, the economic, environmental and health impact of hydrogen penetration in different energy sectors is investigated. Different models and software are being used to analyze cost and benefit of hydrogen in the industry as well as transportation sector. As can be seen in Figure 7-1, first, the cost of different green energy alternatives is calculated in an industrial facility. The effect of integration of hydrogen technologies such as electrolyzer and fuel cell with other renewable energies such as wind and solar energy is investigated in Chapter 3. Chapters 4, 5, and 6 focus on implementing hydrogen economy idea in transportation sector. In Chapter 4, an optimization model is developed to design a hydrogen refueling network along Highway 401 corridor. In Chapter 5, the health and environmental benefit of developing a hydrogen network along Highway 401 in Toronto is analyzed. Chapter 6 focuses on calculating the health benefit of an increased share of Zero-Emission Vehicles (ZEVs) in Toronto.
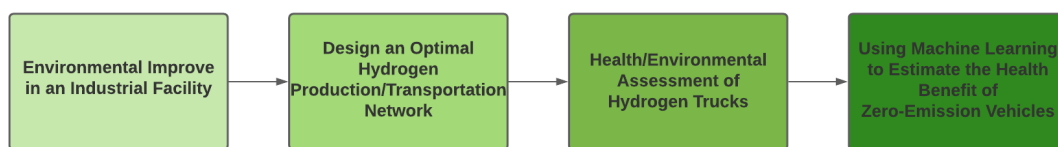


**Figure 7-1 – Overall workflow of the thesis**

A five-year mathematical model for determining the appropriate design of renewable energy systems for meeting particular $CO_2$ emission reduction targets is created earlier in the thesis. The renewable energy technologies will be deployed in a manufacturing industrial

complex that generates electricity using CHP and heats with natural gas. The optimization model was created in order to discover the most cost-effective combination of technology that results in a 4.53 percent annual $CO_2$ emission. The results of the optimization model show that in the first and second years, wind power is the most cost-effective technology for lowering emissions, with costs of 44 and 69 CAD per tonne of $CO_2$, respectively. From the third year on, hydrogen energy was determined to be more cost-effective than wind power. The cost of reducing $CO_2$ emissions does not change significantly from year to year, rising from 107 CAD per tonne of $CO_2$ in the first year to 130 CAD per tonne of $CO_2$ in the fifth. In all years, solar power is proven to be a significantly more expensive technology than wind power for lowering $CO_2$ emissions. Lower capacity factor (in Ontario), more intermittency (requiring more storage capacity), and higher investment costs are the causes for higher solar power costs. Over the course of five years, the optimization model revealed that a hybrid wind/battery/hydrogen energy system has the lowest cost of emission reduction. A wind/battery/hydrogen system's emission reduction cost rises from 44 CAD per tonne of $CO_2$ in the first year to 156 CAD per tonne of $CO_2$ in the fifth year.

In addition, a model is being developed to optimise the sizes and locations of the hydrogen infrastructures required to produce and distribute hydrogen for Ontario's hydrogen corridor route (HWY 401). The researchers employed a novel mathematical modelling and optimization approach that can be applied to various regions/countries. The strategy included the use of the HDSAM tool developed by the H2A Analysis Group, as well as a GAMS-based optimization model. MOVES was also used to calculate health costs and benefits by quantifying pollution emitted by conventional automobiles. The findings

demonstrated that, despite their high capital costs, the initial development of the hydrogen economy and FCEVs can be advantageous, and that the Canadian government should examine it as a potential approach to assist solve the climate change problem and enhance public health. According to our calculations, a 1% share of hydrogen in heavy-duty truck fuel use can save the environment $1.63 million per year and the health system $1.45 million per year. It's worth noting that these expenses represent an underestimate of actual costs, which can be examined further in future research. We also showed that, despite the current high costs of hydrogen generation and distribution, these prices might be reduced by employing optimum energy planning and increased capacity. The results of comparing 0.1 percent and 1% scenarios revealed that the economy of scales could result in a 35 percent reduction in the per kg cost of hydrogen. Higher capacities and market shares necessitate a more in-depth examination of technology development and future costs, which will be covered in future works.

To explore the environmental and health costs associated with Highway 401, Canada's busiest highway, a model was constructed to investigate the impact of hydrogen penetration in the transportation sector. To evaluate the health benefits of replacing fossil-fuel vehicles with ZEVs, an integrated model was developed. The concentrations of PM2.5 and $NO_x$ in the vicinity of Highway 401 were calculated using a combination of MOVES2014b, WRF model, and AERMOD. Then, using hazard ratios from the literature, the $NO_x$ mortality risk was determined. VSL was used to calculate the health cost of $NO_x$ in six situations. GREET was also used to assess $CO_2$ emissions from heavy-duty trucks and passenger vehicles over the course of their lives in six distinct scenarios. The environmental cost was then estimated

168

by multiplying each scenario's total $CO_2$ emissions by the Canadian carbon tax, which is CAD 40 per tonne of $CO_2$. $NO_x$ had the greatest impact on death rates, according to the findings. Because of their lower concentrations or reduced hazard risk, some contaminants are less likely to have a significant influence on human health. Moreover, despite their smaller traffic share, the health impact of truck pollution is greater than that of passenger vehicles. It can be inferred that investing in the decrease of pollution caused by trucks is more prudent. Furthermore, the annual environmental impact of Highway 401 traffic is estimated to be CAD 55 million, which can be lowered to less than CAD 6 million by switching to zero-emission electric vehicles. Furthermore, by changing all trucks to FC trucks, the annual environmental cost can be cut by CAD 49 million. Finally, it was determined that investing in fuel cell trucks takes precedence over investing in electric passenger vehicles. Despite a lower share in Highway 401 traffic, the economic benefit of the 100% FC truck scenario is almost the same as the 100% electric passenger vehicle scenario.

Finally, an integrated model is used to assess the health cost of a fossil-fuel-based urban transportation system. With the current transportation system's health costs in mind, the benefits of replacing fossil-fuel vehicles with electric vehicles can be assessed. A machine learning method called Long-Short Term Memory (LSTM) is used to predict air pollution based on traffic data, weather conditions, and past air pollution data to anticipate air pollution. The resulting model is then utilized to estimate $NO_x$ concentrations in various scenarios of EV market penetration. The impact of reducing the number of fossil-fuel cars is explored using the hazard ratio. Finally, the overall number of deaths avoided in each

scenario is calculated using population density in different neighborhoods. Finally, the health benefit of various EV penetration scenarios is estimated using Value of Statistical Life (VSL). The $NO_x$ reduction is greatest in Toronto West, according to the findings. In addition, when the percentage of fossil-fuel vehicles drops, the $NO_x$ concentration decreases linearly. The reduction in mortality is strongly influenced by the reduction in air pollution as well as population density. Finally, a 10% reduction in fossil-fuel vehicles can save the lives of 70 people simply by reducing $NO_x$ emissions. This can save the economy CAD 560 million per year in monetary terms.

## 7.2 Proposed future work

Based on the findings of these studies, some ideas for improving the discussed model can be suggested:

1- Modelling all sectors together: A comprehensive model can be built, which includes all energy sectors such as transportation, industry, and etc. This model can be optimized using a multi-objective optimization with different objective functions such as environmental, health and energy cost.

2- Considering more pollutants: more detail health cost calculation function can be built to estimate the health benefit of using more hydrogen in the energy system. It should be noted that for such a purpose, a detailed air pollution model must be built.

3- Improving machine learning model: To reach a better estimation of vehicle count effects on total air pollution, different machine learning models can be built. Those models should consider more features and larger datasets. The challenge fir such models is to gather data that can affect the pollutant's concentration.

4- Investigating the rivalry between different ZEV options: The comprehensive model of Ontario energy system can help the policy-makers to decide the optimal steps toward a clean energy system. Such model can decide the priority of developing BEVs or FCEVs.

# References

[1]    S. Imperatives, Report of the World Commission on Environment and Development: Our common future, Accessed Feb. 10 (1987) 1–300.

[2]    M. Ball, M. Weeda, The hydrogen economy--vision or reality?, Int. J. Hydrogen Energy. 40 (2015) 7903–7919.

[3]    G. Marbán, T. Valdés-Sol\'\is, Towards the hydrogen economy?, Int. J. Hydrogen Energy. 32 (2007) 1625–1637.

[4]    W.D. Nordhaus, Revisiting the social cost of carbon, Proc. Natl. Acad. Sci. 114 (2017) 1518–1523.

[5]    K. Ricke, L. Drouet, K. Caldeira, M. Tavoni, Country-level social cost of carbon, Nat. Clim. Chang. 8 (2018) 895–900.

[6]    World Energy Outlook 2018 examines future patterns of global energy system at a time of increasing uncertainties - News - IEA, (n.d.). https://www.iea.org/news/world-energy-outlook-2018-examines-future-patterns-of-global-energy-system-at-a-time-of-increasing-uncertainties (accessed November 16, 2021).

[7]    World Energy Outlook 2018 - YouTube, (n.d.). https://www.youtube.com/watch?v=ejM3VB0z_3M (accessed November 16, 2021).

[8]    A.J. Cohen, M. Brauer, R. Burnett, H.R. Anderson, J. Frostad, K. Estep, K. Balakrishnan, B. Brunekreef, L. Dandona, R. Dandona, others, Estimates and 25-year trends of the global burden of disease attributable to ambient air pollution: an analysis

of data from the Global Burden of Diseases Study 2015, Lancet. 389 (2017) 1907–1918.

[9]  E. Lanzi, others, The Economic Consequences of Outdoor Air Pollution, Organ. Econ. Coop. Dev. Retrieved from Https//Www. Oecd. Org/Environment/Indicators-Modelling-Outlooks/Policy-Highlights-Economic-Cons  Equences-of-Outdoor-Air-Pollution-Web. Pdf. (2016).

[10]  H. Shamsi, E. Haghi, K. Raahemifar, M. Fowler, Five-year technology selection optimization to achieve specific CO2 emission reduction targets, Int. J. Hydrogen Energy. 44 (2019) 3966–3984. https://doi.org/10.1016/j.ijhydene.2018.12.104.

[11]  H. Shamsi, M.-K. Tran, S. Akbarpour, A. Maroufmashat, M. Fowler, Macro-Level optimization of hydrogen infrastructure and supply chain for zero-emission vehicles on a canadian corridor, J. Clean. Prod. 289 (2021) 125163.

[12]  H. Shamsi, M. Munshed, M.-K. Tran, Y. Lee, S. Walker, K. Raahemifar, M. Fowler, others, Health Cost Estimation of Traffic-Related Air Pollution and Assessing the Pollution Reduction Potential of Zero-Emission Vehicles in Toronto, Canada, Energies. 14 (2021) 4956.

[13]  M. Voldsund, K. Jordal, R. Anantharaman, Hydrogen production with CO2 capture, Int. J. Hydrogen Energy. 41 (2016) 4969–4992.

[14]  S. Sharma, S.K. Ghoshal, Hydrogen the future transportation fuel: From production to applications, Renew. Sustain. Energy Rev. 43 (2015) 1151–1158.

[15]  The manufacturing and storage of hydrogen, (n.d.). https://www.slideshare.net/bgba223/the-manufacturing-and-storage-of-hydrogen

(accessed November 16, 2021).

[16]  N.P. Brandon, Z. Kurban, Clean energy and the hydrogen economy, Philos. Trans. R. Soc. A Math. Phys. Eng. Sci. 375 (2017) 20160400.

[17]  A. Maroufmashat, M. Fowler, Transition of future energy system infrastructure; through power-to-gas pathways, Energies. 10 (2017) 1089.

[18]  F. Cell, H.J. Undertaking, Study on Early Business Cases for H2 in Energy Storage and More Broadly Power to H2 Applications, (2017).

[19]  A. Körner, C. Tam, S. Bennett, J. Gagné, Technology roadmap-hydrogen and fuel cells, Int. Energy Agency Paris, Fr. (2015).

[20]  Total greenhouse gas emissions (kt of CO2 equivalent) | Data, (n.d.). https://data.worldbank.org/indicator/EN.ATM.GHGT.KT.CE?end=2012&start=1985 &year_low_desc=true (accessed November 17, 2021).

[21]  CO2 emissions (kt) | Data, (n.d.). https://data.worldbank.org/indicator/EN.ATM.CO2E.KT?end=2013&start=1960&yea r_high_desc=true, (accessed November 17, 2021).

[22]  C. Environmental Sustainability Indicators, GLOBAL GREENHOUSE GAS EMISSIONS CANADIAN ENVIRONMENTAL SUSTAINABILITY INDICATORS, (n.d.). www.canada.ca/en/environment-climate-change/services/environmental-indicators/global- (accessed November 17, 2021).

[23]  Rieussec, Erwan, GREENHOUSE GAS EMISSIONS CANADIAN ENVIRONMENTAL SUSTAINABILITY INDICATORS, (n.d.). www.canada.ca/en/environment-climate-change/services/environmental-

indicators/greenhouse-gas- (accessed November 17, 2021).

[24]    O.W.M. Association, others, Greenhouse gas emissions and the Ontario Waste management industry white paper, (2015).

[25]    T.S. Schmidt, N.U. Blum, R.S. Wakeling, Attracting private investments into rural electrification—A case study on renewable energy based village grids in Indonesia, Energy Sustain. Dev. 17 (2013) 581–595.

[26]    A. Robalino-López, A. Mena-Nieto, J.E. Garc\'\ia-Ramos, System dynamics modeling for renewable energy and CO2 emissions: A case study of Ecuador, Energy Sustain. Dev. 20 (2014) 11–20.

[27]    A.M. Bassi, A.E. Baer, Quantifying cross-sectoral impacts of investments in climate change mitigation in Ecuador, Energy Sustain. Dev. 13 (2009) 116–123.

[28]    M. Beaudin, H. Zareipour, A. Schellenberglabe, W. Rosehart, Energy storage for mitigating the variability of renewable electricity sources: An updated review, Energy Sustain. Dev. 14 (2010) 302–314.

[29]    L. Stamford, A. Azapagic, Life cycle sustainability assessment of UK electricity scenarios to 2070, Energy Sustain. Dev. 23 (2014) 194–211.

[30]    E. Haghi, B. Farshidian, Y. Saboohi, Developing a model for optimal sizing of a small hydropower/PV hybrid system for electrification, in: 2017 IEEE Int. Conf. Smart Energy Grid Eng., 2017: pp. 170–176.

[31]    N. Agarwal, A. Kumar, others, Optimization of grid independent hybrid PV--diesel--battery system for power generation in remote villages of Uttar Pradesh, India, Energy Sustain. Dev. 17 (2013) 210–219.

175

[32] B.K. Bala, S.A. Siddique, Optimal design of a PV-diesel hybrid system for electrification of an isolated island—Sandwip in Bangladesh using genetic algorithm, Energy Sustain. Dev. 13 (2009) 137–142.

[33] E.S. Hrayshat, Techno-economic analysis of autonomous hybrid photovoltaic-diesel-battery system, Energy Sustain. Dev. 13 (2009) 143–150.

[34] H. Belmili, M. Haddadi, S. Bacha, M.F. Almi, B. Bendib, Sizing stand-alone photovoltaic--wind hybrid system: Techno-economic analysis and optimization, Renew. Sustain. Energy Rev. 30 (2014) 821–832.

[35] A. Kaabeche, R. Ibtiouen, Techno-economic optimization of hybrid photovoltaic/wind/diesel/battery generation in a stand-alone power system, Sol. Energy. 103 (2014) 171–182.

[36] T. Ma, H. Yang, L. Lu, A feasibility study of a stand-alone hybrid solar--wind--battery system for a remote island, Appl. Energy. 121 (2014) 149–158.

[37] A. Gonzalez, J.-R. Riba, A. Rius, R. Puig, Optimal sizing of a hybrid grid-connected photovoltaic and wind power system, Appl. Energy. 154 (2015) 752–762.

[38] D. Andress, T.D. Nguyen, S. Das, Reducing GHG emissions in the United States' transportation sector, Energy Sustain. Dev. 15 (2011) 117–136.

[39] P.J. Hall, E.J. Bain, Energy-storage technologies and electricity generation, Energy Policy. 36 (2008) 4352–4355.

[40] T.S. Uyar, D. Be\csikci, Integration of hydrogen energy systems into renewable energy systems for better design of 100\% renewable energy communities, Int. J. Hydrogen Energy. 42 (2017) 2453–2456.

[41] S.B. Walker, U. Mukherjee, M. Fowler, A. Elkamel, Benchmarking and selection of Power-to-Gas utilizing electrolytic hydrogen as an energy storage alternative, Int. J. Hydrogen Energy. 41 (2016) 7717–7731.

[42] F. Zhang, P. Zhao, M. Niu, J. Maddy, The survey of key technologies in hydrogen energy storage, Int. J. Hydrogen Energy. 41 (2016) 14535–14552.

[43] S.E. Hosseini, M.A. Wahid, Hydrogen production from renewable and sustainable energy resources: Promising green energy carrier for clean development, Renew. Sustain. Energy Rev. 57 (2016) 850–866.

[44] E. Haghi, K. Raahemifar, M. Fowler, Investigating the effect of renewable energy incentives and hydrogen storage on advantages of stakeholders in a microgrid, Energy Policy. 113 (2018) 206–222.

[45] H. Ameli, M. Qadrdan, G. Strbac, Techno-economic assessment of battery storage and power-to-gas: a whole-system approach, Energy Procedia. 142 (2017) 841–848.

[46] P.E. Dodds, I. Staffell, A.D. Hawkes, F. Li, P. Grünewald, W. McDowall, P. Ekins, Hydrogen and fuel cell technologies for heating: A review, Int. J. Hydrogen Energy. 40 (2015) 2065–2083.

[47] M. Smaoui, A. Abdelkafi, L. Krichen, Optimal sizing of stand-alone photovoltaic/wind/hydrogen hybrid system supplying a desalination unit, Sol. Energy. 120 (2015) 263–276.

[48] Y. Kalinci, A. Hepbasli, I. Dincer, Techno-economic analysis of a stand-alone hybrid renewable energy system with hydrogen production and storage options, Int. J. Hydrogen Energy. 40 (2015) 7652–7664.

[49] H. Chen, C. Yang, K. Deng, N. Zhou, H. Wu, Multi-objective optimization of the hybrid wind/solar/fuel cell distributed generation system using Hammersley Sequence Sampling, Int. J. Hydrogen Energy. 42 (2017) 7836–7846.

[50] A. Al-Sharafi, A.Z. Sahin, T. Ayar, B.S. Yilbas, Techno-economic analysis and optimization of solar and wind energy systems for power generation and hydrogen production in Saudi Arabia, Renew. Sustain. Energy Rev. 69 (2017) 33–49.

[51] A. Maleki, A. Askarzadeh, Comparative study of artificial intelligence techniques for sizing of a hydrogen-based stand-alone photovoltaic/wind hybrid system, Int. J. Hydrogen Energy. 39 (2014) 9973–9984.

[52] E. Haghi, M. Fowler, K. Raahemifar, Co-benefit analysis of incentives for energy generation and storage systems; a multi-stakeholder perspective, Int. J. Hydrogen Energy. 44 (2019) 9643–9671.

[53] M. Mohsin, A.K. Rasheed, R. Saidur, Economic viability and production capacity of wind generated renewable hydrogen, Int. J. Hydrogen Energy. 43 (2018) 2621–2630.

[54] S. Khanmohammadi, P. Heidarnejad, N. Javani, H.. Ganjehsarabi, Exergoeconomic analysis and multi objective optimization of a solar based integrated energy system for hydrogen production, Int. J. Hydrogen Energy. 42 (2017) 21443–21453.

[55] H. Ishaq, I. Dincer, G.F. Naterer, Performance investigation of an integrated wind energy system for co-generation of power and hydrogen, Int. J. Hydrogen Energy. 43 (2018) 9153–9164.

[56] Independent electricity system operator (IESO), (n.d.). http://www.ieso.ca/-/media/files/ieso/document-library/planning-forecasts/ontario-planning-

outlook/module-5-market-and-system-operations-tx-and-dx-outlook-20160901-pdf.pdf?la=en (accessed November 17, 2017).

[57]   Ministry of Energy Independent Electricity System Operator-Market Oversight and Cybersecurity, (n.d.).

[58]   S.B. Walker, D. van Lanen, U. Mukherjee, M. Fowler, Greenhouse gas emissions reductions from applications of Power-to-Gas in power generation, Sustain. Energy Technol. Assessments. 20 (2017) 25–32.

[59]   A. Sgobbi, W. Nijs, R. De Miglio, A. Chiodi, M. Gargiulo, C. Thiel, How far away is hydrogen? Its role in the medium and long-term decarbonisation of the European energy system, Int. J. Hydrogen Energy. 41 (2016) 19–35.

[60]   D. Steward, G. Saur, M. Penev, T. Ramsden, Lifecycle cost analysis of hydrogen versus other technologies for electrical energy storage, 2009.

[61]   T.J. Stehly, D.M. Heimiller, G.N. Scott, COST OF WIND ENERGY REVIEW.(No. NREL/TP-6A20-70363), Natl. Renew. Energy Lab.(NREL), Golden, CO (United States). (2016).

[62]   R. Fu, D. Feldman, R. Margolis, M. Woodhouse, K. Ardani, US solar photovoltaic system cost benchmark: Q1 2017, 2017.

[63]   Y. Li, A.-C. Orgerie, J.-M. Menaud, Balancing the use of batteries and opportunistic scheduling policies for maximizing renewable energy consumption in a Cloud data center, in: 2017 25th Euromicro Int. Conf. Parallel, Distrib. Network-Based Process., 2017: pp. 408–415.

[64]   I. Nexant, H2A hydrogen delivery infrastructure analysis models and conventional

pathway options analysis results, (2008).

[65]   Power Data, (n.d.). https://www.ieso.ca/power-data (accessed April 1, 2018).

[66]   Global       Adjustment       (GA),       (n.d.).       https://www.ieso.ca/power-data/price-
       overview/global-adjustment (accessed April 1, 2018).

[67]   Historical natural gas rates | Ontario Energy Board, (n.d.). https://www.oeb.ca/rates-
       and-your-bill/natural-gas-rates/historical-natural-gas-rates   (accessed   November   17,
       2021).

[68]   Benchmarking      Guides,      (n.d.).      https://www.nrcan.gc.ca/energy-efficiency/energy-
       efficiency-industry/energy-management-industry/energy-benchmarking-
       industry/benchmarking-guides/5171 (accessed November 17, 2021).

[69]   I. Dincer, M.A. Rosen, Sustainability aspects of hydrogen and fuel cell systems,
       Energy Sustain. Dev. 15 (2011) 137–146.

[70]   K. Alanne, S. Cao, Zero-energy hydrogen economy (ZEH2E) for buildings and
       communities including personal mobility, Renew. Sustain. Energy Rev. 71 (2017)
       697–711.

[71]   C. Marino, A. Nucara, M. Pietrafesa, A. Pudano, An energy self-sufficient public
       building using integrated renewable sources and hydrogen storage, Energy. 57 (2013)
       95–105.

[72]   J.I. Levene, M.K. Mann, R.M. Margolis, A. Milbrandt, An analysis of hydrogen
       production from renewable electricity sources, Sol. Energy. 81 (2007) 773–780.

[73]   E. Haghi, M. Fwoler, K. Raahemifar, Economic analysis of hydrogen production in
       context of a microgrid, in: 2017 IEEE Int. Conf. Smart Energy Grid Eng., 2017: pp.

79–84.

[74] D. Apostolou, G. Xydis, A literature review on hydrogen refuelling stations and infrastructure. Current status and future prospects, Renew. Sustain. Energy Rev. 113 (2019) 109292.

[75] P. Bögel, C. Oltra, R. Sala, M. Lores, P. Upham, E. Dütschke, U. Schneider, P. Wiemann, The role of attitudes in technology acceptance management: Reflections on the case of hydrogen fuel cells in Europe, J. Clean. Prod. 188 (2018) 125–135.

[76] T.A. Boden, G. Marland, R.J. Andres, Global, regional, and national fossil-fuel CO2 emissions, Carbon Dioxide Inf. Anal. Center, Oak Ridge Natl. Lab. US Dep. Energy, Oak Ridge, Tenn., USA Doi. 10 (2009).

[77] P. Perera, K. Hewage, R. Sadiq, Are we ready for alternative fuel transportation systems in Canada: A regional vignette, J. Clean. Prod. 166 (2017) 717–731.

[78] J.S. Lwebuga-Mukasa, T. Oyana, A. Thenappan, S.J. Ayirookuzhi, Association between traffic volume and health care use for asthma among residents at a US--Canadian border crossing point, J. Asthma. 41 (2004) 289–304.

[79] M.M. Finkelstein, M. Jerrett, M.R. Sears, Traffic air pollution and mortality rate advancement periods, Am. J. Epidemiol. 160 (2004) 173–177.

[80] M. Brauer, C. Reynolds, P. Hystad, Traffic-related air pollution and health in Canada, CMAJ. 185 (2013) 1557–1558.

[81] J. Hall, R. Kerr, Innovation dynamics and environmental technologies: the emergence of fuel cell technology, J. Clean. Prod. 11 (2003) 459–471.

[82] D.C. Rosenfeld, J. Lindorfer, K. Fazeni-Fraisl, Comparison of advanced fuels—

which technology can win from the life cycle perspective?, J. Clean. Prod. 238 (2019) 117879.

[83]   M.-K. Tran, M. Fowler, A review of lithium-ion battery fault diagnostic algorithms: Current progress and future challenges, Algorithms. 13 (2020) 62.

[84]   M.-K. Tran, M. Fowler, Sensor fault detection and isolation for degrading lithium-ion batteries in electric vehicles using parameter estimation with recursive least squares, Batteries. 6 (2020) 1.

[85]   A. Alaswad, A. Baroutaji, H. Achour, J. Carton, A. Al Makky, A.-G. Olabi, Developments in fuel cell technologies in the transport sector, Int. J. Hydrogen Energy. 41 (2016) 16499–16508.

[86]   Y. Ligen, H. Vrubel, H.H. Girault, Mobility from renewable electricity: Infrastructure comparison for battery and hydrogen fuel cell vehicles, World Electr. Veh. J. 9 (2018) 3.

[87]   U. Mukherjee, S. Walker, A. Maroufmashat, M. Fowler, A. Elkamel, Power-to-gas to meet transportation demand while providing ancillary services to the electrical grid, in: 2016 IEEE Smart Energy Grid Eng., 2016: pp. 221–225.

[88]   J. Kast, R. Vijayagopal, J.J. Gangloff Jr, J. Marcinkoski, Clean commercial transportation: Medium and heavy duty fuel cell electric trucks, Int. J. Hydrogen Energy. 42 (2017) 4508–4517.

[89]   A. Maroufmashat, M. Fowler, S.S. Khavas, A. Elkamel, R. Roshandel, A. Hajimiragha, Mixed integer linear programing based approach for optimal planning and operation of a smart urban energy network to support the hydrogen economy, Int.

J. Hydrogen Energy. 41 (2016) 7700–7716.

[90]   U. Mukherjee, A. Maroufmashat, J. Ranisau, M. Barbouti, A. Trainor, N. Juthani, H. El-Shayeb, M. Fowler, Techno-economic, environmental, and safety assessment of hydrogen powered community microgrids; case study in Canada, Int. J. Hydrogen Energy. 42 (2017) 14333–14349.

[91]   S. Hardman, E. Shiu, R. Steinberger-Wilckens, T. Turrentine, Barriers to the adoption of fuel cell vehicles: A qualitative investigation into early adopters attitudes, Transp. Res. Part A Policy Pract. 95 (2017) 166–182.

[92]   M.B. Stevens, M.W. Fowler, A. Elkamel, S. Elhedhli, Macro-level optimized deployment of an electrolyser-based hydrogen refuelling infrastructure with demand growth, Eng. Optim. 40 (2008) 955–967.

[93]   E. Çabukoglu, G. Georges, L. Küng, G. Pareschi, K. Boulouchos, Fuel cell electric vehicles: An option to decarbonize heavy-duty transport? Results from a Swiss case-study, Transp. Res. Part D Transp. Environ. 70 (2019) 35–48.

[94]   J.J. Brey, A.F. Carazo, R. Brey, Exploring the marketability of fuel cell electric vehicles in terms of infrastructure and hydrogen costs in Spain, Renew. Sustain. Energy Rev. 82 (2018) 2893–2899.

[95]   M. Reuß, T. Grube, M. Robinius, D. Stolten, A hydrogen supply chain with spatial resolution: Comparative analysis of infrastructure technologies in Germany, Appl. Energy. 247 (2019) 438–453.

[96]   N. Liu, F. Xie, Z. Lin, M. Jin, Evaluating national hydrogen refueling infrastructure requirement and economic competitiveness of fuel cell electric long-haul trucks,

Mitig. Adapt. Strateg. Glob. Chang. 25 (2020) 477–493.

[97]  W. Li, R. Long, H. Chen, F. Chen, X. Zheng, Z. He, L. Zhang, Willingness to pay for hydrogen fuel cell electric vehicles in China: A choice experiment analysis, Int. J. Hydrogen Energy. 45 (2020) 34346–34353.

[98]  S. Hardman, G. Tal, Who are the early adopters of fuel cell vehicles?, Int. J. Hydrogen Energy. 43 (2018) 17857–17866.

[99]  F. Liu, F. Zhao, Z. Liu, H. Hao, The impact of fuel cell vehicle deployment on road transport greenhouse gas emissions: the China case, Int. J. Hydrogen Energy. 43 (2018) 22604–22621.

[100]  A.H. Hajimiragha, C.A. Canizares, M.W. Fowler, S. Moazeni, A. Elkamel, S. Wong, Sustainable convergence of electricity and transport sectors in the context of a hydrogen economy, Int. J. Hydrogen Energy. 36 (2011) 6357–6375.

[101]  R.-H. Lin, Z.-Z. Ye, B.-D. Wu, A review of hydrogen station location models, Int. J. Hydrogen Energy. 45 (2020) 20176–20183.

[102]  E. Haghi, H. Shamsi, S. Dimitrov, M. Fowler, K. Raahemifar, Assessing the potential of fuel cell-powered and battery-powered forklifts for reducing GHG emissions using clean surplus power; a game theory approach, Int. J. Hydrogen Energy. 45 (2020) 34532–34544.

[103]  Ministry of Transportation Provincial Highways Traffic Volumes 2016, Ontario, (n.d.). https://www.library.mto.gov.on.ca/SydneyPLUS/TechPubs/Portal/tp/tvSplash.aspx (accessed November 17, 2021).

[104] S. McWhorter, G. Ordaz, Onboard Type IV Compressed Hydrogen Storage Systems-Current Performance and Cost, US Dep. Energy, Washington, DC, DOE Progr. Rec. 13013 (2013).

[105] D. Peterson, J. Vickers, D. Desantis, K. Ayers, M. Hamdan, K. Harrison A A Approved, K. Randolph, E. Miller, S. Satyapal, DOE Hydrogen and Fuel Cells Program Record Title: Hydrogen Production Cost From PEM Electrolysis-2019 ] Originators, (1900). http://www.hydrogen.energy.gov/h2a_prod_studies.html: (accessed November 17, 2021).

[106] H2A: Hydrogen Analysis Production Models | Hydrogen and Fuel Cells | NREL, (n.d.). https://www.nrel.gov/hydrogen/h2a-production-models.html (accessed November 17, 2021).

[107] Hydrogen Delivery Scenario Analysis Model (HDSAM), (n.d.). https://hdsam.es.anl.gov/index.php?content=hdsam (accessed November 17, 2021).

[108] C. Ainscough, D. Peterson, E. Miller, Hydrogen production cost from PEM electrolysis, DOE Hydrog. Fuel Cells Progr. Rec. 14004 (2014).

[109] D. Sawyer, S. Stiebert, C. Welburn, Evaluation of total cost of air pollution due to transportation in Canada, Transp. Canada, Ottawa, ON, Canada. (2007).

[110] J. Sotes, others, A clearer view on Ontario's emissions: Electricity emissions factors and guidelines, Atmos. Fund. (2019).

[111] M.-K. Tran, M. Akinsanya, S. Panchal, R. Fraser, M. Fowler, Design of a hybrid electric vehicle powertrain for performance optimization considering various powertrain components and configurations, Vehicles. 3 (2021) 20–32.

[112] M.-K. Tran, S. Sherman, E. Samadani, R. Vrolyk, D. Wong, M. Lowery, M. Fowler, Environmental and Economic Benefits of a Battery Electric Vehicle Powertrain with a Zinc--Air Range Extender in the Transition to Electric Vehicles, Vehicles. 2 (2020) 398–412.

[113] M.-K. Tran, A. Bhatti, R. Vrolyk, D. Wong, S. Panchal, M. Fowler, R. Fraser, A Review of Range Extenders in Battery Electric Vehicles: Current Progress and Future Perspectives, World Electr. Veh. J. 12 (2021) 54.

[114] D. Brugge, J.L. Durant, C. Rioux, Near-highway pollutants in motor vehicle exhaust: a review of epidemiologic evidence of cardiac and pulmonary health risks, Environ. Heal. 6 (2007) 1–12.

[115] J. Gasana, D. Dillikar, A. Mendy, E. Forno, E.R. Vieira, Motor vehicle air pollution and asthma in children: a meta-analysis, Environ. Res. 117 (2012) 36–45.

[116] T. Aldhafeeri, M.-K. Tran, R. Vrolyk, M. Pope, M. Fowler, A review of methane gas detection sensors: Recent developments and future perspectives, Inventions. 5 (2020) 28.

[117] A.J. Cohen, H. Ross Anderson, B. Ostro, K.D. Pandey, M. Krzyzanowski, N. Künzli, K. Gutschmidt, A. Pope, I. Romieu, J.M. Samet, others, The global burden of disease due to outdoor air pollution, J. Toxicol. Environ. Heal. Part A. 68 (2005) 1301–1307.

[118] M. Jerrett, M.M. Finkelstein, J.R. Brook, M.A. Arain, P. Kanaroglou, D.M. Stieb, N.L. Gilbert, D. Verma, N. Finkelstein, K.R. Chapman, others, A cohort study of traffic-related air pollution and mortality in Toronto, Ontario, Canada, Environ. Health Perspect. 117 (2009) 772–777.

[119] R.T. Burnett, S. Cakmak, J.R. Brook, The effect of the urban ambient air pollution mix on daily mortality rates in 11 Canadian cities, Can. J. Public Heal. 89 (1998) 152–156.

[120] J.R. Brook, R.T. Burnett, T.F. Dann, S. Cakmak, M.S. Goldberg, X. Fan, A.J. Wheeler, Further interpretation of the acute effect of nitrogen dioxide observed in Canadian time-series studies, J. Expo. Sci. \& Environ. Epidemiol. 17 (2007) S36--S44.

[121] L.I. Bai, S. Shin, R.T. Burnett, J.C. Kwong, P. Hystad, A. van Donkelaar, M.S. Goldberg, E. Lavigne, R. Copes, R. V Martin, others, Exposure to ambient air pollution and the incidence of congestive heart failure and acute myocardial infarction: A population-based study of 5.1 million Canadian adults living in Ontario, Environ. Int. 132 (2019) 105004.

[122] Health Impacts of Air Pollution in Canada: Estimates of morbidity and premature mortality outcomes, 2019. https://publications.gc.ca/collections/collection_2019/sc-hc/H144-51-2019-eng.pdf (accessed November 17, 2021).

[123] P. Grennfelt, A. Engleryd, M. Forsius, Ø. Hov, H. Rodhe, E. Cowling, Acid rain and air pollution: 50 years of progress in environmental science and policy, Ambio. 49 (2020) 849–864.

[124] L. Pinault, D. Crouse, M. Jerrett, M. Brauer, M. Tjepkema, Spatial associations between socioeconomic groups and NO2 air pollution exposure within three large Canadian cities, Environ. Res. 147 (2016) 373–382.

[125] A.G. Touchaei, H. Akbari, C.W. Tessum, Effect of increasing urban albedo on

meteorology and air quality of Montreal (Canada)--Episodic simulation of heat wave in 2005, Atmos. Environ. 132 (2016) 188–206.

[126] M.D. Adams, Air pollution in Ontario, Canada during the COVID-19 State of Emergency, Sci. Total Environ. 742 (2020) 140516.

[127] D.R. McCubbin, M.A. Delucchi, The health costs of motor-vehicle-related air pollution, J. Transp. Econ. Policy. (1999) 253–286.

[128] N.Z. Muller, R. Mendelsohn, Measuring the damages of air pollution in the United States, J. Environ. Econ. Manage. 54 (2007) 1–14.

[129] G.S. Martinez, J. V Spadaro, D. Chapizanis, V. Kendrovski, M. Kochubovski, P. Mudu, Health impacts and economic costs of air pollution in the metropolitan area of Skopje, Int. J. Environ. Res. Public Health. 15 (2018) 626.

[130] Y. Xia, D. Guan, X. Jiang, L. Peng, H. Schroeder, Q. Zhang, Assessment of socioeconomic costs to China's air pollution, Atmos. Environ. 139 (2016) 147–156.

[131] X. Lu, T. Yao, J.C.H. Fung, C. Lin, Estimation of health and economic costs of air pollution over the Pearl River Delta region in China, Sci. Total Environ. 566 (2016) 134–143.

[132] D. Giannadaki, E. Giannakis, A. Pozzer, J. Lelieveld, Estimating health and economic benefits of reductions in air pollution from agriculture, Sci. Total Environ. 622 (2018) 1304–1316.

[133] D.J. Nowak, S. Hirabayashi, M. Doyle, M. McGovern, J. Pasher, Air pollution removal by urban forests in Canada and its effect on air quality and human health, Urban For. \& Urban Green. 29 (2018) 40–48.

[134] L. Minet, T. Chowdhury, A. Wang, Y. Gai, I.D. Posen, M. Roorda, M. Hatzopoulou, Quantifying the air quality and health benefits of greening freight movements, Environ. Res. 183 (2020) 109193.

[135] MOtor Vehicle Emission Simulator (MOVES), (n.d.). https://www.epa.gov/moves.

[136] Air Quality Dispersion Modeling—Preferred and Recommended Models: AERMOD Modeling System., (n.d.). https://www.epa.gov/scram/air-quality-dispersion-modeling-preferred-and-recommended-models.

[137] J.G. Powers, J.B. Klemp, W.C. Skamarock, C.A. Davis, J. Dudhia, D.O. Gill, J.L. Coen, D.J. Gochis, R. Ahmadov, S.E. Peckham, others, The weather research and forecasting model: Overview, system efforts, and future directions, Bull. Am. Meteorol. Soc. 98 (2017) 1717–1737.

[138] A. Faustini, R. Rapp, F. Forastiere, Nitrogen dioxide and mortality: review and meta-analysis of long-term studies, Eur. Respir. J. 44 (2014) 744–753.

[139] Mortality rates, by age group, (n.d.). https://www150.statcan.gc.ca/t1/tbl1/en/tv.action?pid=1310071001.

[140] R.C. Bosworth, A. Hunter, A. Kibria, The value of a statistical life: economics and politics, Strat. Logan, UT, USA. (2017).

[141] A. Zhang, A.E. Boardman, D. Gillen, I. Waters, others, Towards estimating the social and environmental costs of transportation in Canada, Rep. Transp. Canada. 7 (2004).

[142] W.M. Hodan, W.R. Barnard, Evaluating the contribution of PM2. 5 precursor gases and re-entrained road emissions to mobile source PM2. 5 particulate matter emissions, MACTEC Fed. Programs, Res. Triangle Park. NC. (2004).

[143] U. Mukherjee, R.K. Saari, C. Bachmann, W. Wang, Multipollutant impacts to US receptors of regional on-road freight in Ontario, Canada, J. Air \& Waste Manag. Assoc. 70 (2020) 1121–1135.

[144] Final consumption – Key World Energy Statistics 2020 – Analysis - IEA, (n.d.). https://www.iea.org/reports/key-world-energy-statistics-2020/final-consumption (accessed November 29, 2021).

[145] J. Jakubiak-Lasocka, J. Lasocki, R. Siekmeier, Z. Chłopek, Impact of Traffic-Related air pollution on health, Adv. Exp. Med. Biol. 834 (2014) 21–29. https://doi.org/10.1007/5584_2014_14.

[146] P.J. Landrigan, R. Fuller, N.J.R. Acosta, O. Adeyi, R. Arnold, N. (Nil) Basu, A.B. Baldé, R. Bertollini, S. Bose-O'Reilly, J.I. Boufford, P.N. Breysse, T. Chiles, C. Mahidol, A.M. Coll-Seck, M.L. Cropper, J. Fobil, V. Fuster, M. Greenstone, A. Haines, D. Hanrahan, D. Hunter, M. Khare, A. Krupnick, B. Lanphear, B. Lohani, K. Martin, K. V. Mathiasen, M.A. McTeer, C.J.L. Murray, J.D. Ndahimananjara, F. Perera, J. Potočnik, A.S. Preker, J. Ramesh, J. Rockström, C. Salinas, L.D. Samson, K. Sandilya, P.D. Sly, K.R. Smith, A. Steiner, R.B. Stewart, W.A. Suk, O.C.P. van Schayck, G.N. Yadama, K. Yumkella, M. Zhong, The Lancet Commission on pollution and health, Lancet. 391 (2018) 462–512. https://doi.org/10.1016/S0140-6736(17)32345-0.

[147] A.J. Badyda, P. Dabrowiecki, W. Lubinski, P.O. Czechowski, G. Majewski, Exposure to traffic-related air pollutants as a risk of airway obstruction, Adv. Exp. Med. Biol. 755 (2013) 35–45. https://doi.org/10.1007/978-94-007-4546-9_5.

[148] M.H. Forouzanfar et al., Global, regional, and national comparative risk assessment of 79 behavioural, environmental and occupational, and metabolic risks or clusters of risks, 1990–2015: a systematic analysis for the Global Burden of Disease Study 2015, Lancet. 388 (2016) 1659–1724. https://doi.org/10.1016/S0140-6736(16)31679-8.

[149] M.-K. Tran, M. Fowler, A review of lithium-ion battery fault diagnostic algorithms: Current progress and future challenges, Algorithms. 13 (2020). https://doi.org/10.3390/a13030062.

[150] H. Kopackova, P. Libalova, Smart city concept as socio-technical system, in: 2017 Int. Conf. Inf. Digit. Technol., IEEE, 2017: pp. 198–205.

[151] E. von Schneidemesser, K. Steinmar, E.C. Weatherhead, B. Bonn, H. Gerwig, J. Quedenau, Air pollution at human scales in an urban environment: Impact of local environment and vehicles on particle number concentrations, Sci. Total Environ. 688 (2019) 691–700.

[152] L.M.B. Ventura, F. de Oliveira Pinto, A. Gioda, D. Márcio de Almeida, Inspection and maintenance programs for in-service vehicles: An important air pollution control tool, Sustain. Cities Soc. 53 (2020) 101956.

[153] W. Ke, S. Zhang, X. He, Y. Wu, J. Hao, Well-to-wheels energy consumption and emissions of electric vehicles: Mid-term implications from real-world features and air pollution control progress, Appl. Energy. 188 (2017) 367–377.

[154] L. Kebede, G. Tulu, R.T. Lisinge, Diesel-fueled public transport vehicles and air pollution in Addis Ababa, Ethiopia: Effects of vehicle size, age and kilometers travelled, Atmos. Environ. X. (2021) 100144.

[155] I. Bougoudis, K. Demertzis, L. Iliadis, HISYCOL a hybrid computational intelligence system for combined machine learning: the case of air pollution modeling in Athens, Neural Comput. Appl. 27 (2016) 1191–1206.

[156] F. Lautenschlager, M. Becker, K. Kobs, M. Steininger, P. Davidson, A. Krause, A. Hotho, OpenLUR: Off-the-shelf air pollution modeling with open features and machine learning, Atmos. Environ. 233 (2020) 117535.

[157] R.O. Sinnott, Z. Guan, Prediction of air pollution through machine learning approaches on the cloud, in: 2018 IEEE/ACM 5th Int. Conf. Big Data Comput. Appl. Technol., 2018: pp. 51–60.

[158] H.J. Lee, R.B. Chatfield, A.W. Strawa, Enhancing the Applicability of Satellite Remote Sensing for PM 2.5 Estimation Using MODIS Deep Blue AOD and Land Use Regression in California, United States, Environ. Sci. Technol. 50 (2016) 6546–6555. https://doi.org/10.1021/acs.est.6b01438.

[159] C. Wen, S. Liu, X. Yao, L. Peng, X. Li, Y. Hu, T. Chi, A novel spatiotemporal convolutional long short-term neural network for air pollution prediction, Sci. Total Environ. 654 (2019) 1091–1099. https://doi.org/10.1016/j.scitotenv.2018.11.086.

[160] W. Tong, L. Li, X. Zhou, A. Hamilton, K. Zhang, Deep learning PM2.5 concentrations with bidirectional LSTM RNN, Air Qual. Atmos. Heal. 12 (2019) 411–423. https://doi.org/10.1007/s11869-018-0647-4.

[161] C.J. Huang, P.H. Kuo, A deep cnn-lstm model for particulate matter (Pm2.5) forecasting in smart cities, Sensors (Switzerland). 18 (2018). https://doi.org/10.3390/s18072220.

[162] J. Fan, Q. Li, J. Hou, X. Feng, H. Karimian, S. Lin, A spatiotemporal prediction framework for air pollution based on deep RNN, ISPRS Ann. Photogramm. Remote Sens. Spat. Inf. Sci. 4 (2017) 15.

[163] D. Qin, J. Yu, G. Zou, R. Yong, Q. Zhao, B. Zhang, A Novel Combined Prediction Scheme Based on CNN and LSTM for Urban PM2.5 Concentration, IEEE Access. 7 (2019) 20050–20059. https://doi.org/10.1109/ACCESS.2019.2897028.

[164] I. Šimić, M. Lovrić, R. Godec, M. Kröll, I. Bešlić, Applying machine learning methods to better understand, model and estimate mass concentrations of traffic-related pollutants at a typical street canyon, Environ. Pollut. 263 (2020). https://doi.org/10.1016/j.envpol.2020.114587.

[165] Z. Li, S.H.L. Yim, K.F. Ho, High temporal resolution prediction of street-level PM2.5 and NOx concentrations using machine learning approach, J. Clean. Prod. 268 (2020) 121975. https://doi.org/10.1016/j.jclepro.2020.121975.

[166] T. Boningari, P.G. Smirniotis, Impact of nitrogen oxides on the environment and human health: Mn-based materials for the NOx abatement, Curr. Opin. Chem. Eng. 13 (2016) 133–141. https://doi.org/10.1016/j.coche.2016.09.004.

[167] J.E. Jonson, J. Borken-Kleefeld, D. Simpson, A. Nyíri, M. Posch, C. Heyes, Impact of excess NOx emissions from diesel cars on air quality, public health and eutrophication in Europe, Environ. Res. Lett. 12 (2017). https://doi.org/10.1088/1748-9326/aa8850.

[168] R. Fu, Z. Zhang, L. Li, Using LSTM and GRU neural network methods for traffic flow prediction, in: 2016 31st Youth Acad. Annu. Conf. Chinese Assoc. Autom.,

2016: pp. 324–328.

[169] X. Qing, Y. Niu, Hourly day-ahead solar irradiance prediction using weather forecasts by LSTM, Energy. 148 (2018) 461–468.

[170] S.H.I. Xingjian, Z. Chen, H. Wang, D.-Y. Yeung, W.-K. Wong, W. Woo, Convolutional LSTM network: A machine learning approach for precipitation nowcasting, in: Adv. Neural Inf. Process. Syst., 2015: pp. 802–810.

[171] T.-Y. Kim, S.-B. Cho, Predicting residential energy consumption using CNN-LSTM neural networks, Energy. 182 (2019) 72–81.

[172] Y.-T. Tsai, Y.-R. Zeng, Y.-S. Chang, Air pollution forecasting using RNN with LSTM, in: 2018 IEEE 16th Intl Conf Dependable, Auton. Secur. Comput. 16th Intl Conf Pervasive Intell. Comput. 4th Intl Conf Big Data Intell. Comput. Cyber Sci. Technol. Congr. (DASC/PiCom/DataCom/CyberSciTech, 2018: pp. 1074–1079.

[173] Air Quality Ontario, (n.d.). http://www.airqualityontario.com/ (accessed November 29, 2021).

[174] vz_challenge/transportation/traffic_volumes at master · CityofToronto/vz_challenge · GitHub, (n.d.). https://github.com/CityofToronto/vz_challenge/tree/master/transportation/traffic_volumes (accessed December 19, 2021).

[175] Weather Dashboard for Toronto, (n.d.). https://toronto.weatherstats.ca/ (accessed December 15, 2021).

[176] D.L. Crouse, P.A. Peters, P.J. Villeneuve, M.-O. Proux, H.H. Shin, M.S. Goldberg, M. Johnson, A.J. Wheeler, R.W. Allen, D.O. Atari, others, Within-and between-city

contrasts in nitrogen dioxide and mortality in 10 Canadian cities; a subset of the Canadian Census Health and Environment Cohort (CanCHEC), J. Expo. Sci. \& Environ. Epidemiol. 25 (2015) 482–489.